UCLouvain

FACULTE DES SCIENCES

Faculté des sciences

Foldamer-based pyridoxal phosphate mimics as organocatalysts for transamination reactions

Auteure : Beeckmans Estelle

Promoteur : Prof. Singleton Michael

Lecteur·rices : Prof. Hermans Sophie, Prof. Riant Olivier, Prof. Robiette Raphaël

Année académique 2023-2024

Master [120] en sciences chimiques, à finalité approfondie

"*Science is an inherently optimistic enterprise, the working assumption being that Nature is comprehensible*" - Rebecca Skloot

"*I finally became convinced that the theory of creation actually had a much better scientific basis than the theory of evolution, for the creation model was actually better able to explain the physical and biological complexity in the world*" – Roy Spencer

Acknowledgement

Dans un premier temps, je tiens évidemment à remercier mon promoteur, le professeur Michael Singleton, pour m'avoir accueilli dans son laboratoire et pour avoir pris le temps de m'orienter dans la bonne direction lors des moments de doute. Son expertise et ses conseils avisés ont été des éléments clés pour la réalisation de ce mémoire. J'aimerais aussi spécialement remercier les professeurs Olivier Riant, Sophie Hermans et Raphaël Robiette qui prendront le temps de lire et d'évaluer ce mémoire. J'espère que celui-ci sera à la hauteur de leurs attentes.

J'aimerais aussi remercier tous les membres du laboratoire pour leur aide précieuse mais surtout, pour leur humour décalé qui redonne le sourire même pendant les trop longues journées. Un grand merci à Charles, Louis, Maëlle, Loïc, Corentin et encore plus spécialement merci à Seb qui a pris énormément de son temps pour corriger mon mémoire et en faire ce qu'il est aujourd'hui. Je remercie aussi spécialement mon encadrant, Ugo, pour sa gentillesse et son approche bienveillante qui m'ont appris beaucoup de choses, dont l'autonomie en laboratoire. J'espère être amenée à retrouver une équipe aussi chouette que celle-ci à l'avenir et, en attendant, je leur souhaite à tous le meilleur pour la suite.

Finalement, je suis particulièrement reconnaissante envers ma famille, et principalement envers ma mère, qui a supporté mes hauts et mes bas à travers mes 5 années d'étude et qui m'a encouragé tout au long de ce mémoire même si elle ne comprenait rien à ce que je lui racontais. Merci à Garance, Greg, Romain et Lauraleen, des amis en or que j'espère garder encore longtemps et qui m'ont permis de surmonter tant de blocus. Merci à Manon qui n'a jamais arrêté de croire en moi et de m'encourager depuis notre rencontre lors de notre tout premier jour à l'université et finalement, merci à Angie, qui me permet de déconnecter de ce monde universitaire et de rêver à autre chose de temps à autre.

Abstract

Pyridoxal-5'-phosphate, the biologically active form of vitamin B6, has been intriguing scientists for decades thanks to its ability to catalyze many different biological reactions involving amine substrates. This coenzyme can bind to more than 140 enzymes to help them in their function, each of them catalysing its own reaction due to the difference in the environment. Indeed, the selectivity of PLP has been demonstrated to be highly dependent on the environment around the reaction center. Depending on the residues interacting with this reaction center and thus, depending on the specific 3D folding of each enzyme, the selectivity of PLP is tuned, leading to a highly versatile catalyst.

Inspired by PLP, this master's thesis aims to develop a new type of PLP-like organocatalyst where the local environment around the active site can be specifically controlled. For this, we make use of foldamers, oligomers able to fold on themselves to adopt a specific 3D structure, similar to what occurs with enzymes. These structures combine the best of enzymes and organocatalysts by allowing specific placement of relevant functional groups on well-defined and stable backbones. This makes them ideal tools for studying how the change in environment induced by the specific folding of foldamers around a PLP-mimic influences the reactivity.

This master's thesis therefore describes the synthesis of a trimeric sequence containing a PLP analogue thanks to a combinatorial approach. The aldehyde group of the PLP-mimic was obtained by direct functionalization of the trimer, allowing to avoid additional protecting and deprotecting steps and providing a new post-synthetic functionalization example for AOF. The catalytic potential of this new trimeric PLP-mimic towards a transamination reaction with benzylamine and a sacrificial ketone was investigated. We first attempted to optimize the conditions for this reaction with the monomeric PLP-mimic and then compared the reactivity of the monomeric and trimeric PLP analogues. Based on what we observed, the trimer can perform this reaction faster than the monomer, giving one of the rare AOF acting as a catalyst. These promising results provide a new type of reactivity not previously reported for foldamers and open new possibilities for organocatalyst design.

Table of content

Abbreviations table

Abbreviation	*Full name*
ACHC	*Trans-2-aminocyclohexanecarboxylic acid*
AOF	*Aromatic oligoamide foldamer*
ATP	*Adenosine triphosphate*
BBI	*Benzylamine-benzaldehyde imine*
BHT	*Butylated hydroxytoluene*
CBL	*Cystathionine β-lyase*
DBU	*1,8-diazabicyclo(5.4.0)undec-7-ene*
DCC	*Dicyclohexylcarbodiimide*
DCM	*Dichloromethane*
DIAD	*Diisopropyl azodicarboxylate*
DMAD	*Dimethyl acetylenedicarboxylate*
DMF	*Dimethylformamide*
DMSO	*Dimethylsulfoxide*
d.r.	*Diastereomeric ratio*
e.e.	*Enantiomeric excess*
EDC	*1-ethyl-3-(-3-dimethylaminopropyl)carbodiimide*
HAAs	*β-hydroxy-α-amino acids*
HATU	*Hexafluorophsophate azabenzotriazole tetramethyl uronium*
LDC	*Lysine decarboxylase*
NAD(P)H	*Nicotinamide adenine dinucleotide (phosphate)*
PL	*Pyridoxal*
PLP	*Pyridoxal phosphate*
PM	*Pyridoxamine*
PMP	*Pyridoxamine phosphate*
PN	*Pyridoxine*
QQP	*Quinoline-quinoline-pyridine sequence*
TA	*Threonine Aldolase*
THF	*Tetrahydofuran*
TLC	*Thin layer chromatography*
TMB	*Trimethoxybenzene*
TPL	*L-tyrosine phenol-lyase*
β_3-hLys	*β_3-homolysine*

1 State of the art

Nature has always amazed us for numerous reasons, especially for its incredible complexity. Earth has been developing for billions of years to give this astonishing diversity in which we live today. Despite the daunting complexity of nature's processes, they have been inspiring scientists for a long time and led to a new area in chemistry; biomimetic chemistry. This type of chemistry stands at the border between biology and chemistry and focuses on developing artificial compounds with bioinspired properties[1,2].

One of the main inspirations in this field lies in enzymes; proteins acting as highly efficient natural catalysts. Indeed, enzymes are able to drastically increase kinetics of bioprocesses and are essential for the development of all living organisms[3]. In addition, enzymes also demonstrate remarkable specificity, meaning that they usually catalyze the conversion of only one type of substrate[4].

However, many enzymes cannot function properly on their own and often rely on small organic molecules called coenzymes[5]. Such compounds can bind to an enzyme and help it perform its catalytic activity owing to cooperative interactions between them[6]. Therefore, coenzymes are able to turn enzymes with limited efficiency into powerful catalysts.

Some of the most famous coenzymes are ATP and NAD(P)H[7] but another intriguing example is the Pyridoxal Phosphate (PLP), a compound found in vitamin B6. This molecule has been extensively studied and serves as a powerful coenzyme in many biological reactions involving amine compounds. Yet, the reactivity of PLP is significantly influenced by its surroundings, notably by all the cooperative interactions taking place between PLP and the enzyme it is linked to.

In the present work, we aim at synthesizing an artificial PLP-like molecule with a controlled environment in order to tune the reactivity of the mimic. Indeed, thanks to supramolecular structures called foldamers, one can modulate the environment around the PLP-mimic and thus, the interactions responsible for its reactivity.

1.1 Pyridoxal Phosphate

Pyridoxal Phosphate was discovered, in the 1950's, to be the biologically active form of vitamin B6[8]. This vitamin comprises six water-soluble compounds all containing a pyridine ring as their core (figure 1). In the same family, five other structurally related derivatives can be converted to PLP thanks to different enzymes[9]; pyridoxal (PL), pyridoxine (PN), pyridoxamine (PM) and their phosphate derivatives with PMP that will later be discussed in section 1.1.3.

PLP plays the role of a coenzyme, which means that it is a small organic compound which enhances the catalytic efficiency of enzymes through specific binding[10]. Therefore, a lot of enzymes rely on PLP (and hence, vitamin B6). Indeed, since its discovery in 1951, already more than 140 PLP-dependent enzymes have been discovered[11] which represents around 4% of known enzymes.

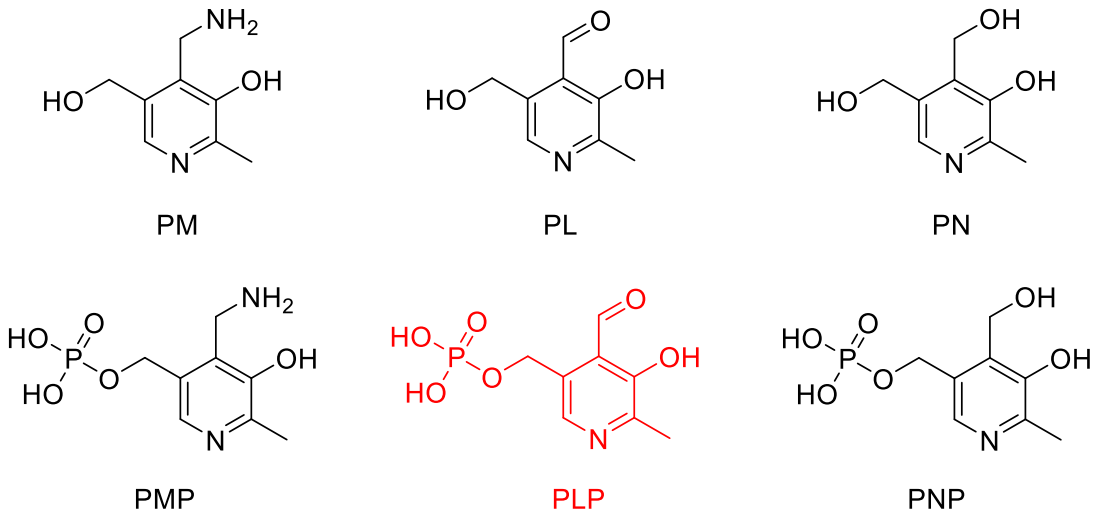

Figure 1. Structure of the six compounds of vitamin B6 with Pyridoxal Phosphate in red.

Over the years, PLP has acquired an important place in science since it has been found to be directly related to many metabolic processes such as lipid metabolism, amino acid biosynthesis, neurotransmitter production and more[12]. Its ability to participate in all of these pathways is a result of its great reaction versatility.

What is really impressive is that this exact same coenzyme is involved in many different transformations but how exactly does one single species realize so many reactions? It all depends on the interactions with its environment and thus, on the enzyme it is linked to. Indeed, depending on the residues interacting with PLP, its properties are modulated and thus,

it allows the catalysis of many different reactions by only this compound. This concept can be illustrated by some examples of PLP-dependent enzymes able to catalyze different reactions due to their respective environment.

A first example of a PLP-dependent enzyme is Lysine Decarboxylase (LDC)[13]. This enzyme catalyzes the decarboxylation of L-lysine into cadaverine (figure 2)[14].

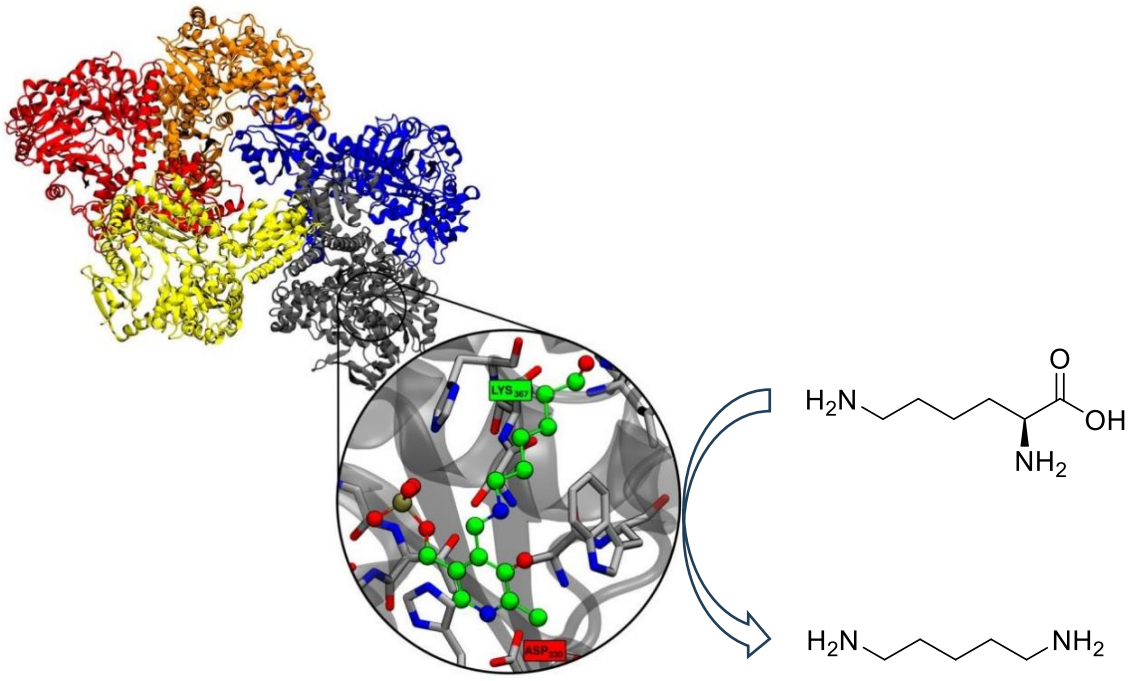

Figure 2. Structure of Lysine Decarboxylase with a representation of its active site and decarboxylation of L-lysine into cadaverine. Adapted from [13].

LDC has drawn attention in the industrial field because of its product, cadaverine, that can be used to produce polyurethanes and polyamides, two polymers with many applications in everyday life[15]. Since this bio-based production of cadaverine seems to be a great alternative to the production of these polymers (normally produced from petroleum resources), intensive work has already been conducted on LDC, notably by trying to enhance its catalytic efficiency by increasing PLP levels[16].

Another example of a PLP-dependent enzyme is Threonine Aldolase (TA). This enzyme catalyzes the formation of a new carbon-carbon bond between glycine and acetaldehyde to form threonine (figure 3). TA's can be divided into two categories; L-TA and D-TA depending on which isomer of threonine they can accept, respectively, L-threonine and D-threonine.

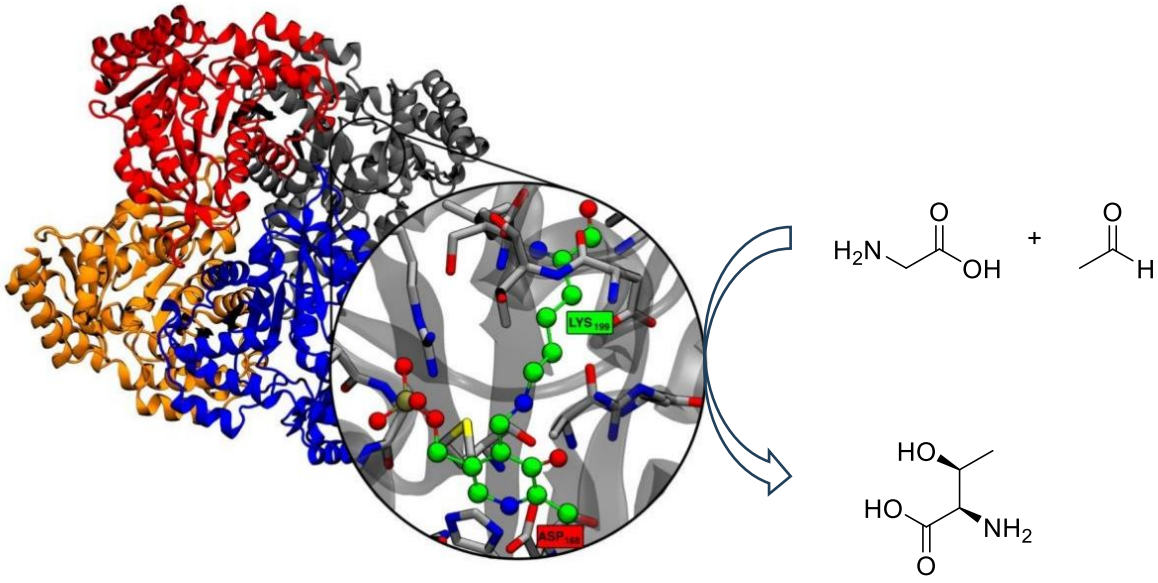

Figure 3. Structure of L-Threonine Aldolase with a representation of its active site and condensation of acetaldehyde and glycine into L-threonine. Adapted from [13]

TA is therefore able to catalyze the condensation between glycine and any aldehyde, allowing the synthesis of many β-hydroxy-α-amino acids (HAAs). Hence, TA has drawn attention in the pharmaceutical field since HAAs are important amino acids used as building blocks in the synthesis of diverse natural products, drugs, antibiotics (penicillin, amoxicillin or cefotoxin[17]) and more[18].

There are a lot of other PLP-dependent enzymes that could be highlighted for their applications such as L-Tyrosine Phenol-Lyase (TPL) that allows the production of a treatment for Parkinson's disease, Cystathionine β-Lyase (CBL) which gives interesting products for the food industry, etc.

1.1.1 Mechanistic versatility

PLP reactivity was exemplified by the decarboxylation and the aldol condensation realized by, respectively, LDC and TA but a closer look at the mechanisms for these diverse transformations shows a number of similar intermediates. Indeed, PLP is involved in the catalysis of a plethora of reactions but all of them share a few common first steps.

PLP being a coenzyme, it needs to bind reversibly to the substrate. This is done in two steps; thanks to its aldehyde group, the "free" PLP will first bind to a lysine residue from the enzyme to form the *internal* aldimine. Then, this internal aldimine can undergo a transaldimination with the amine substrate to form the *external* aldimine (Scheme 1)[19].

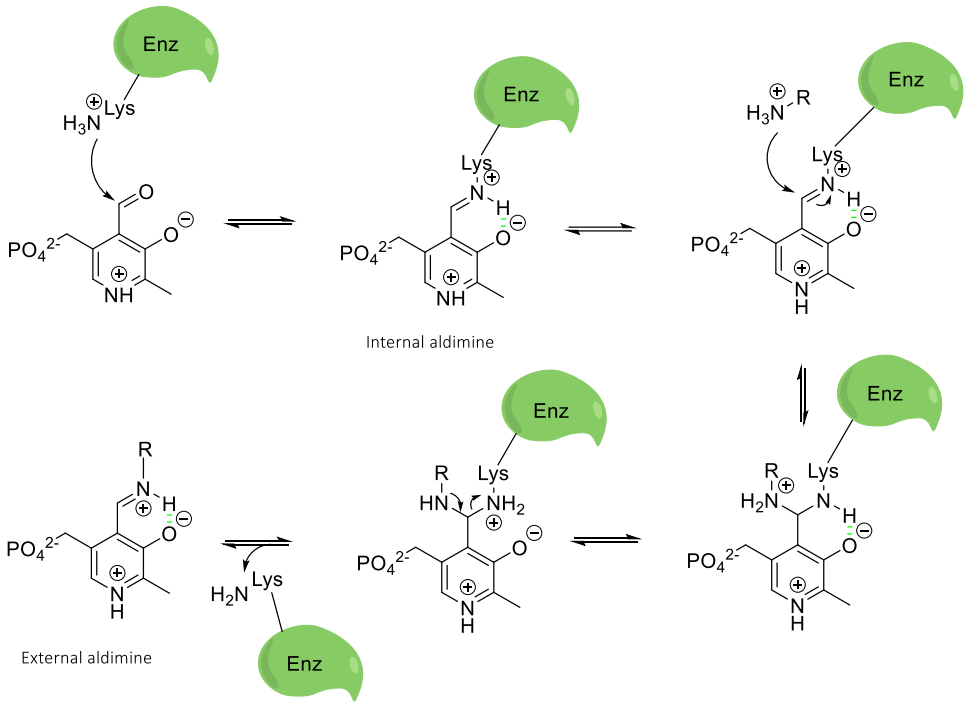

Scheme 1. Formation of the internal aldimine followed by a transaldimination to form the external aldimine.

This condensation into an aldimine is a common reaction when talking about an aldehyde but PLP has an enhanced reactivity thanks to two structural features; its pyridine ring draws the electrons, making C_4' a better electrophile (figure 4) and its phenoxide anion is able to stabilize the iminium not only by hydrogen bonding but also by resonance.

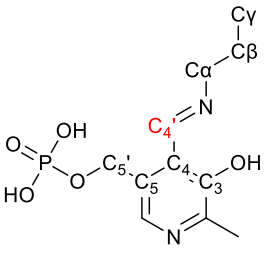

Figure 4. Atom labels of PLP.

From this external aldimine, PLP, cooperatively with the enzyme, is then able to catalyze a plethora of reactions involving amine substrates. Indeed, many different reactions are then possible either on the α-, β-, or γ-carbon such as racemisation, decarboxylation, transamination, elimination, etc. (figure 5).

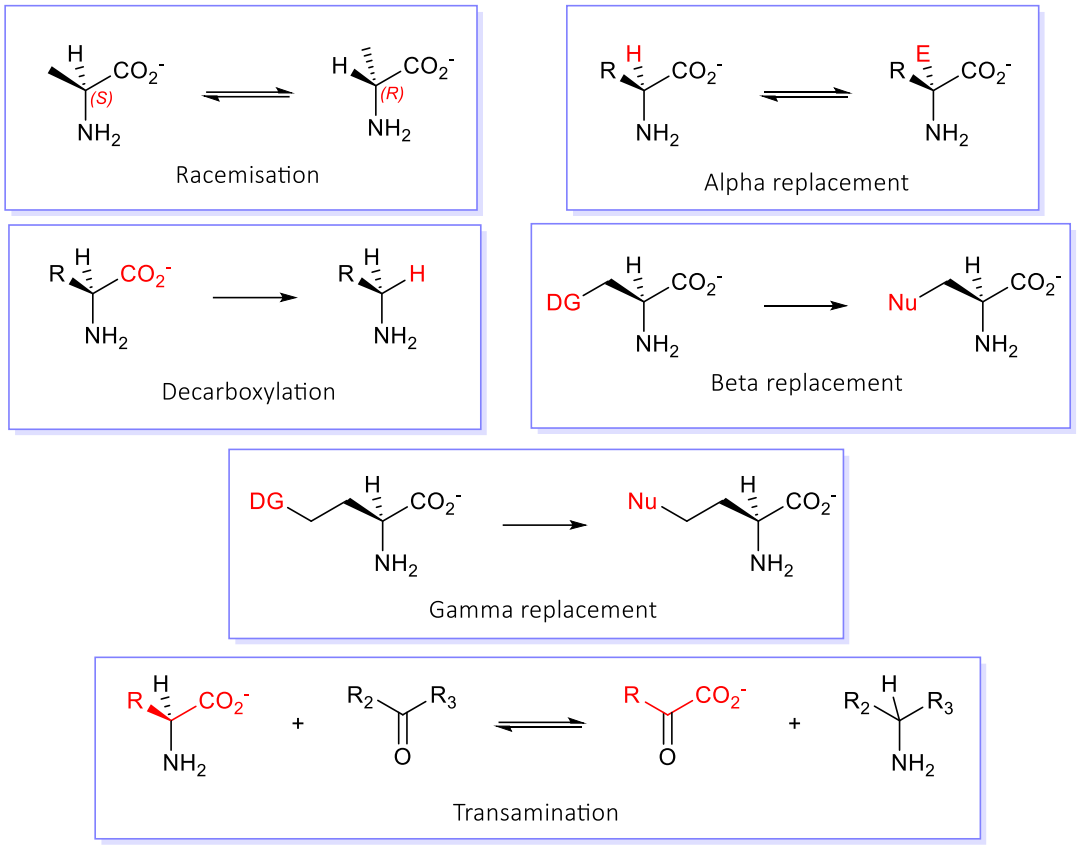

Figure 5. General overview of reactions catalyzed by PLP-dependent enzymes.

The great versatility of PLP mostly comes from its "electron sink" property, meaning that it is able to stabilize the negative charge that is formed on the quinonoid intermediate either by deprotonation, decarboxylation, or heterolytic cleavage of a bond on the α-carbon (scheme 2).

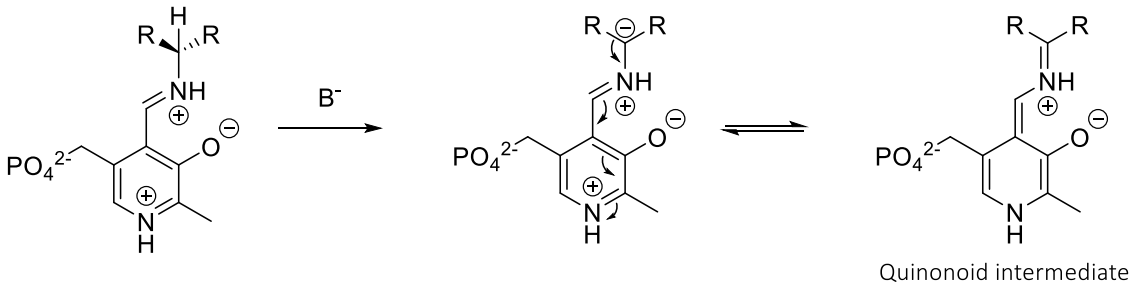

Scheme 2. Stabilisation of the negative charge by the quinonoid intermediate.

Therefore, the majority of PLP-catalyzed reactions share a common mechanism by these first steps and the diversification takes place starting with the quinonoid intermediate. The mechanisms of these different reactions are shown on scheme 3[20].

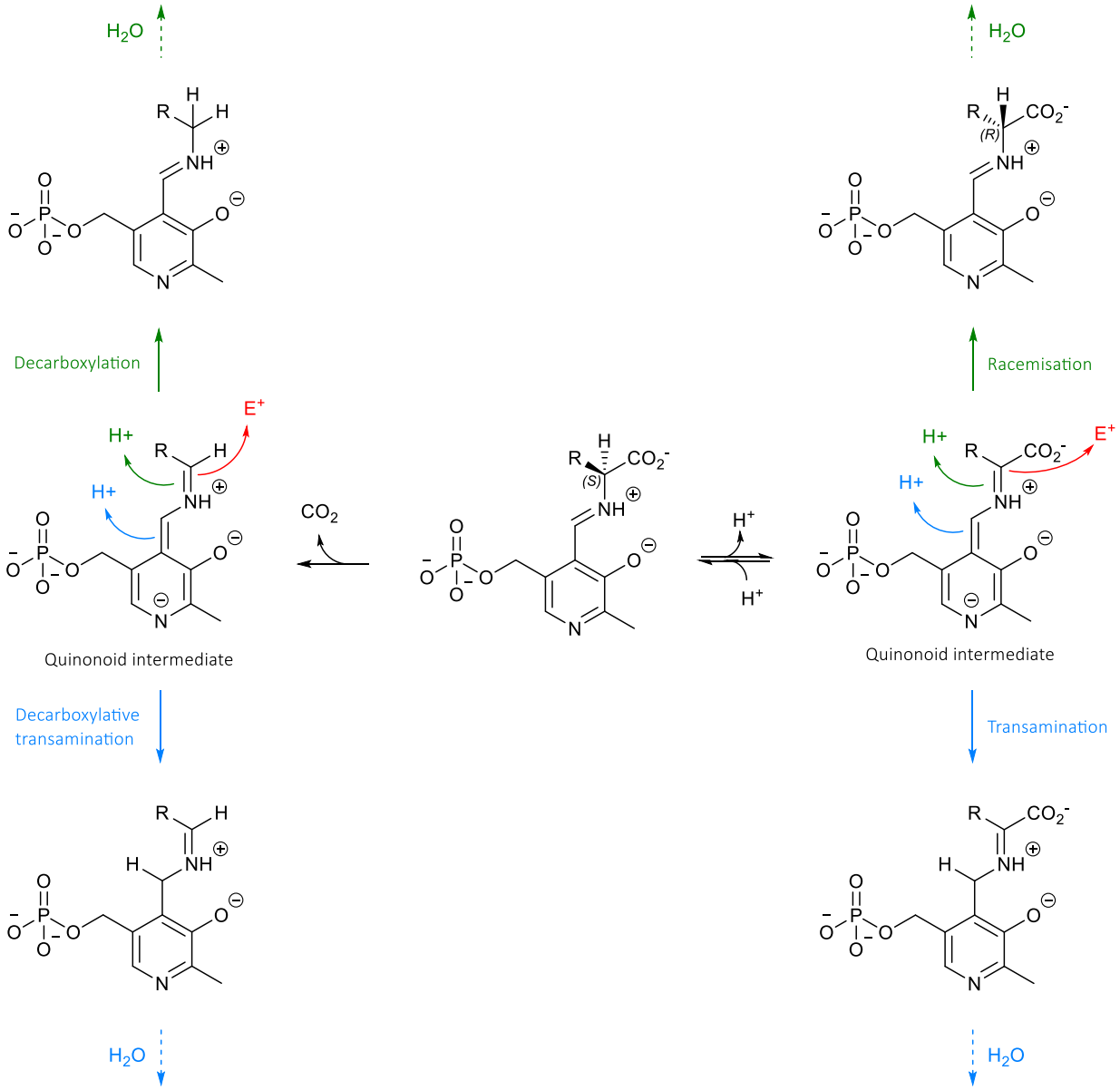

Scheme 3. Mechanism of some PLP-assisted reactions on the α-carbon.

In this scheme are shown the mechanism of 4 PLP-assisted α-carbon reactions; racemisation, decarboxylation, transamination and decarboxylative transamination. In the first place, the quinonoid intermediate can be formed either by deprotonation or decarboxylation. Then, from both pathways, a transamination can take place, as well as an alpha-replacement (not fully shown here but represented by the red arrows).

With several possible reactions, the efficiency of PLP lies in its ability to favour one reaction at the expense of the others. Therefore, the next challenge is to determine which factor controls this selectivity. To answer to this question, scientists have tried to study the correlation between the structure of different PLP-dependent enzymes and the reactions they catalyze.

1.1.2 Selectivity determination

In the first place, scientists hypothesized that the selectivity was depending on the fold type of the enzyme[21]. Indeed, there exist seven Fold Types in total for all enzymes and all the already discovered PLP-dependent enzymes are part of Fold Types I to V (figure 6).[22,23]

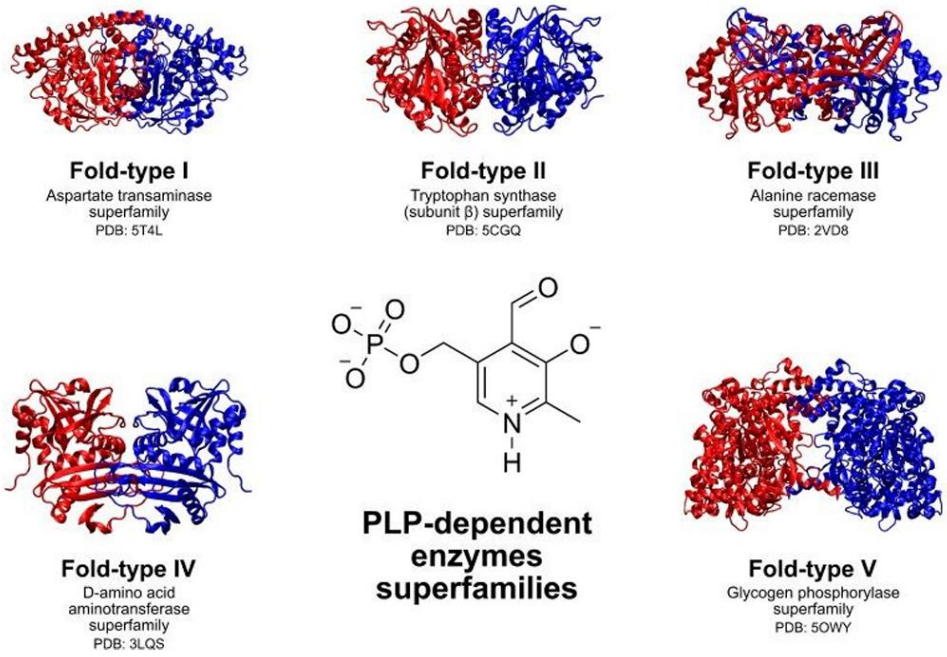

Figure 6. 3D structure of Fold Types I to V (and example of a PLP-dependent enzyme of each family). Printed from [13]

Therefore, scientists were considering that each Fold Type could be correlated to the selectivity. For example, at the time, they were only considering three different Fold Types and they hypothesized that each of them was specific to reactions on a certain position. They therefore called them α-, β- and γ-families to describe reactions taking place on the α-, β- and γ-carbon.

Nevertheless, it has now been proven that there is no correlation between the Fold Type and the selectivity since several Fold Types can catalyze the same reactions and each reaction can be catalyzed by, at least, two different Fold Types.

Therefore, what is determining the type of reaction catalyzed by PLP? It is actually the close environment around the reaction center. Indeed, the interactions between the diverse residues of the enzyme and the PLP will determine the selectivity.

Two of the main ideas for how the local environment relates to selectivity are the Dunathan stereoelectronic hypothesis and Tuning of the Electron Sink.

Dunathan stereoelectronic hypothesis

Dunathan postulated that the orientation of the substituents on the α-carbon determines the type of reaction. He suggested that the bond to be broken must be oriented perpendicular to the pyridine ring[24]. Indeed, the perpendicular bond is therefore aligned with the π-orbitals of the pyridine ring. This allows a minimum of energy in the transition state since, in this way, the π-orbital in formation is in conjugation with the already existing π-orbitals of the pyridine ring, allowing the extension of the electronic delocalization to the bond that is breaking (figure 7).

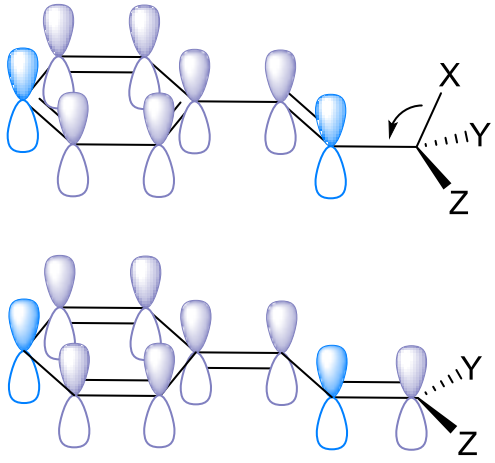

Figure 7. Schematic representation of the π-orbitals in the quinonoid intermediate. The perpendicular bond being the most labile since it allows a minimum of energy in the transition state. The nitrogen atoms are represented by blue orbitals. Adapted from [24]

Thus, such a hypothesis allows us to differentiate reactions taking place on the position α, such as decarboxylation or deprotonation in which a carboxylate group or a proton are respectively oriented perpendicular to the pyridine ring (figure 8).

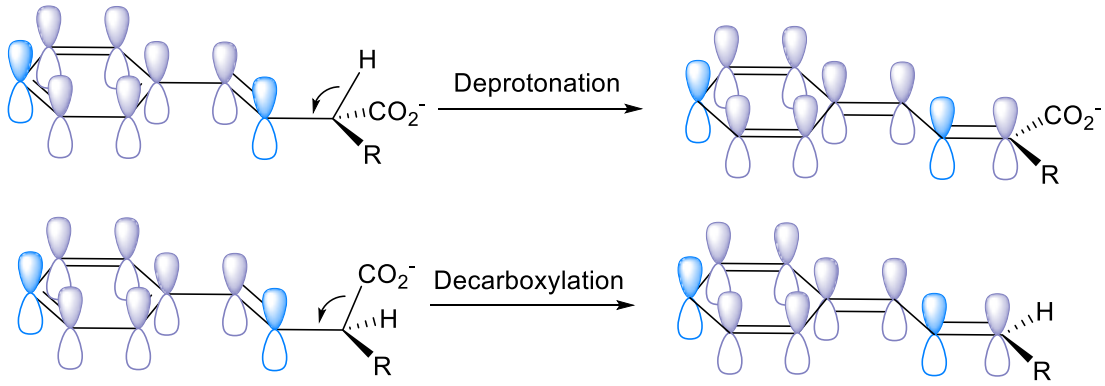

Figure 8. Representation of the Dunathan hypothesis differentiating reactions on the C_α. Adapted from [25].

The orientation of the substituents on the C_α is depending on the interactions with the close environment. Indeed, rotation around the C_α-N bond can happen and thus, allow different orientations for the three substituents. However, this rotation must be partially restricted by the specific surroundings of the external aldimine thanks to, notably, non-covalent interactions and steric hindrance. By restricting this rotation, one of the substituents will be preferably placed perpendicular to the pyridine ring and will thus be selectively cleaved. An example of this is shown in figure 9 where diverse residues are orienting the hydrogen or carboxylate group perpendicular to the pyridine ring thanks to hydrogen bonds and steric hindrance.

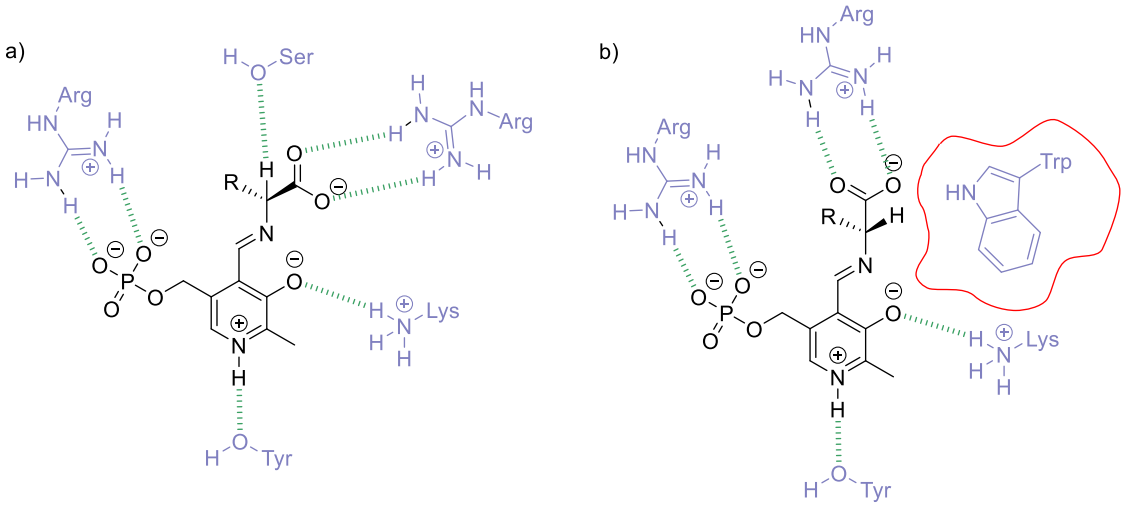

Figure 9. Schematic representation of the influence of the neighbouring amino acid residues on the orientation of the substituents on C_α. (a) Hydrogen perpendicular to the pyridine ring due to hydrogen bonding and (b) carboxylate perpendicular to the pyridine ring due to hydrogen bonding and steric hindrance of a tryptophan residue.

This hypothesis is useful to differentiate reactions taking place on the C_α and can be extended to reactions requiring more steps, such as transamination or β- and γ-replacement. However, other interactions between all the residues of the enzyme and other parts of the PLP have also been linked to selectivity.

Tuning of the Electron Sink

Indeed, another effect due to the environment explaining the selectivity is the tuning of the intrinsic electron sink ability of the PLP. Depending on the specific arrangement of residues surrounding PLP, the protonated or deprotonated form of the aromatic nitrogen of PLP will be favoured. This will increase or decrease its electron sink ability and will thus impact the type of reaction that will be catalyzed (figure 10)[25].

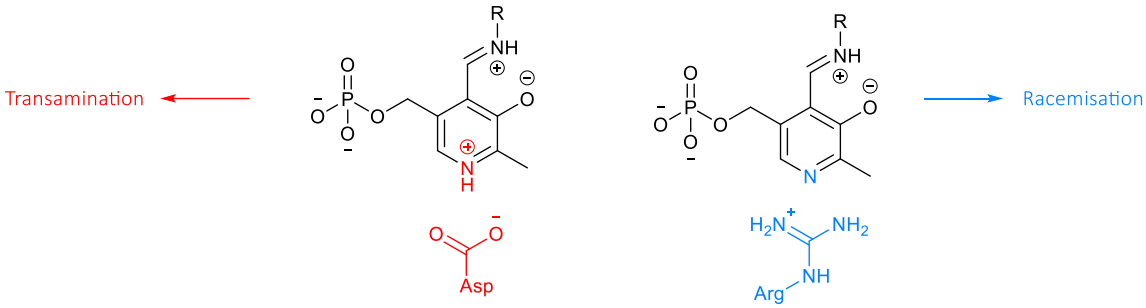

Figure 10. Control of the electron sink ability of the coenzyme PLP depending on the residues close to the reaction center.

In the case of a neighbouring negatively charged residue, like aspartate, the PLP will be maintained in its protonated form, enhancing its electron-withdrawing abilities. In these conditions, a transamination will be favoured since the deprotonation of the C_α will be facilitated thanks to the stabilization by the quinonoid intermediate but, mainly, the C_4' will be the favoured site of reprotonation.

Conversely, in the case of a neighbouring positively charged residue, like arginine, PLP is maintained in its deprotonated form, decreasing its electron-withdrawing abilities. These conditions rather favour racemisation since this reaction seems to require less electron delocalization.[26]

Thus, this electron sink control implies interactions between the aromatic nitrogen of PLP and the surrounding residues but other parts of PLP can also interact with the neighbouring residues. For example, in a transamination reaction, as described above, the protonated form of PLP must be favoured but it is not the only condition. Indeed, this reaction is also facilitated thanks to a closely located lysine (or lysine-like) residue that will be able to capture the proton on C_α and then, transfer a proton to C_4' (scheme 4).

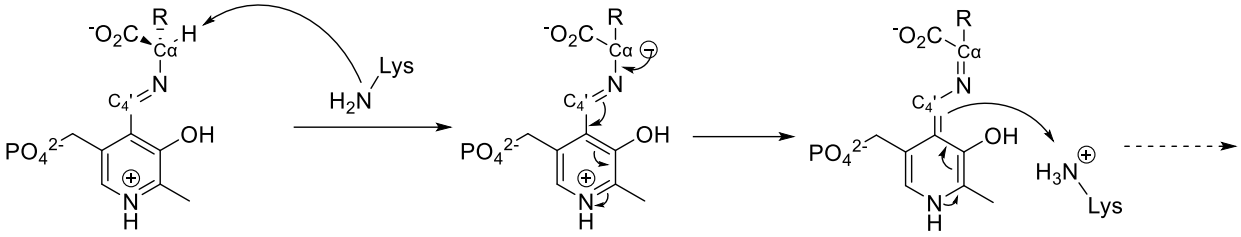

Scheme 4. First steps of a transamination reaction showing the deprotonation and reprotonation steps realized by a close lysine residue.

Another example highlighting the importance of the interactions with other parts of PLP is the racemisation reaction. As described above, the deprotonated form of PLP must be favoured but this reaction is also possible thanks to the steric hindrance provided by some residues on one face of the PLP. Indeed, the proximity between some residues of the enzyme and one face of PLP prevents any water molecule to reach and protonate this face (figure 11).

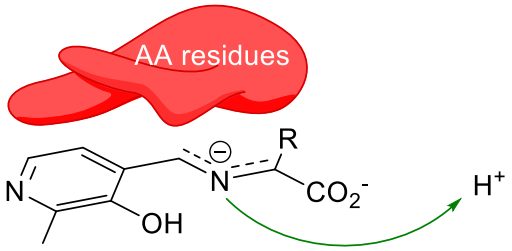

Figure 11. Representation of the steric hindrance provided by some residues on the upper face of the coenzyme, forcing the reprotonation to happen on the lower face.

1.1.3 Some previous PLP-mimics

Intrigued by the great properties of PLP, many research groups started to develop similar molecules, called PLP-mimics, in order to catalyze different reactions based on amine substrates.

In 1952, the Metzler group investigated the deamination of serine catalyzed by pyridoxal only[27]. Indeed, pyridoxal is able to catalyze diverse reactions without being linked to an enzyme though at much slower rates. Nevertheless, they discovered that reactions with pyridoxal alone could be accelerated by metals such as aluminium, copper or iron. Indeed, these metals are able to chelate with the aldimine as shown on scheme 5. This chelation stabilizes the aldimine and provides a coplanarity between the pyridine ring and the imine, allowing the acceleration of the reaction.

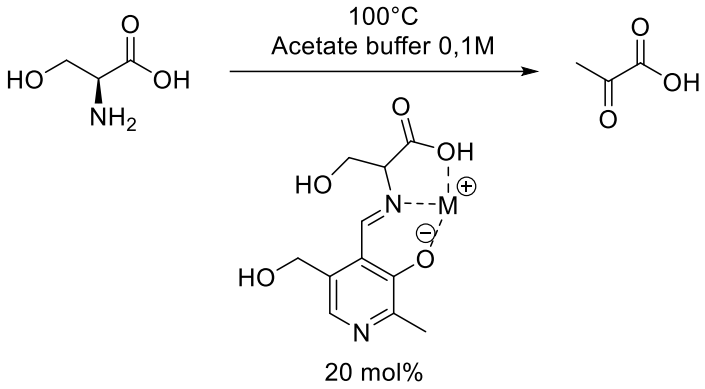

Scheme 5. Deamination of serine catalyzed by Metzler's pyridoxal-mimic (chelated with a metal). Adapted from [27]

This is one of the few examples of PLP analogues since, more often, scientists have looked into the amine counterpart of PLP; PMP (Pyridoxamine Phosphate). Its purpose is as exactly the same as PLP: catalyzing reactions such as transamination by forming an aldimine with carbonyl compounds (scheme 6). Indeed, during transamination reactions, the cofactor cycles between the PLP and PMP forms, making both potential starting points for different PLP catalyzed reactions. Therefore, one can also look into some of the work conducted on PMP analogues.

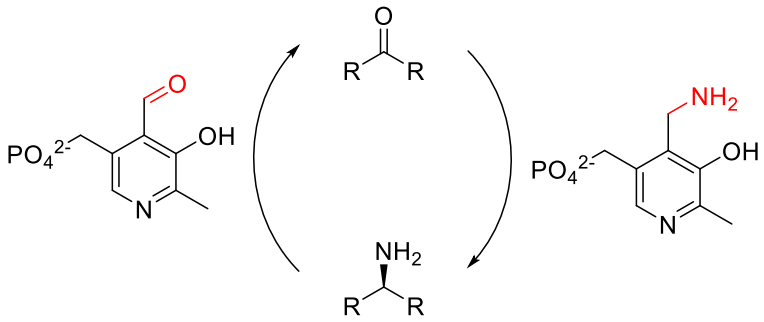

Scheme 6. Structure of pyridoxamine phosphate (right) and use in transamination reaction.

In 1978, Kuzuhara's group reported the synthesis of a pyridoxamine analogue able to catalyze the stereoselective transamination of ketoacids in order to synthesize optically active amino acids (scheme 7)[28].

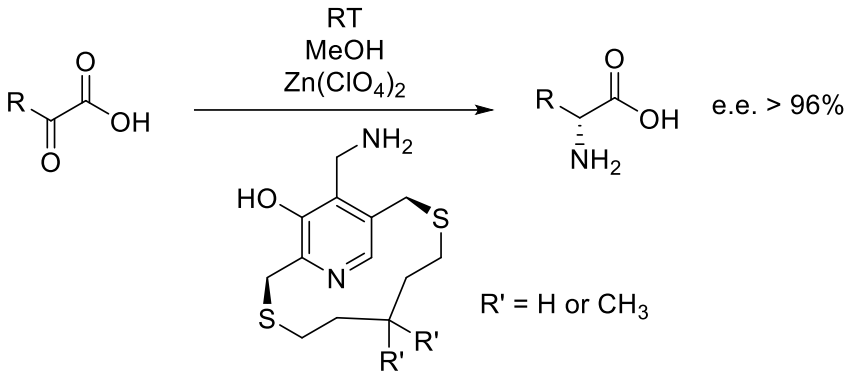

Scheme 7. Kuzuhara's pyridoxamine analogue for stereoselective transamination of ketoacids into optically active amino acids. Adapted from [28]

They synthesized this pyridoxamine analogue by adding an "ansa chain" with the purpose of hindering one face of the aromatics to favour the reprotonation on one face only, allowing a stereoselective transamination. They succeeded in developing an efficient way of asymmetric synthesis of α-amino acids by using the branched ansa chain (R' = CH_3), that showed higher enantiomeric excess than for R' = H, in presence of Zn^{2+} (up to 96% of enantiomeric excess)[29].

The Breslow group also investigated the transamination of α-amino acids by developing diverse pyridoxamine analogues with basic side chains (figure 12)[30, 31]. These arms are indeed sufficiently flexible to bend and extend so that they can pass the hydrogen from one carbon to the other one.

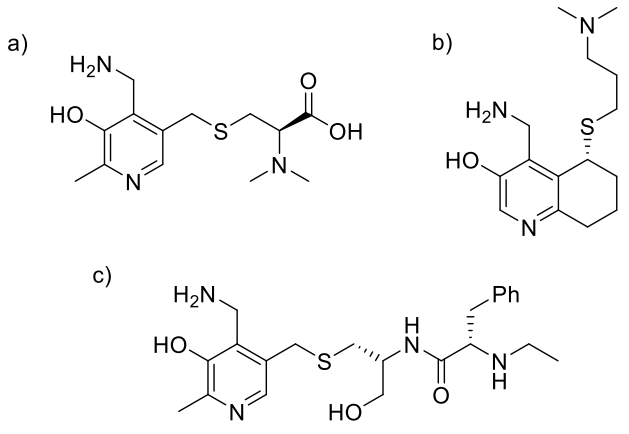

Figure 12. Pyridoxamine analogues with basic side chains developed by Breslow group.

They reached enantiomeric excess up to 92% by using these pyridoxamine analogues in presence of Zn^{2+} with the higher e.e. obtained for the bicyclic analogue (b) thanks to the geometric locking of the basic side arm on one face of the pyridoxamine (R enantiomer) that allows the deprotonation-reprotonation mechanism to happen on one face only[32].

Breslow and coworkers also got interested in supramolecular analogues in order to better mimic the structure of enzymes by adding a level of control that is reminiscent of enzymes, namely, molecular recognition. Once again, they studied the asymmetric transamination of ketoacids into optically active amino acids and developed different types of supramolecular mimics. For example, in 1980, they developed a pyridoxamine analogue linked to a β-cyclodextrin. Indeed, as described above, the basic side chain grafted on pyridoxamine catalyzes the proton transfer in the transamination reaction but, by also grafting a β-cyclodextrin with an inherent chirality, they induce an optical activity[33]. This analogue was later enhanced by Tabushi group by grafting a basic ethylenediamine side chain on the β-cyclodextrin and not on the pyridoxamine analogue[34] (figure 13). This important idea drastically accelerated the rate of the reaction up to 2000 fold compared to pyridoxamine. The inherent chirality of the β-cyclodextrin also induced excellent ee's up to 98%, proving that small PLP models can actually be powerful synthetic tools.

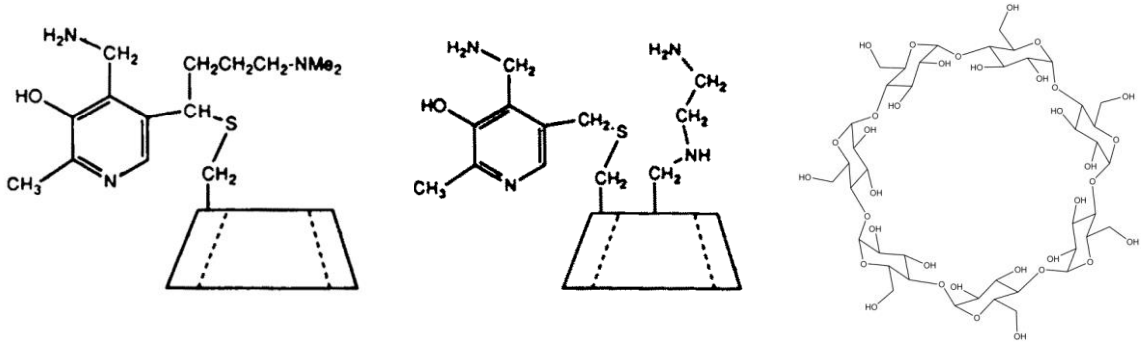

Figure 13. Schematic representation of the cyclodextrin pyridoxamine analogue of Breslow (left), the cyclodextrin pyridoxamine analogue of Tabushi (middle) and structure of a β-cyclodextrin (right). Adapted from [34].

Besides the usual transamination reactions, PLP analogues have been used to promote other reactions. For example, the Zhao and Yuan groups investigated the use of a pyridoxal analogue as catalyst for an asymmetric Mannich reaction[35] (scheme 8).

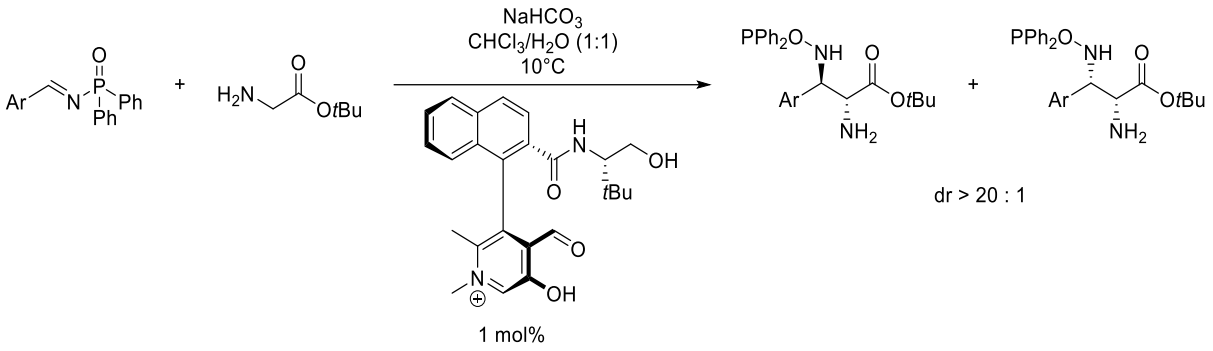

Scheme 8. Mannich reaction and structure of Zhao and Yuan's pyridoxal analogue. Adapted from [35].

In this pyridoxal analogue, two features have a great importance for the catalysis. First, the N-methylation is essential since without it, the authors have noticed that the pyridoxal is completely inactive. Indeed, this methylation increases the electron-withdrawing property of pyridoxal, enhancing its catalytic activity.

Secondly, the side chain has a great influence on the selectivity of the catalyst. Thanks to the amide and hydroxy groups of the side chain (that are both H-bond donors), the catalyst is able to form 2 hydrogen bonds with the substrate, allowing it to orientate the substrate with a specific spatial arrangement to enhance the selectivity (figure 14)[35].

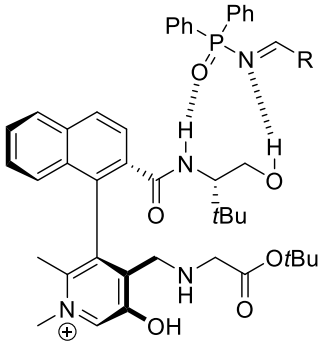

Figure 14. Representation of the hydrogen bonds between the catalyst and the substrate to specifically orientate it. Adapted from [35].

In all of these examples, a common feature for the good reactivity is the presence of a controlled local environment. Indeed, as described in a previous section, the residues surrounding the coenzyme can interact with it and thus, have a great impact on the reactivity. In all the previous examples, the coenzyme required reasonable synthetic modifications in order to reach good rates and/or enantiomeric excess, with some of these examples using supramolecular structures to control the environment.

In a related way, in nature, the control of the environment around PLP is operated by the folding of amino acid residues into larger ordered structures. Therefore, inspired by these

secondary structures, the use of synthetic oligomers could provide similar potential for controlling the environment and tuning the reactivity of PLP. One possibility for such compounds is to use structures called foldamers.

1.2 Foldamers

1.2.1 General characteristics

Enzymes are really impressive biological molecules since, starting from a set of only 20 natural amino acids, they can form long linear sequences that fold into high-ordered structures. As the consequence of this unique folding, they are able to achieve remarkable functions such as catalysis, electron transfer and many more. Therefore, it is not surprising that scientists got inspired by them and have tried, for decades, to mimic the complex structures of enzymes by assembling non-natural monomers into sequences able to fold into well-defined structures called "foldamers".

The term "foldamer" was first introduced by S. H. Gellman in the late 1990's as any polymer with a strong tendency to adopt a specific compact conformation[36]. Since the introduction of this term, scientists are constantly enriching the field by assembling diverse non-natural building blocks in order to better control the intramolecular interactions and therefore, the folding of such structures[37].

Nowadays, these foldamers are described by Jeffrey S. Moore as "any oligomer that folds into a conformationally ordered state in solution, the structures of which are stabilized by a collection of non-covalent interactions between non-adjacent monomer units" [38]. This definition is more restrictive than the one given by Gellman since it implies non-covalent interactions between *non*-adjacent units. Therefore, considering this latest definition greatly reduces the number of compounds that can be considered as foldamers. For example, with Moore's definition, stable linear strands would not be considered foldamers.

Therefore, for the purpose of this project, the broader definition given to foldamers are "oligomers able to fold on themselves to adopt a specific three-dimensional structure thanks to non-covalent interactions such as hydrogen bonds, electrostatic interactions and π-stacking" [39]. Such a definition, better takes into account the diverse range of secondary structures that have been reported for foldamers.

Among these 3D structures, foldamers can fold into well-known single and double helical structures, β-sheet structures, and many more (figure 15)[40].

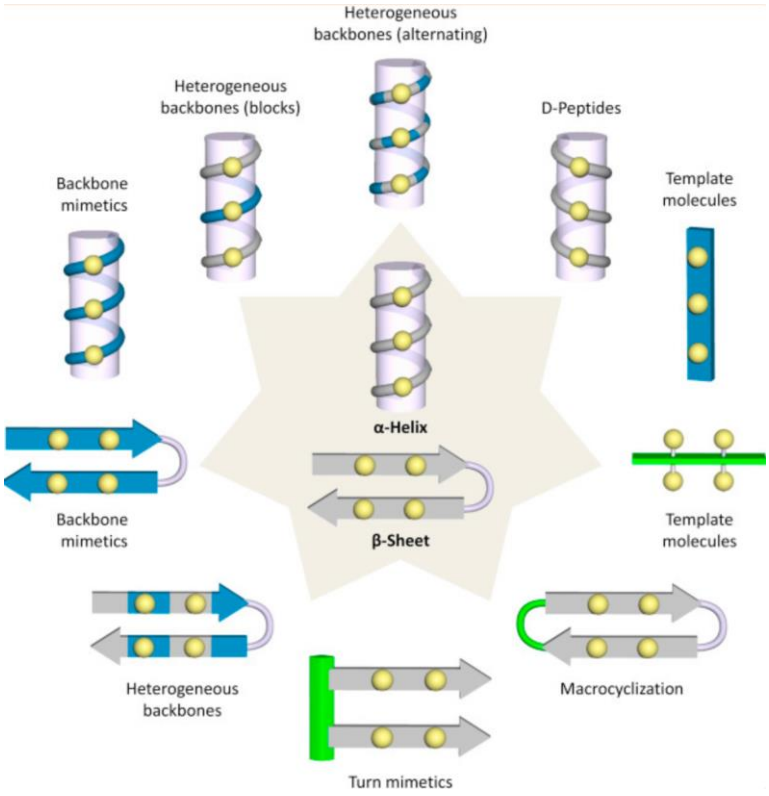

Figure 15. Illustrations of some secondary structures of foldamers. Printed from [40]

Throughout the years and the intensive research on foldamers, it has been determined that such structures must present some desired features:

- Predictability of their folding: in the framework of this project, we need to control the adopted structure of the foldamer (herein, a helix).
- Ease of synthesis: as large structures need to be synthesized for this project, we want a quick and easy way to synthesize them.
- Stability of the folded structure: in order for the foldamer to play a specific function (herein, catalysis), its structure must be stable.
- Tunability: as we want to achieve a wide range of foldamers by using the same synthetic pathways, the monomer units must be easily tunable.

The field of foldamer is incredibly wide and therefore, they can be divided into two large classes depending on the monomer units: backbones with aliphatic monomers and backbones with aromatic monomers.

1.2.2 Aliphatic foldamers

This class of foldamers consists in saturated carbon units usually separated by amide groups but can also be separated by urea groups or hydrazide groups. The monomer units of aliphatic foldamers are quite diverse; α-peptides, β-peptides, γ-peptides, peptoids,… (figure 16).

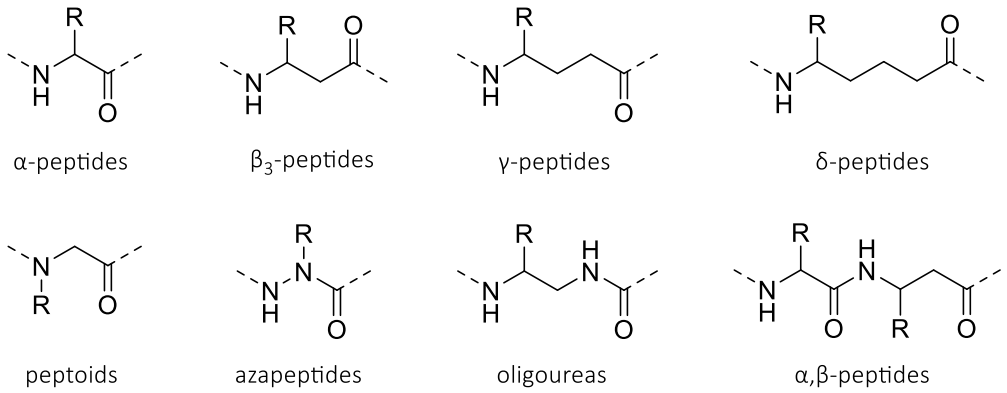

Figure 16. Some monomeric units used for aliphatic foldamers.

1.2.3 Aliphatic foldamers as catalysts

Even prior to the introduction of the term "foldamer", scientists were assembling α-peptides in order to mimic natural peptides since these are composed of α-amino acids. It is only later, coinciding with the introduction of foldamers, that the use of β-peptides was considered. Indeed, in 1996, Seebach[41] and Gellman[42] developed foldamers composed of β-peptides able to fold into stable helical secondary structures (figure 17).

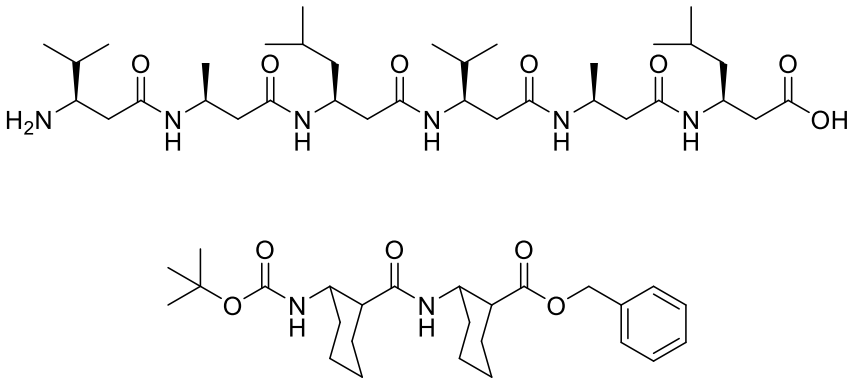

Figure 17. Structures of the β-peptide foldamers synthesized by Seebach (above) and Gellman (below).

These β-peptides actually demonstrate a better stability in their secondary structure than their α-peptides counterparts. Indeed, even though the extra carbon adds a freely rotating

bond in the structure that would decrease the tendency to form highly ordered structures, it has been proven that these β-peptide foldamers are able to form surprisingly stable helices[43]. The hypothesis on this stability is that the increased degree of freedom allows for a better arrangement of dihedral angles for hydrogen bonding.

The majority of the complex operations carried out by enzymes are, among other things, due to their tertiary structure (3D arrangement of the secondary structure units) and aliphatic foldamers have shown the ability to fold into discrete tertiary structures as well, hinting for these structures to demonstrate the same abilities than enzymes, such as catalysis[44]. Indeed, several groups have already reported the self-assembly of these foldamers into helix bundle like tertiary structures[45] and therefore, tried to use them as catalysts.

Another study concerning foldamers used as catalyst was led by the Hilvert group. They investigated a retro-aldol reaction with a β-peptide decamer as a catalyst[46] (scheme 9).

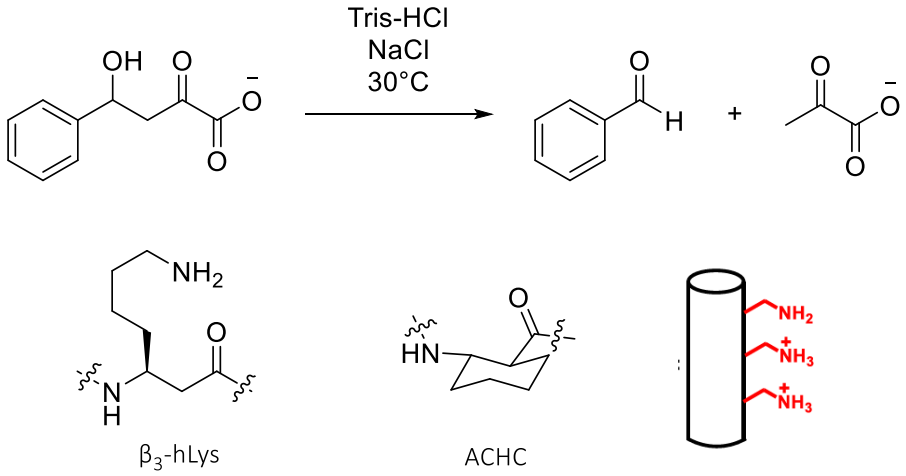

Scheme 9. Retro-aldol reaction catalyzed by Hilvert's β-peptide foldamer. Adapted from [46].

The aliphatic foldamer consisted in the repeating sequence "ACHC-ACHC-β_3-hLys" which gives an amphiphilic helix. The purpose of the trans-2-aminocyclohexanecarboxylic acid (ACHC) sequence is to stabilize the helical structure as well as providing the hydrophobic residues that drive the self-assembly in aqueous solution while the β_3-homolysine (β_3-hLys) purpose is to catalyze the retro-aldol reaction thanks to its amine function. Hilvert's group proved that this self-assembly is actually an important feature of the catalysis since it brings the positive charge of each ammonium in close proximity, allowing the lowering of the pKa of at least one ammonium group[47].

Another study was led by Guichard's group on a urea-based foldamer able to successfully catalyze the enantioselective Michael addition of malonates to nitro-olefins (up to 99% of enantioselectivity with a low catalyst loading of 0,1 mol% foldamer)[48]. This foldamer showed a stable helical secondary structure that was stabilized by hydrogen bonds between both NH groups of one urea group and the carbonyl of a neighbouring urea group[49] (scheme 10).

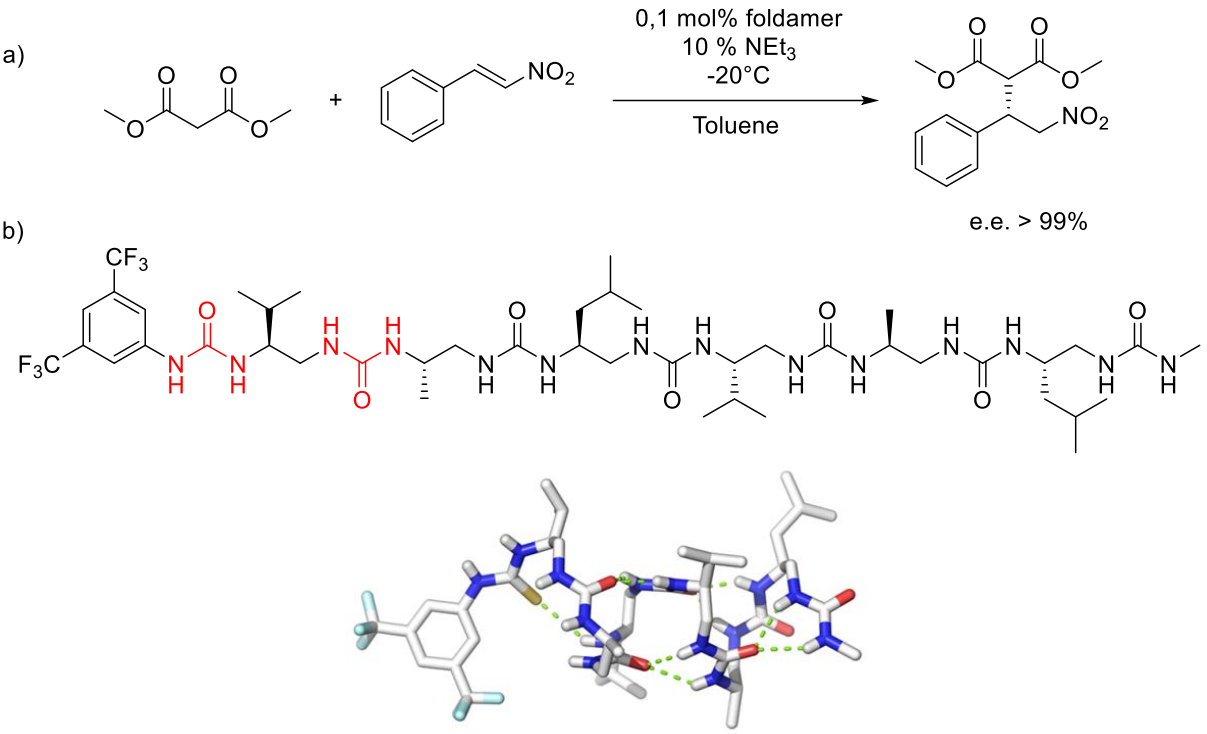

Scheme 10. a) Enantioselective addition of malonate to nitro-olefin and b) Guichard's urea-based foldamer used as catalyst for this reaction. Adapted from [49].

The particularity of this foldamer is that it seems that the active site involved in the catalysis are the two neighbouring N-terminus urea groups (in red on scheme 10) thanks to their H-bond donor groups able to recognize the substrate. In this way, the urea groups are thus able to assist the reaction by bringing the nitro-olefine and the diethylmalonate in close proximity. This differs from other foldamer-based catalysts since, usually, the active site consists in a side chain and not in the backbone of the foldamer itself.

One last example consists in a cyclodextrin-peptide hybrid developed by Ueno's group[50]. Indeed, as all enzymes require several functional groups working together, Ueno's group got inspired by it and developed cyclodextrin-peptide hybrids bearing three functional groups; a cyclodextrin, an imidazole and a carboxylate group. This peptide hybrid is able to fold into an α-helix thanks to the main component being alanine[51] and the α-helix is further stabilized by 2

pairs of intramolecular salt bridges (combination of two non-covalent interactions) between glutamine and arginine residues[52] (scheme 11).

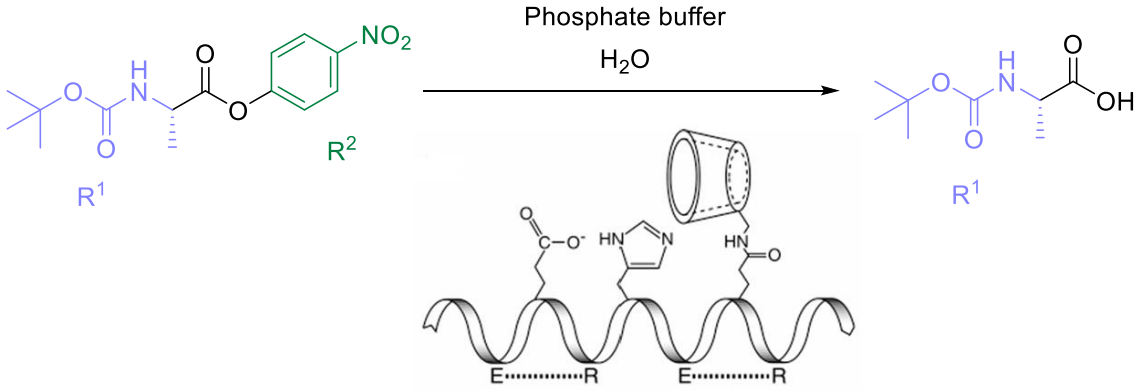

Scheme 11. Cyclodextrin-peptide hybrid developed by Ueno's group in order to catalyse hydrolysis. Adapted from [50]

They then showed that this structure was able to catalyze the hydrolysis of esters thanks to the three functional groups. Indeed, the cyclodextrin is able to bind a guest (here, the ester chain) by H-bonding in its central cavity, making this group the substrate binding site. In addition, a hydrogen bond is formed between the carboxylate group and the imidazole, enhancing the nucleophilicity of the imidazole making it a better catalyst (scheme 12)[53].

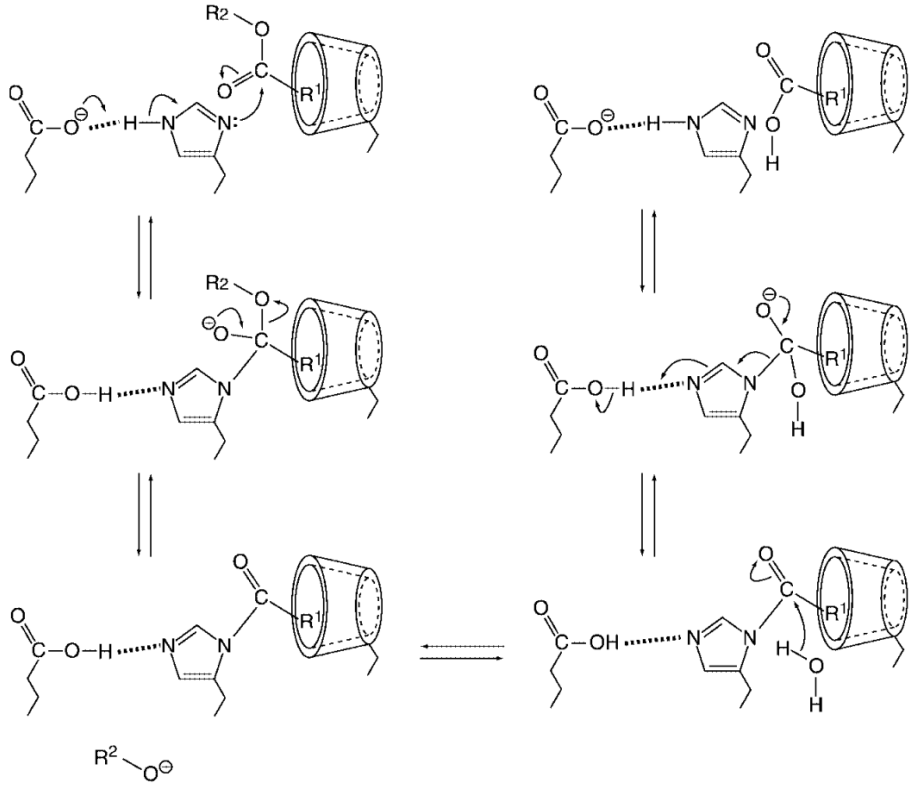

Scheme 12. Schematic representation of the mechanism for ester hydrolysis assisted by Ueno's catalyst. Printed from [50].

Aliphatic foldamers are therefore useful catalysts but they present some limitations. First, it is important to note that their secondary 3D structure is quite flexible since, as mentioned earlier, the different monomers are usually linked together by amide bonds (figure 18). In such bonds, the link C-N is well rigid and planar thanks to its partial double bond character but, on the opposite, the bonds C-C_α and N-C_α (defined by the angles of rotation Φ and Ψ) are not as rigid and can freely rotate. Therefore, the secondary structure of aliphatic foldamers is highly dependent of the different R groups[54] and small changes in the environment or in the sequence itself can easily disrupt the conformation of the foldamer.

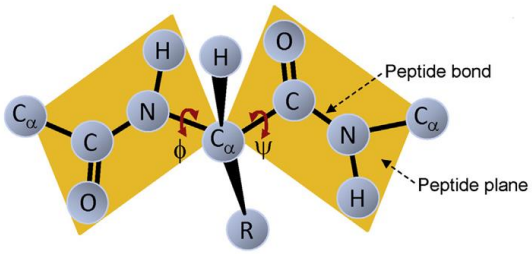

Figure 18. Representation of an amide bond with the Φ and Ψ rotation angles. Printed from [54].

Another limitation of aliphatic foldamers is that their secondary structure is primarily stabilized by hydrogen bonds between remote units (and not neighbouring units). Hence, their structure is not always predictable.

Therefore, another class of foldamers has emerged in 1994, thanks to the Hamilton group, and overcome these problems: aromatic foldamers[55].

1.2.4 Aromatic foldamers

Aromatic foldamers are similar to aliphatic foldamers with the only difference that the monomers are, in this case, aromatic and heteroaromatic units such as benzene, pyridine, quinoline and even bulkier structures such as diazaanthracene and naphtalenediimide[56] (figure 19).

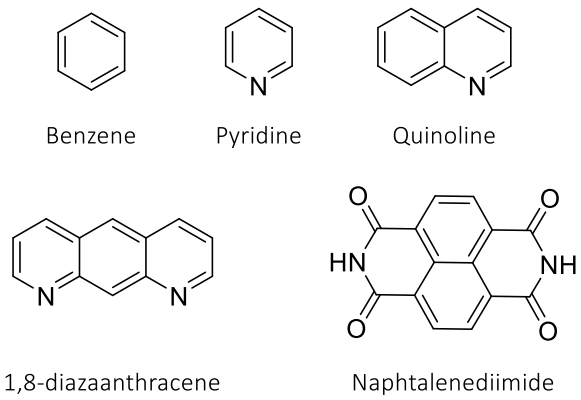

Figure 19. Some examples of aromatic monomers

As for aliphatic foldamers, the aromatic units can be linked together by amide bonds, enaminones, hydrazides or ureas. However, Aromatic Oligoamide Foldamers (AOF) are the most studied type of foldamer and are the ones that will interest us for this project.

The biggest interest in AOF is their enhanced stability thanks to the conjugation between the aromatic groups and the neighbouring amide bonds. Indeed, a minimum of energy is observed when those groups are coplanar, no matter the conformation (syn/anti)[57] and therefore, the bonds C-C_α and N-C_α cannot rotate as freely as in aliphatic foldamers, enhancing the stability of the secondary structure. Moreover, contrary to aliphatic foldamers, hydrogen bonds are formed between close units, making their structure more predictable.

More importantly, this conjugation also allows to control the conformation, syn or anti, thanks to repulsive and attractive interactions, by adding functional groups on the aromatic moieties (figure 20). For example, to favour the anti conformation, one can add a H-bond acceptor at the ortho position on the aromatic moiety to form a stabilizing H-bond with the amide proton (figure 20a). This hydrogen bond acceptor can also be endocyclic and, in this case, the H-bond allows the formation of a 5-membered ring (figure 20b). Obviously, the bond is longer and not as well oriented as in a 6-membered ring however, the anti conformation is still favoured thanks to the important steric repulsion between the amide carbonyl group and the endocyclic H-bond acceptor in the syn conformation.

On the other hand, the syn conformation will be favoured when a hydrogen bond donor is added to ortho position of the aromatic moiety (figure 20c and d). In this case, the anti conformation could theoretically also be stabilized by hydrogen bonds however, it is not favoured because the hydrogen bond is weaker than in the syn conformation thanks to either, poorer H-bond donors and acceptors (figure 20c) or a less favourable orientation (figure 20d)[58].

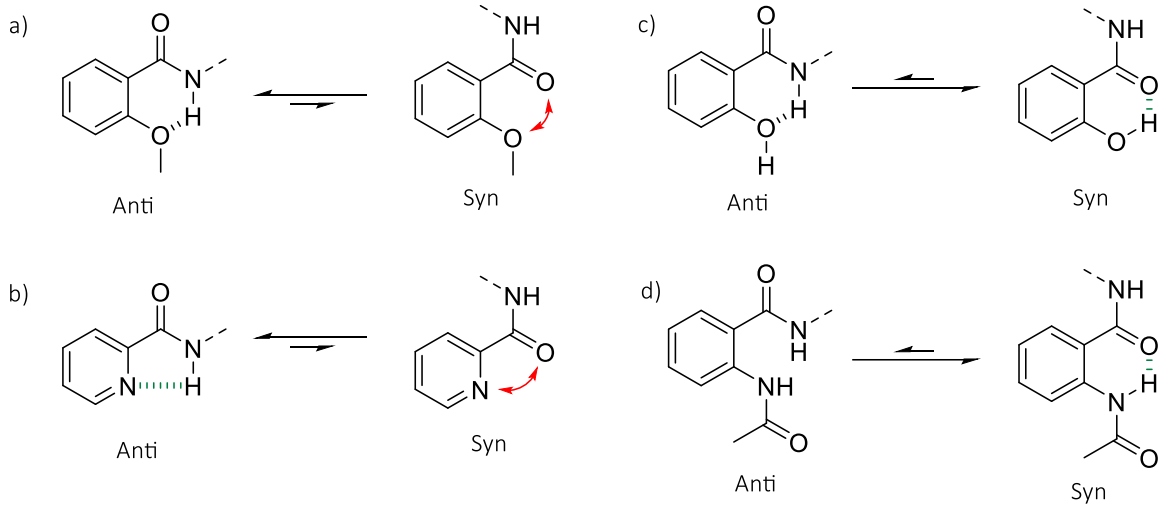

Figure 20. Conformational preferences depending on the substituents on the aryl moiety.

In a similar way, the conformation of the bond between N and C_α can also be discriminated with H-bond acceptors and donors.

Thanks to these rotational restrictions, one can accurately define the conformation that will be observed for Aromatic Oligoamide Foldamers by predicting the interactions between adjacent units. Based on this idea, AOF can be programmed to adopt various secondary structures with the simplest one being the linear conformation.

Linear aromatic foldamers

Linear aromatic foldamers can be synthesized thanks to several building blocks: anthranilic acid, bipyridine, pyrazine, picolinic acid and many more[59,60]. These linear foldamers can actually be subdivided into two categories: those with all their hydrogen bonds taking place on one side, thus presenting a facial polarity and a slight curvature (figure 21c and d), and those with their hydrogen bonds taking place on both sides of the foldamer, thus being strictly linear (figure 21a and b)[61].

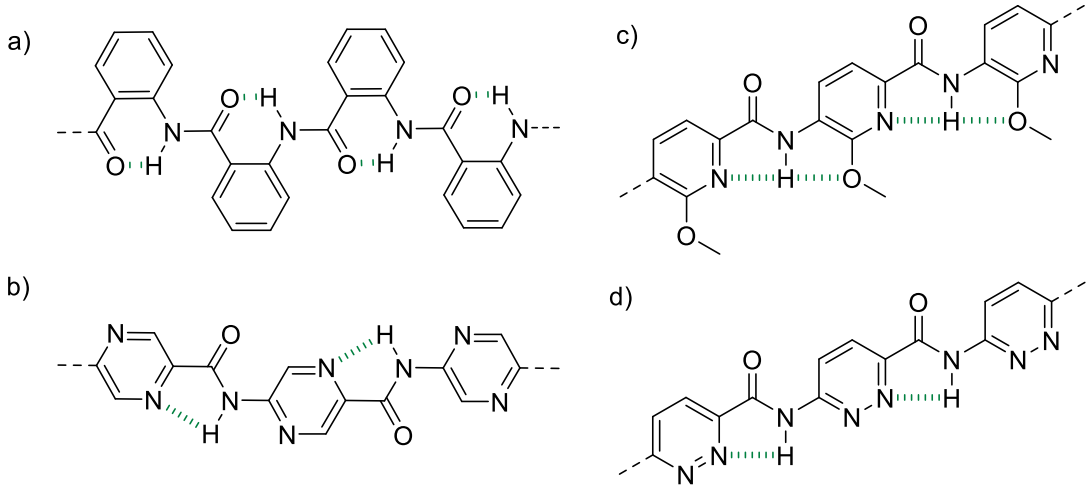

Figure 21. Examples of linear Aromatic Oligoamide Foldamers with H-bonds all on the same side (c and d) and on both sides (a and b). The aromatic unit being (a) benzene, (b) pyridine, (c) pyrazine and (d) pyridazine.

The facial polarity of linear foldamers with all their hydrogen bonds on one side can actually be exploited for different applications and, notably, for molecular recognition. Thus, for example, in 2003, the Hamilton group developed an AOF able to mimic the recognition of α-helices thanks to the distance between the side chains being similar to the distance between amino-acid residues in α-helices[61].

However, even though the linear conformation is the simplest one, the most well-studied secondary structure adopted by Aromatic Oligoamide Foldamers (and aliphatic foldamers) is the helical conformation.

Helical aromatic foldamers

When the angle between the amine and acid substituents is smaller than 180° (figure 22a), the strand will show a bending. This type of bent structure has notably been achieved by using meta-substituted, six-membered, aromatic amino-acids such as, for example, oligomers of 2,6-diaminopyridine (figure 22).

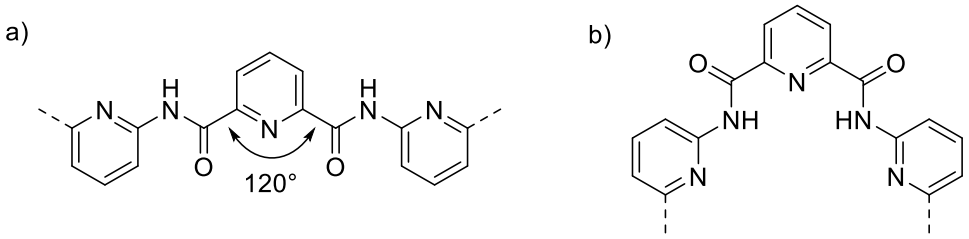

Figure 22. Both conformations of 2,6-diaminopyridine with the favoured bent structure represented on the right. The aforementioned angle between amine and acid substituents is represented on the left structure.

For short oligomers, monomers remote from each other will not be able to interact and the foldamer will develop a planar but "crescent-like" structure (figure 23).

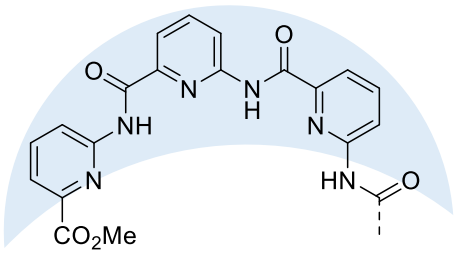

Figure 23. Representation of the crescent but planar shape adopted by short oligomers.

When the oligomer is long enough, monomers remote from each other will be able to interact and the planarity will thus be deviated, allowing the formation of helical structures (figure 24)[62,63].

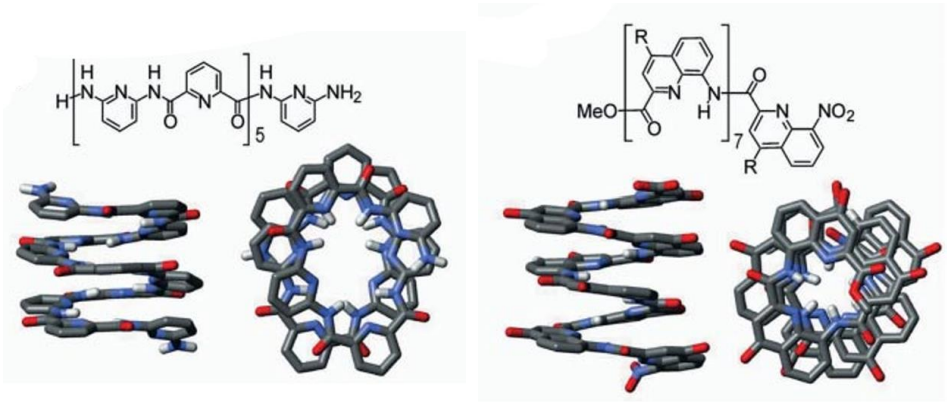

Figure 24. Solid state structure of two helical Aromatic Oligoamide Foldamers. Printed from [58].

The bending of the structure implies a partial loss of the stabilizing conjugation between aromatic and amide groups, but this energetic cost can actually be counterbalanced by π-π interactions taking place between the aromatic units once they are stacked in the helical structure.

A really interesting characteristic of these helical structures is that one can tune the diameter of the helix and the number of monomers per turn by playing with 3 parameters:

- The relative orientation between the amine and acid moieties: as demonstrated by the Gong group[64], very large diameters can be obtained by alternating para and meta substituted monomers (figure 25a) while, on the opposite, using monomers in which the amine and acid moieties define an angle of 60° can generate highly curved helices (figure 25b).

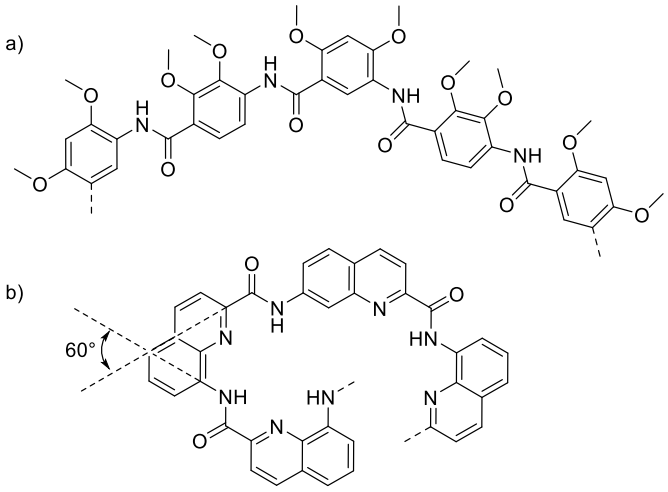

Figure 25. a) Gong's foldamer alternating para and meta substituents presenting a very large diameter and b) foldamer constituted of 60° angles between acid and amine moieties thus presenting a very hollow diameter.

- Size of the monomers: for a fixed orientation between amine and acid moieties, larger monomers form larger diameters while smaller monomers form smaller diameters (figure 26)

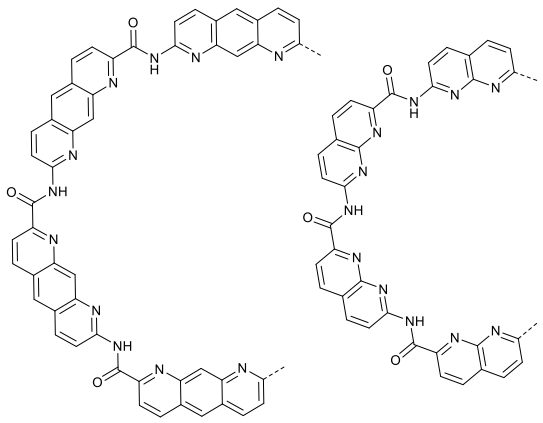

Figure 26. Influence of the monomer size on the diameter of the helix. Adapted from [58].

- Position of the hydrogen bonds: H-bonds forming on the outer rim of a helix will straighten it and increase the diameter while H-bonds forming on the inner rim of a helix will decrease the diameter of it. For example, one can take an oligomer of meta-substituted monomers with a 120° angle between amine and acid moieties. Such a structure will be composed of 6 monomers per turn but inner H-bonds will decrease the diameter to 4,5 units per turn while outer H-bonds will increase it to 8 units per turn (figure 27)

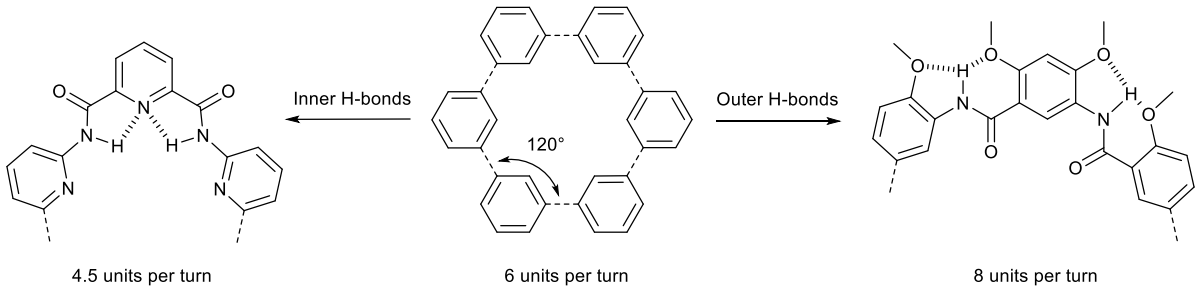

Figure 27. Influence of the position of the hydrogen bonds (outer or inner rim) on the diameter of the helix. Adapted from [58].

In addition to the stabilization of the helical structure, aromatic surfaces in an AOF can also be involved in intermolecular interactions and cause unexpected aggregation into double helices (figure 28)[65,66].

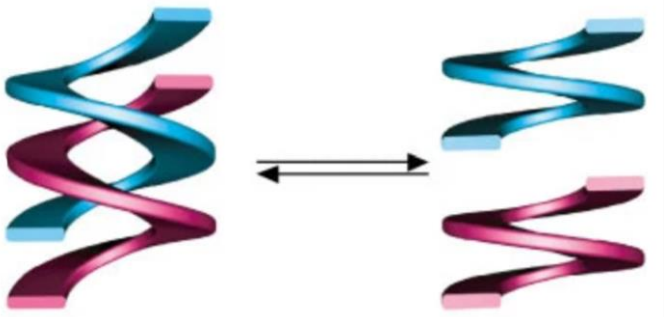

Figure 28. Equilibrium of the aggregation of two single helices into a double helix. Adapted from [65].

This aggregation is possible thanks to a slight extension of the single helices. This extension causes an even larger deviation of the planarity and a larger torsion of the amide bonds which should normally imply a destabilization of the structure. However, the energetic cost of this elongation seems to be well counterbalanced by the π-π interactions taking place between the two helices.

1.2.5 Helical aromatic foldamers as catalysts

Helical AOF have several applications in, for example, molecular recognition or even transport of a guest when their diameter is large enough to encapsulate a molecule (figure 29)[67].

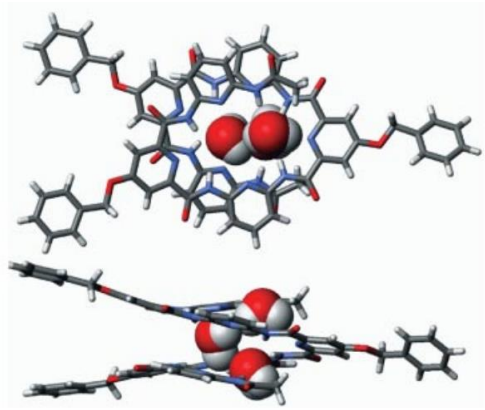

Figure 29. Crystal structure of a helical AOF with water molecules encapsulated in its cavity. Printed from [58].

However, contrary to aliphatic foldamers, there are only a few examples of helical AOF used as catalysts and one of them has been realized by Zhang and Jiang's group. They synthesized several chiral biphosphine ligands grafted on quinoline foldamers which were able to coordinate with rhodium to give chiral catalysts for hydrogenation reactions[68] (figure 30).

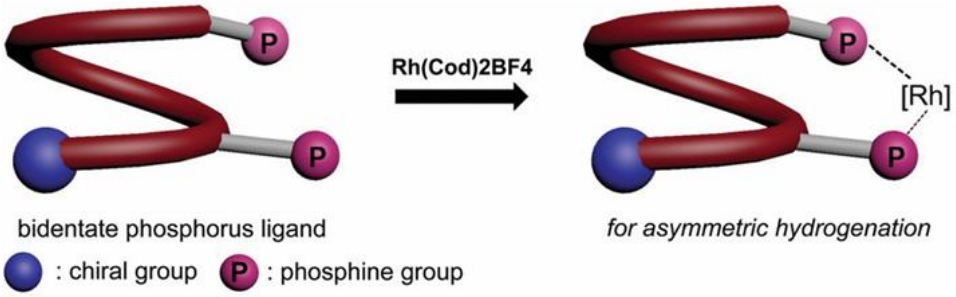

Figure 30. Zhang et Jiang's chiral catalysts based on quinoline foldamers for hydrogenation reaction. Adapted from [68].

They demonstrated that the chirality and the bulkiness of the rhodium complex formed had a great influence on the enantioselectivity of the hydrogenation reaction.

Another work was conducted by Zeng and coworkers, in 2017, on a foldamer-based organocatalyst able to catalyze the arylation between an unactivated aromatic C-H bond and an aryl iodide (scheme 13).

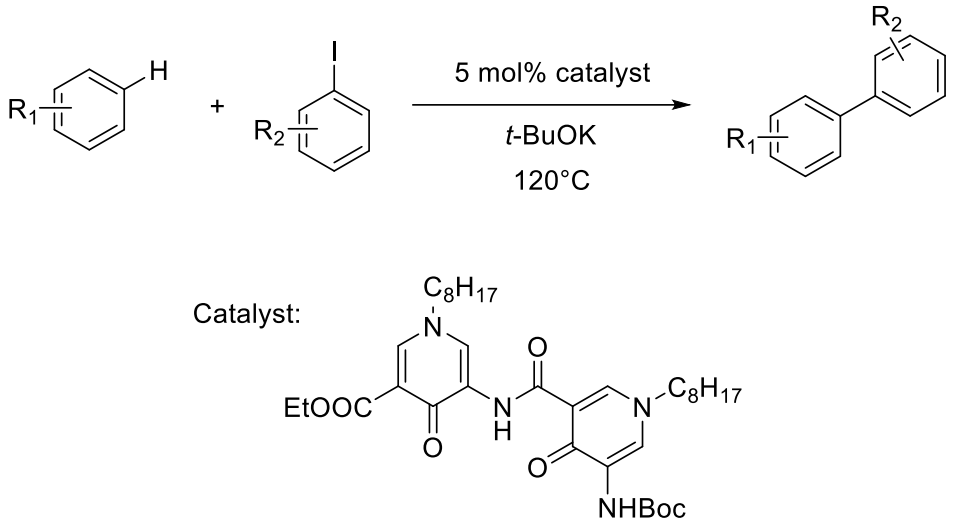

Scheme 13. Zeng's foldamer-based catalyst for an arylation reaction between unactivated aromatic CH bond and aryl iodide. Adapted from [69].

They synthesized 5 pyridone foldamers as catalysts for this reaction (monomer, dimer, trimer, tetramer and pentamer) that all give a crescent-shaped structure. All catalysts were able to give the arylation product but the dimer gave the highest yield of 96% for a catalytic loading of 5 mol%.

Even though they were not able to explain the better catalytic efficiency of the dimer, all five foldamers catalyze this reaction because they can strongly bind K^+ of the base thanks to their oxygen atoms (carbonyl) pointing towards the inside of the cavity. Indeed, when the same reaction was attempted with other bases, such as *t*-BuONa or *t*-BuOLi, no product was obtained because the catalysts cannot bind Na^+ and Li^+ as strongly as K^+.[69]

These two examples show that helical AOF can be used as efficient catalysts thanks to their different properties. Indeed, when compared to aliphatic foldamers, they present an increased stability, a more predictable structure and moreover, their helical structure allows the interaction between remote functional groups. For all these features, such supramolecular structures were chosen as the modular scaffold to control the environment around our PLP-mimic and thus, its reactivity.

1.3 Previous work

This project is not at its beginning and has already been started one year ago by another member of the group. Therefore, it is important to cover what has already been investigated last year before entering in what was studied in this master's thesis.

The very first step of the project consisted in designing and synthesizing our own PLP-mimic and this step was successfully achieved last year[70] (figure 31).

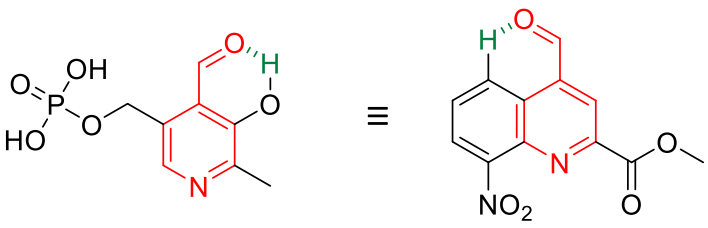

Natural PLP Our PLP-mimic

Figure 31. Our PLP-mimic (right) compared to natural PLP (left).

One can note that our PLP-mimic is not an exact replica of the natural PLP but this is easily explained by the fact that the π-deficient system and the aldehyde group of PLP are the two most important groups for its reactivity. Therefore, the design of this PLP-mimic was not randomly chosen but was thoroughly thought out based on the structure of the foldamer we will use to control the environment around the mimic. Indeed, for diverse reasons that will be explained in the next section (objectives), the sequence of monomers we are using to build our foldamers is the quinoline-quinoline-pyridine sequence (QQP). As both monomers of this sequence are already π-deficient, we simply aimed at modifying one of them to include an aldehyde group.

If we chose the quinoline moiety to be modified, instead of the pyridine one, it is because of the possible hydrogen bond between the oxygen of the aldehyde and the hydrogen in position para of the nitro group. Indeed, we hope that this nitro group will be electron-withdrawing enough for the proton in position para to be a suitable H-bond donor. By this hydrogen bond, as in the natural PLP, we aim at slowing the rotation of the aldehyde to enhance the electron delocalization since the π-orbitals in formation will then be greatly aligned with the π-orbitals of the quinoline ring.

The reactivity of our PLP-mimic alone was also investigated last year since one of the crucial parts of this project is to determine if our PLP-mimic can show a similar reactivity to the natural PLP. Therefore, they first tested the ability of our mimic to form the important imine species with an amine substrate, here, benzylamine (scheme 14). By monitoring the reaction, they observed the formation of this new species in 4 hours.

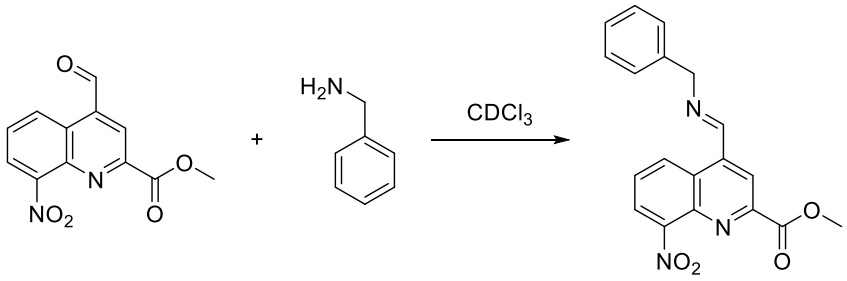

Scheme 14. Imine condensation between our PLP-mimic and benzylamine.

They then investigated the ability of the mimic to act as a catalyst in a transamination reaction (scheme 15).

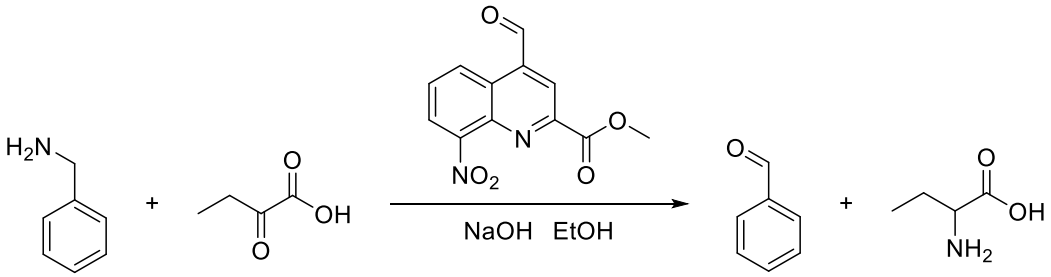

Scheme 15. Catalytic transamination.

This reaction was investigated by adding NaOH to a solution of benzylamine in the presence of a sacrificial ketone, useful to regenerate the catalyst (explained in more detail in section 3.3). This experiment was tried several times with varying equivalents of benzylamine and sacrificial ketone in order to determine the optimal loading of the catalyst. It was finally established that a catalytic loading of 10 mol% gives a yield of 28%, proving that our PLP-mimic, by itself, allows the catalysis of a transamination reaction.

2 Objectives

As described above, Pyridoxal Phosphate has been at the heart of many studies thanks to its interesting versatility, and lots of different PLP-like molecules have already been synthesized. However, one of the biggest challenges of these PLP-mimics is that, as demonstrated in section 1.2.3, their reactivity/selectivity is highly dependent of their environment. Therefore, some groups have already tried to incorporate a PLP-mimic into a supramolecular structure to improve its catalytic efficiency. However, in most cases, the structures used can offer a general environment but are limited in being able to design specific interactions. In this work*, we will aim at incorporating a PLP-mimic into supramolecular structures called Aromatic Oligoamide Foldamers in order to control its environment and thus, its selectivity and reactivity*. As described in the introduction, these AOF have been extensively studied and have shown the interesting ability to adopt specific 3D secondary structures for organizing cooperative functional groups, making them highly interesting for controlling the local environment around PLP-mimic.

This project will be divided into two principal objectives: synthesis and reactivity assays.

2.1 Objective 1: Synthesis

2.1.1 Monomer synthesis

Starting from the previously synthesized PLP-mimic described in section 1.3, the following step is to incorporate it into different Aromatic Oligoamide Foldamers. Therefore, we must first synthesize the different monomers composing it. These monomers can be classified into two groups; reactive monomers containing the PLP-mimic motif and structural monomers which constitute the rest of the oligomers (figure 32).

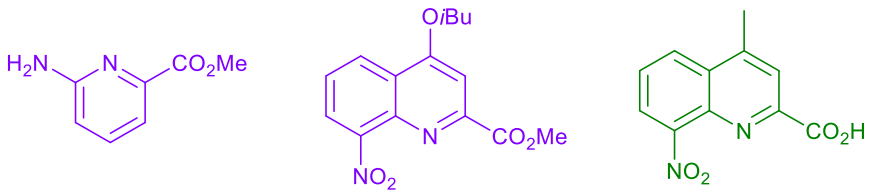

Figure 32. Monomers used in the synthesis of the different foldamers of this project. Structural monomers are represented in purple and the reactive monomer is represented in green.

As can be seen on figure 32, the reactive monomer does not bear the aldehyde function characteristic of the PLP motif. The reason is that, in the reaction allowing the coupling of the different monomers, the aldehyde moiety of the PLP-mimic can react with amine groups to

form undesirable products. Therefore, the preferred strategy in this work will consist in the direct functionalization of the oligomers by oxidizing the methyl position of the reactive moiety. Such strategy will allow us to synthesize different foldamers bearing our mimic by avoiding additional protection and deprotection steps of the aldehyde group.

2.1.2 Oligomer synthesis

Within the framework of this project, we chose the sequence "quinoline-quinoline-pyridine" (QQP) for our foldamers by getting inspired by the work of Huc's group. Indeed, the Huc group studied a foldamer composed of quinolines only that exhibits 2.5 monomers per turn which allows the stacking of the side chains only every two turns[64]. Such stacking results in a distance too important between the side chains to control the direct environment of our PLP-mimic. Therefore, we slightly modified Huc's sequence by exchanging a quinoline moiety with a pyridine unit in order for this QQP foldamer to exhibit 3 monomers per turn. Doing so allows the stacking of the side chains on the same face every turn and makes it possible to control the direct environment around our PLP-mimic. The stacking of the side chains and the structure of the two foldamers are compared on figure 33.

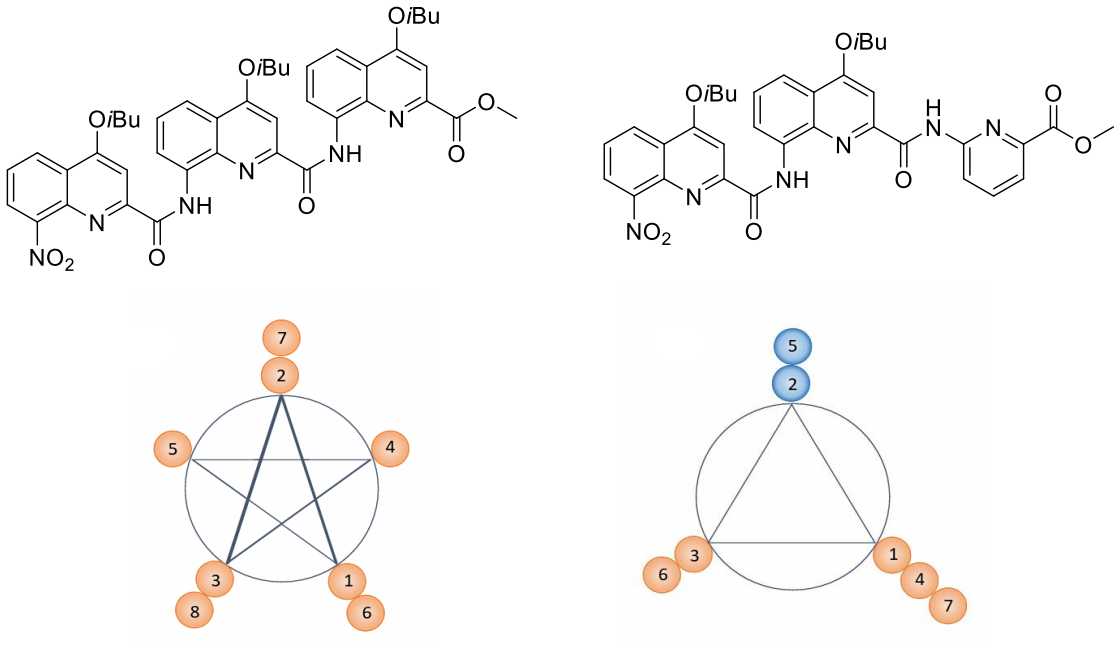

Figure 33. Structure of Huc's foldamer (above left) and our QQP sequence (above right) and comparison of the stacking of the side chains (below). Orange balls represent quinoline residues and blue balls represent pyridine residues.

This QQP sequence has already been synthesized by our group up to a heptamer and was further characterized to show the desired property of folding into a helix[71]. Moreover, as

can be seen on the crystal structure of this heptamer (figure 34), the characterization confirmed the alignment of the side chains every turn, as desired.

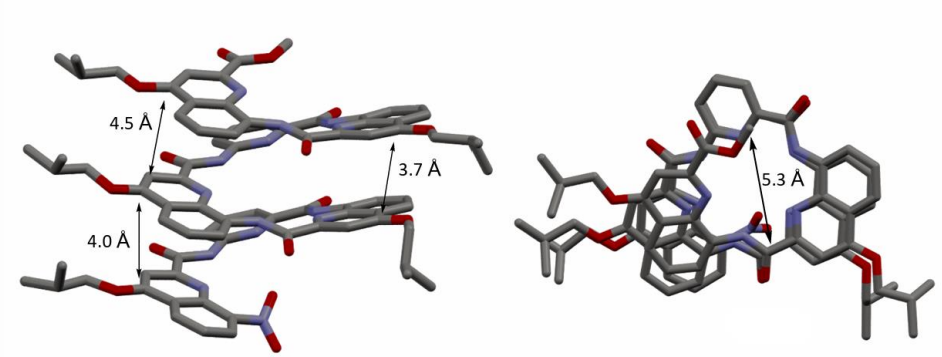

Figure 34. Side view (left) and top view (right) of the crystal structure of the QQP heptamer previously synthesized by our group.

Therefore, *the first objective of my master's thesis consists in the incorporation of our PLP-mimic into this QQP sequence by exchanging a structural quinoline monomer for a reactive quinoline monomer containing the pyridoxal motif.* Several foldamers must be synthesized by changing the length of the foldamer (trimers, hexamers…) and the position of the PLP-mimic in it. However, in this thesis, the main focus will be on the synthesis of a trimer sequence with the aldehyde containing monomer in first position (Q*QP sequence where Q* is the aldehyde containing monomer).

2.2 Objective 2: Reactivity assays

Once this trimer is synthesized, the next step is to study its reactivity since the incorporation of the PLP-mimic into a foldamer tunes the environment around it which must result in a change in the reactivity.

To do so, similarly than for the monomer, the ability of the trimeric PLP-mimic to catalyze a transamination reaction will be investigated. However, beforehand, the conditions used to investigate this reaction will be screened through changing the base, the solvent and the sacrificial ketone to optimize this reaction. These conditions will then be used to extend the study of the reactivity to the trimeric catalyst and compare it with the reactivity obtained for the monomeric catalyst.

Therefore, *the second objective of my master's thesis consists in the study of the reactivity of the trimeric PLP-mimic versus the monomeric one towards a transamination reaction in order to determine how the change in environment affects the reactivity.*

3 Results and discussion

This section can be divided into three parts. The first one will detail the strategy of synthesis that will be used to synthesize the different oligomers. Then, the synthesis of the different building blocks and the problems encountered during this synthesis will be detailed. This second part will be further divided into 2 subgroups; monomer and oligomer synthesis. Finally, the third part will focus on the reactivity assays.

3.1 Strategy of synthesis

Oligomer synthesis relies on a combinatorial approach in which we can combine different compounds in order to generate a large chemical library[72]. Such an approach is used to minimize the number of steps in the synthesis of long oligomers but also to rapidly optimize the properties of these oligomers by easily combining many different units.

Here, the idea of the strategy is to first synthesize the different monomers required in the synthesis of our oligomers. There are three of them that will be needed to synthesize our trimer (M, Q and P on figure 35). Then, a large quantity of the dimer will be synthesized by combining the pyridine (P) and the quinoline isobutoxy (Q) monomers. Finally, this dimer can be coupled with diverse monomers, notably with the precursor of the PLP-mimic, in order to obtain trimers. Different trimers can later be combined with each other to yield hexamers. This can allow us to generate a library of trimers and hexamers quickly (figure 35).

All of these monomers are assembled together thanks to coupling reactions. There exist many types of coupling reactions but, in this case, the different monomers are coupled by amide coupling which requires the reaction between an amine compound and an activated carboxylic acid[73]. Therefore, in this project, each monomer is bearing nitro and ester functions in order to be protected towards amide coupling but these functions must be first deprotected into amine and carboxylic acid groups prior to the coupling reactions.

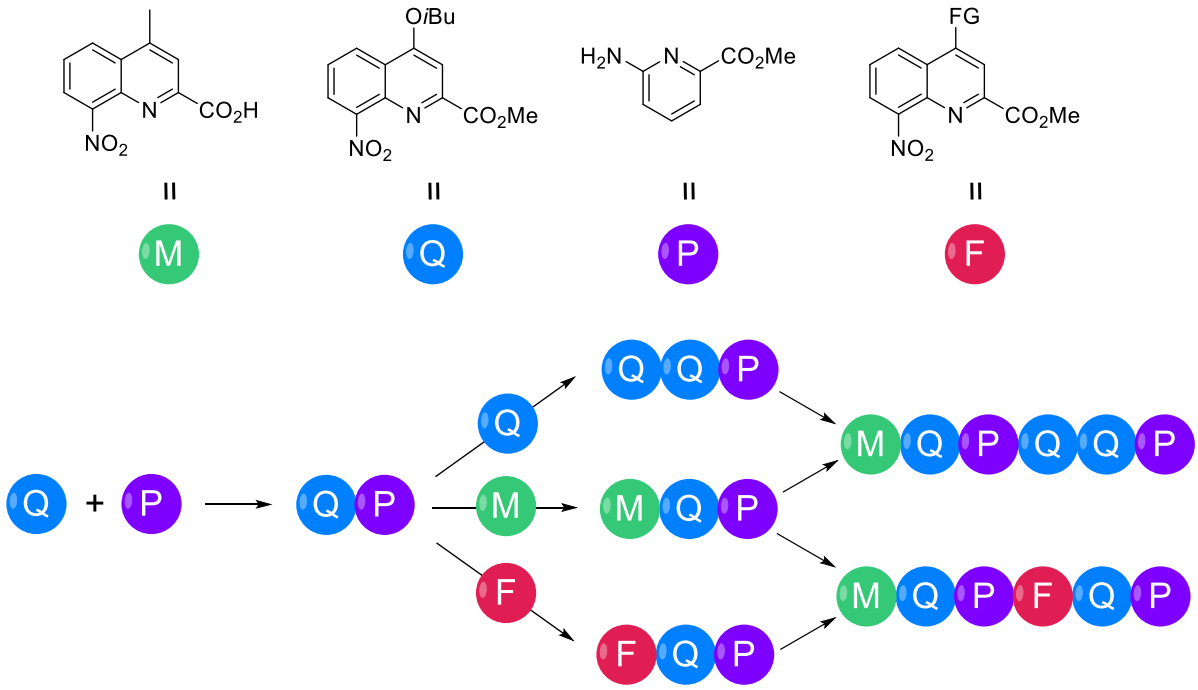

Figure 35. Schematic representation of the combinatory method for the synthesis of the different oligomers. Each monomer is represented by a coloured ball (FG being a functional group such as a basic side chain).

First, ester groups will be saponified into the corresponding carboxylic acids. However, carboxylic acids are not very reactive species and thus, they need to be further activated. This can be realized either with coupling reagents such as HATU, EDC.HCl, DCC or by transforming carboxylic acids into reactive derivatives such as acid chlorides or anhydrides[74]. In this project, it is the second method, the activation into an acid chloride, that will be used. Secondly, nitro groups will be reduced into amine groups. This will be realized thanks to hydrogen and palladium on carbon.

3.2 Synthesis of monomers

The initial objective of this work consists in the synthesis of the three main building blocks of the sequence QQP (figure 36) which will be later assembled to develop the different AOFs. Even if these building blocks seem simple, some challenges were encountered during their synthesis and emphasis will be put on those aspects.

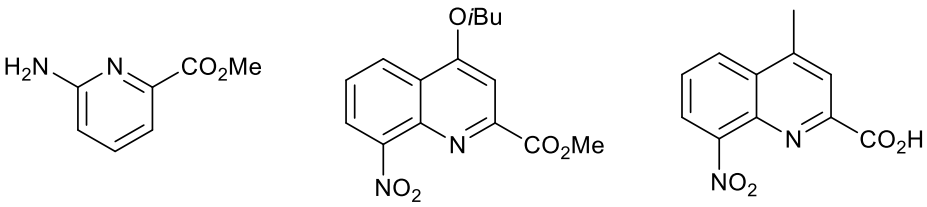

Figure 36. Structure of the three building blocks of the sequence QQP.

3.2.1 Pyridine monomer

The first monomer to be synthesized was the pyridine monomer. This synthesis was quite simple and straightforward since, starting from the commercial substrate *6-aminopicolinic acid* ***1.1***, only an esterification step was realized to yield the desired *pyridine monomer* ***1.2*** (scheme 16). This step is essential to protect the carboxylic acid for further coupling of the monomers.

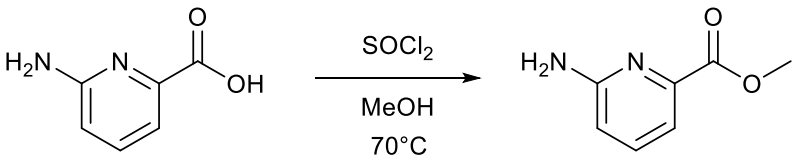

1.1 1.2

Scheme 16. Esterification reaction by thionyl chloride activation.

Usually, putting a carboxylic acid in presence of $SOCl_2$ results in the formation of an acid chloride that can then be followed by a nucleophilic attack. However, in this case, the solvent (methanol) acts as a nucleophile and is added simultaneously with $SOCl_2$. Therefore, in these conditions, $SOCl_2$ will rather react with MeOH to produce anhydrous HCl that will then be able to realize a well-known Fischer esterification[75]. Anhydrous conditions are preferred for a Fischer esterification in order to drive the reaction towards the formation of the ester.

This reaction was realized twice; the first time, with only two equivalents of $SOCl_2$, gave a yield of 52% while the second time, with five equivalents of $SOCl_2$, gave a yield of 82%. Indeed, as the reaction is not realized under anhydrous conditions and that water is formed during the esterification, a part of $SOCl_2$ is neutralized and thus, the reaction requires larger amounts of thionyl chloride. Moreover, larger amounts of HCl (and thus, $SOCl_2$) are required since HCl is also used to protonate the pyridine nitrogen in these conditions.

3.2.2 Isobutoxy quinoline monomer

Then, in the sequence QQP, two different quinoline moieties needed to be synthesized; one bearing a side chain useful for the solubility of the trimer (here, an isobutoxy side chain) and one bearing the precursor of the aldehyde function (the PLP-mimic). Therefore, the second monomer to be synthesized was this isobutoxy quinoline monomer:

I. Synthesis of the quinolinone intermediate

Starting from the commercial reagent *2-nitroaniline* ***1.3***, the quinolinone intermediate was synthesized in two steps; a Michael addition onto DMAD followed by a thermocyclization with polyphosphoric acid (scheme 17).

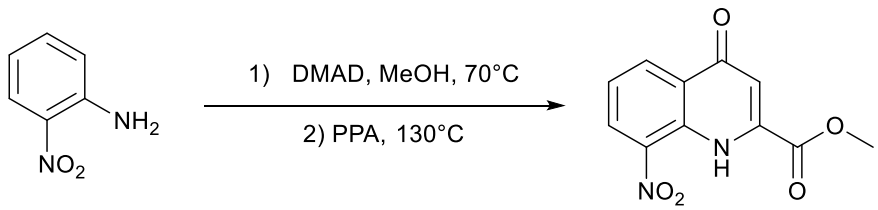

1.3 1.4

Scheme 17. Quinolinone intermediate synthesis.

In the first step, the amine moiety is sufficiently nucleophilic to attack the sp carbon of DMAD which is itself electrophilic enough thanks to the electron-withdrawing ester groups on both of its ends.

The second step consists in a thermocyclization in presence of polyphosphoric acid which is a strong acid that can protonate the oxygen of the carbonyl to make it more electrophilic (scheme 18). This cyclization corresponds to an electrophilic aromatic substitution where the aromatic cycle plays the role of the nucleophile that attacks an electrophilic carbonyl center to finally yield the *quinolinone intermediate* ***1.4***. The formation of the fumarate (red

species) was confirmed by ^{1}H-NMR with the appearance of a signal at 5,84 ppm integrating for one proton corresponding to the proton of the double bond.

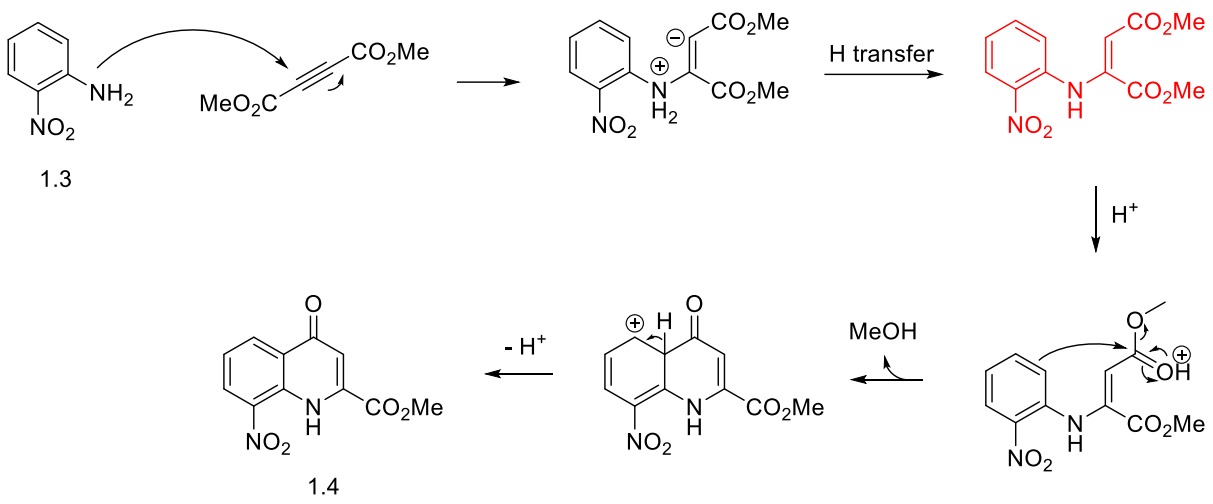

Scheme 18. Mechanism for the quinolinone formation (nucleophilic attack on DMAD followed by a thermocyclization). The stereochemistry of the fumarate has been inverted for ease of representation.

This quinolinone synthesis was only realized once during my master's thesis. However, I only performed the first step of the sequence (with a yield of 43% due to external factors such as probe dysfunction) since this quinolinone intermediate was already available in the laboratory. This first step was performed on large scale (50 g) to ensure large quantities of this quinolinone intermediate since it is the precursor of all the quinoline derivatives targeted in this project. Indeed, this intermediate will then be modified either by O-alkylation or by substitution of the 4-position to yield the two quinoline monomers of the sequence QQP.

II. Mitsunobu reaction

Once the *quinolinone intermediate* ***1.4*** was synthesized, one last step was remaining to obtain the *isobutoxy quinoline monomer* ***1.5***; a Mitsunobu reaction (scheme 19).

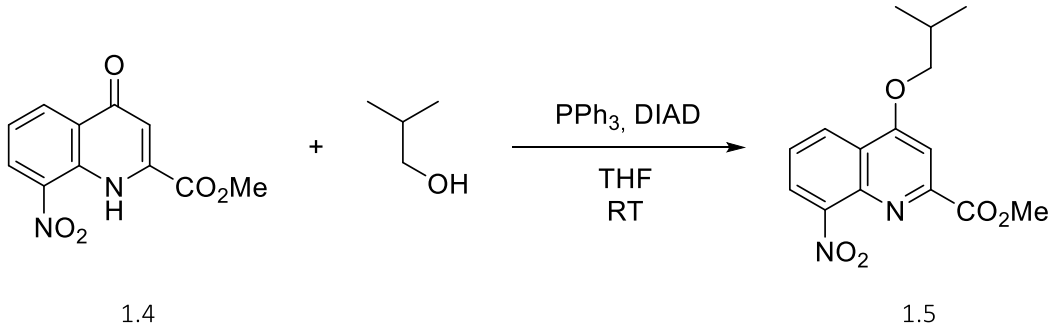

Scheme 19. Mitsunobu reaction to afford the isobutoxy quinoline monomer.

The mechanism of this reaction has been widely studied and, even though it is still debated, the current accepted mechanism is outlined in scheme 20[76]. As can be seen on this mechanism, the betaine (species formed by the reaction between DIAD and PPh_3) deprotonates the nitrogen of the quinolinone intermediate, which plays the role of the acidic nucleophile, allowing the formation of the quinoline species. A subsequent attack of the negatively charged oxygen of the quinoline on the carbon of the isobutanol (made more electrophilic thanks to the bond with PPh_3) allows the formation of the desired *isobutoxy quinoline monomer* ***1.5***.

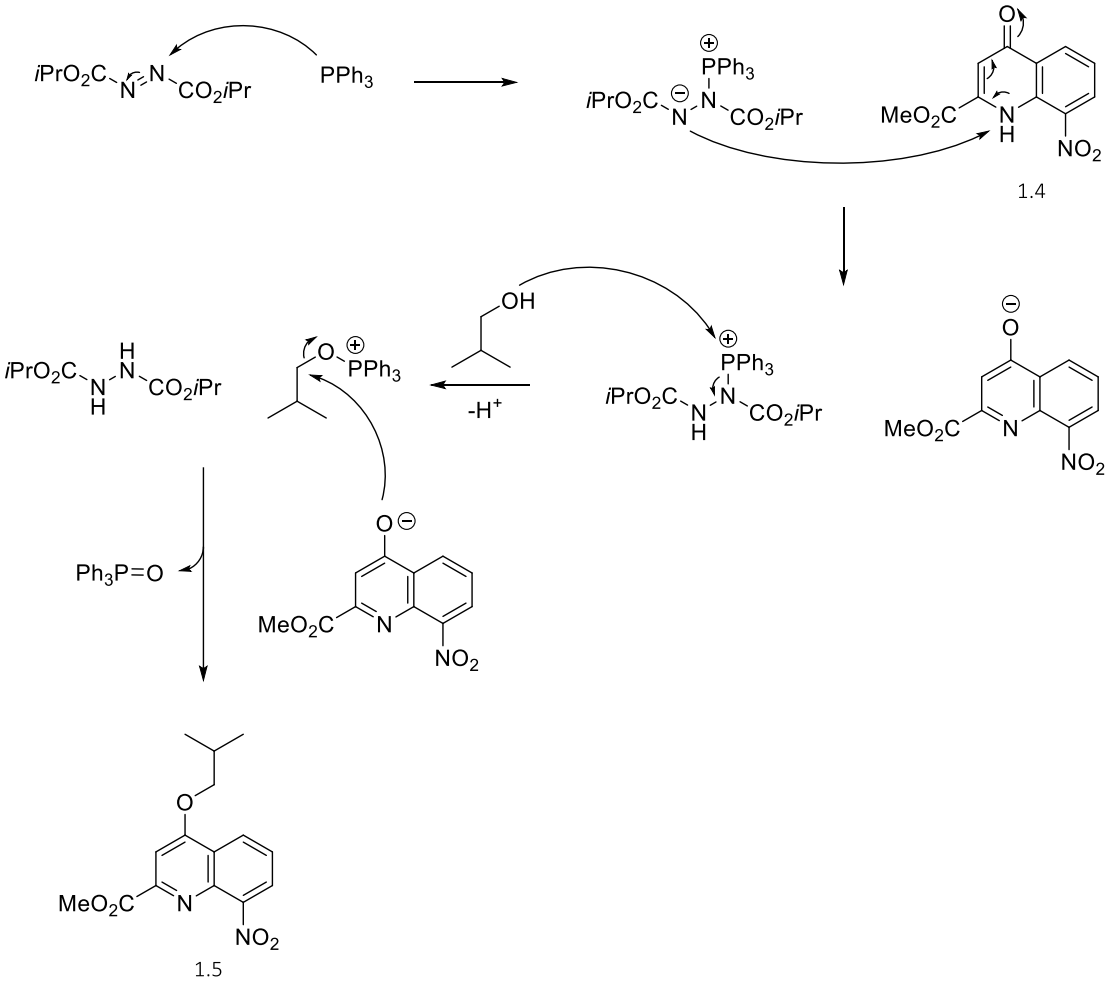

Scheme 20. Mechanism of the Mitsunobu reaction to afford the isobutoxy quinoline monomer.

At first, as previously reported by the group, the reaction was let to run for 3 hours but did not reach completion as showed by a comparative TLC between the quinolinone intermediate and the reaction mixture. This was maybe due to the presence of water that can interfere with the reaction. Therefore, an additional 0,2 equivalent of isobutanol, DIAD and PPh_3 were added and the reaction was let to run for 18 hours to finally afford the *isobutoxy*

quinoline monomer ***1.5*** with yields ranging from 77% to 87% after a recrystallisation in MeOH/$CHCl_3$. In the future, to prevent this problem, the reaction must be directly run with higher equivalents of these reagents. The ^1H NMR spectrum before recrystallisation indeed showed that no more quinolinone intermediate was present in the medium, by comparing with the ^1H NMR spectrum of this intermediate. However, there were still a lot of impurities due to the larger equivalents of PPh_3, isobutanol and DIAD that were introduced. After recrystallisation, the formation of the product **1.5** was finally demonstrated by ^1H NMR spectroscopy that displayed no other signals than the product as well as a small signal for water.

3.2.3 Methyl quinoline monomer

The last monomer to be synthesized was the one that will finally bear the aldehyde function and therefore, the one that will finally be modified into the PLP-mimic. There are (at least) two ways to synthesize our trimer bearing a PLP-mimic unit. On one hand, the oxidation step affording the PLP-mimic can be realized on the methyl monomeric unit to afford the monomeric PLP-mimic which can then be directly coupled to a dimeric unit. On the other hand, this methyl monomeric unit can be coupled to the dimeric unit and the oxidation step would take place on the trimer. However, as briefly explained in the objectives, the PLP-mimic as a monomer could not be directly coupled with other monomers since, during coupling reactions, the aldehyde function of the PLP-mimic was able to react with the amine function of other monomers to give an imine species. Therefore, the second approach was preferred and we synthesized a quinoline monomer bearing a methyl function in order for it to be oxidized once incorporated into an oligomer to give the PLP-mimic.

This last monomer was synthesized in three steps starting from the *quinoline intermediate* ***1.4*** for which the synthesis has already been described above (scheme 18).

I. Chlorination

Starting from the *quinolinone intermediate* ***1.4***, the first step in the synthesis of the desired monomer consisted in the chlorination of the carbon in para position of the nitrogen to yield a *chlorinated intermediate* ***1.6*** (scheme 21).

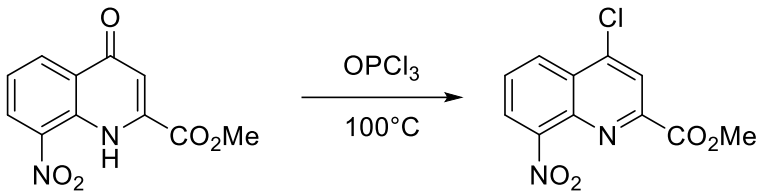

1.4 1.6

Scheme 21. Chlorination reaction

This type of reaction has been widely used to replace a large variety of functional groups (alcohol, enol, CH groups and more) [77]. The phosphorus compound used here, $OPCl_3$, is preferred by our laboratory for safety reasons but can be replaced by PCl_5, another well-known chlorinating agent.

The ^1H NMR spectrum of the product being quite similar to the one of the reagent in terms of multiplicity and integration, the two NMR spectra had to be compared in order to see if a change in the chemical shift was observed as a result of the substitution of the oxo group with a chlorine atom. Indeed, a downfield shift of all the aromatic protons were observed due to the electron-withdrawing ability of the chlorine atom (figure 37). Therefore, the *chlorinated intermediate* ***1.6*** was obtained with a really good yield of 95% and with a good purity, as displayed by the ^1H NMR spectrum that shows no other signals than the ones corresponding to the product (and water).

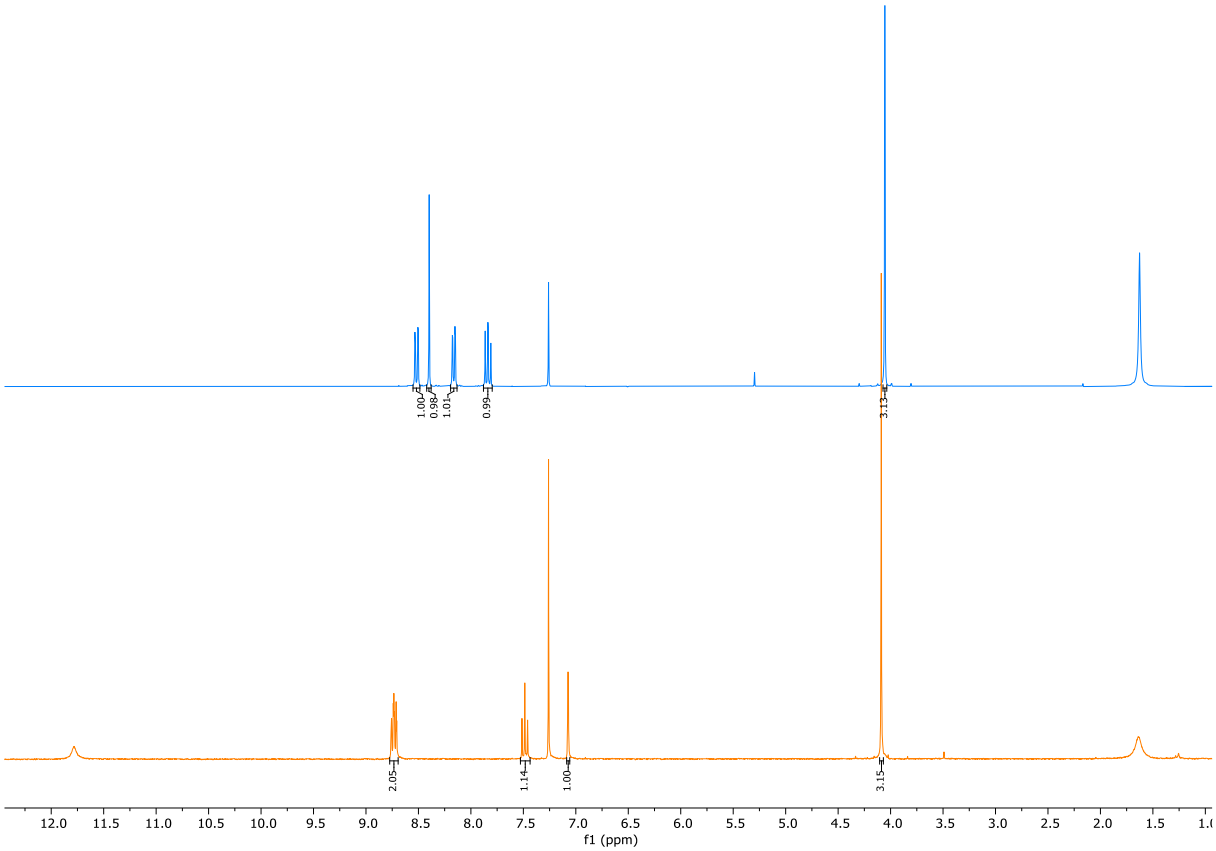

Figure 37. Comparison of ^{1}H NMR spectra between the quinolinone intermediate 1.4 (orange) and the chlorinated intermediate 1.6 (blue).

II. Nucleophilic aromatic substitution

The next step of this synthesis consisted in a nucleophilic aromatic substitution in which a nucleophilic species, diethylmalonate, attacks the aromatic core that is electron deficient (scheme 22).

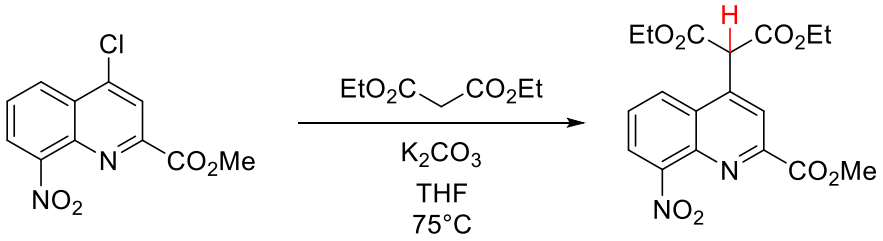

1.6 1.7

Scheme 22. Nucleophilic aromatic substitution.

The mechanism of the reaction, stepwise or concerted, is quite debated and different recent studies are emerging to try to bring evidence of a concerted mechanism[78]. However, a two-steps mechanism (addition-elimination), similar to the one of the chlorination step, has been postulated by Bunnett in 1951 and is currently accepted[79,80].

Such an addition-elimination mechanism is possible thanks to two important features. First, the aromatic ring needs to be electron deficient enough with an electron-withdrawing group in position ortho or para of the leaving group in order to stabilize the Meisenheimer complex that is formed in the first addition step of the mechanism. Here, the nitrogen of the quinoline species plays that role. Secondly, the reaction requires a good leaving group as, in this case, a chlorine atom.

At first, as previously reported by the group, the reaction was let to run for 18 hours but a first ^{1}H NMR spectrum showed that the reaction was far from finished. Indeed, the product was forming because of a signal appearing at 5,35 ppm corresponding to the red proton on scheme 22 however, there was still 3 times more of the chlorinated intermediate. Therefore, the reaction was let to run for 18 hours again to finally afford the pure product **1.7** with a quite good yield of 74%.

III. Decarboxylation

The last step in the synthesis of the *methyl quinoline monomer **1.8*** consisted in the reaction of *compound **1.7*** in an acidic environment while heating (scheme 23).

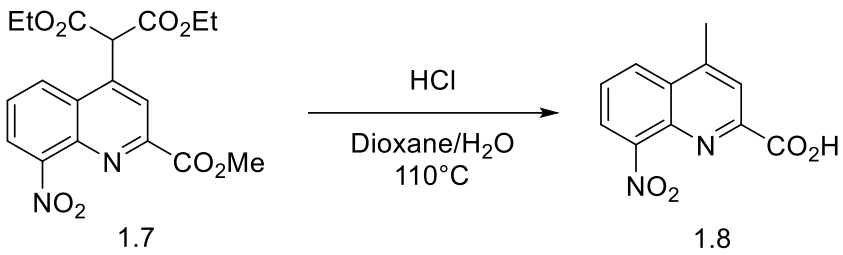

Scheme 23. Last step in the formation of the methyl quinoline monomer (hydrolysis and decarboxylation)

Two important things are happening in this last step. First, the acidic environment allows the hydrolysis of every ester group on compound **1.7**, thus forming three carboxylic acids. Then, heating allows decarboxylation of the two carboxylic acids derived from diethylmalonate to form the *desired monomer **1.8*** (scheme 24). As can be seen in the mechanism, the first decarboxylation is concerted and passes through a cyclic transition state[81]. Moreover, this first decarboxylation actually does not require the assistance of the π-deficient ring and can thus happen with any malonate species. However, the second decarboxylation cannot happen with any carboxylic acid since it requires the delocalization of the electrons into the quinoline ring.

When realized, this reaction gave a low yield of 23%. Indeed, the compound is sensitive to acidic conditions and heat and an extended reaction time led to substantial degradation.

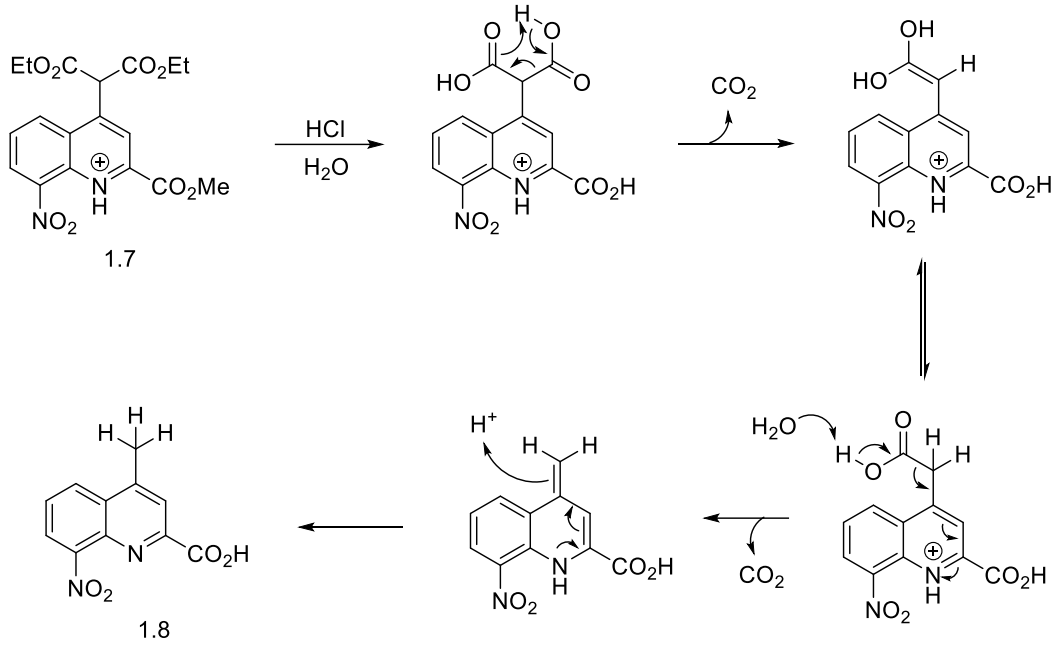

Scheme 24. Mechanism of the decarboxylation reaction.

Now that the three monomers were synthesized (*compounds **1.2**, **1.5** and **1.8***), they needed to be assembled in order to synthesize the different trimers:

3.3 Synthesis of oligomers

3.3.1 Dimer synthesis

I. Activation of the monomer

In order to synthesize the dimer, the *isobutoxy quinoline monomer **1.5***, bearing an ester function, was first hydrolyzed into the corresponding *carboxylic acid **2.1***. Then, this carboxylic acid was transformed into a reactive *acid chloride **2.2*** by using thionyl chloride $SOCl_2$ (scheme 25).

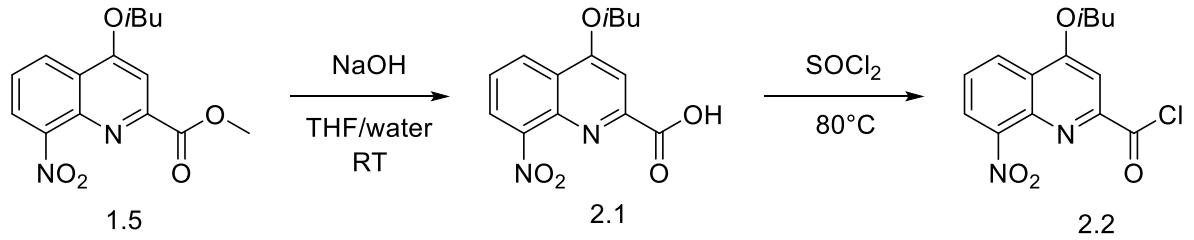

Scheme 25. Hydrolysis of the ester and activation of the resulting carboxylic acid into an acid chloride.

The basic hydrolysis of an ester is preferred to the acid one since it presents diverse advantages such as an irreversible reaction whereas an equilibrium is reached for the acidic hydrolysis[82]. The first time this reaction was realized, the solvent consisted in a mixture of THF/MeOH (2:1) but no reaction was observed after 5 hours. Indeed, the solution turned into a gel and no reaction could happen. Some water was added and the mixture was heated at 40°C for two days to get rid of this gel. After this observation, all the next saponification reactions were run into a solvent mixture of THF/water (2:1) and, as confirmed by ^{1}H NMR spectroscopy, the signal corresponding to the methyl group of the ester disappeared to only yield the pure *carboxylic acid* ***2.1*** with quantitative yields in only 3 to 4 hours.

Concerning the formation of the acid chloride, it can be prepared with different reagents such as thionyl chloride, oxalyl chloride $(COCl)_2$, phosphorus oxychloride $POCl_3$, phosphorus trichloride PCl_3 and phosphorus pentachloride PCl_5[83]. However, thionyl chloride and oxalyl chloride are the most common low-cost chlorinating agents and therefore, $SOCl_2$ was used. The obtained compound being highly reactive, it tends to decompose towards moisture and thus, precautions must be taken. First, the only work-up that is required is the evaporation of $SOCl_2$ with dry toluene since the acid chloride must be rapidly put under vacuum after synthesis to prevent its decomposition. Secondly, the product must be used within a few hours following its synthesis. Finally, ^{1}H NMR spectroscopy of the compound has been realized only the first time it was synthesized and showed the formation of the product in only 3 hours but the purity of the product was not confirmed every time it was synthesized. Moreover, for every step involving this chlorination reaction, the acid chloride was directly used in the next step and thus, the yield was assumed to be 100%.

II. Amide coupling

The next step in the synthesis of the dimer was the amide coupling between the *acid chloride* ***2.2*** and the *pyridine monomer* ***1.2*** (scheme 26).

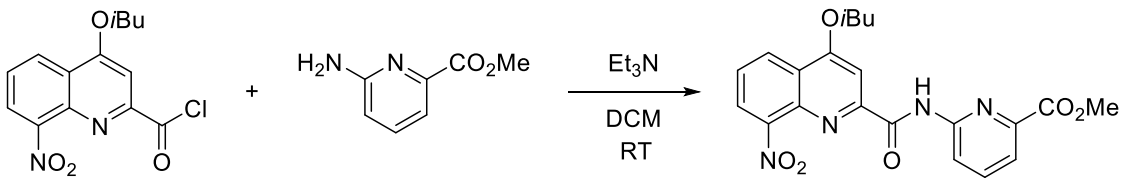

2.2 1.2 2.3

Scheme 26. Coupling reaction between the pyridine monomer and the *acid chloride to yield the* dimer.

In this coupling reaction, an excess of base (Et_3N) was needed since triethylamine has two roles. First, it is required as a catalyst that attacks the reactive acid chloride to yield an even more reactive intermediate that can then be attacked by the nucleophilic species. Secondly, it is also required as a base to prevent the formation of HCl which should be released during the reaction and which should convert the amine into an less reactive HCl salt[88].

The formation and purity of the product **2.3** was proven by ^1H NMR spectroscopy with the appearance of a signal at 10.56 ppm which corresponds to the proton of the amide bond. However, concerning the purity, the first time this coupling was realized, a simple recrystallisation in MeOH was required to yield a pure product. On the contrary, the other attempts of synthesis of the dimer gave mixtures of products that were harder to purify. Indeed, acidic and basic extractions, as well as recrystallisations in MeOH, were not sufficient to purify the mixtures. Silica pads were also tried but with no better success. Therefore, one way of purification that was found consisted in a really slow recrystallisation by adding a large quantity of methanol to the mixture and then, adding DCM until the solid was dissolved. DCM was then evaporated really slowly on a rotary evaporator without heating. In these conditions, the product was successfully obtained with yields ranging between 50 and 60%.

3.3.2 Trimer synthesis

I. Reduction of the dimer

In order to synthesize the trimer, the nitro group of the *dimer **2.3*** first needed to be reduced into an *amine group **2.4*** (scheme 27).

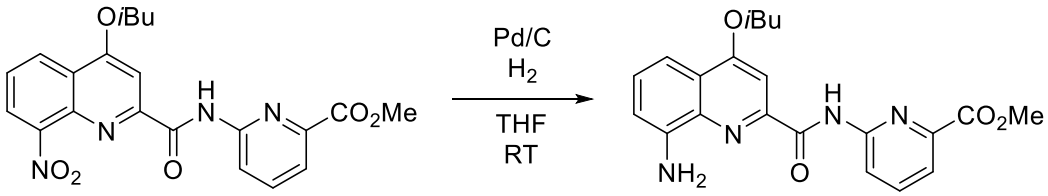

2.3 2.4

Scheme 27. Reduction of the nitro group of the dimer into an amine group.

Reductions can be realized by many ways, however, in the case of a nitro group, the most efficient way is by using palladium on carbon and H_2[84,85].

This reaction was realized several times during my master's thesis. The first try gave a really bad yield of 19% but this was explained by the use of ethyl acetate as the solvent. Indeed,

the reagent was not soluble in ethyl acetate and was thus lost during the work-up (filtration on celite). The second try gave a mixture of different products but one hypothesis to explain this is the use of THF containing BHT as the solvent since BHT could have caused some side reactions. For the third attempt of this reduction, the method was changed since, instead of using an external source of hydrogen (H_2 balloon), it was synthesized in situ by using ammonium metavanadate (NH_4VO_3), ammonium formate (NH_4COOH) and Pd/C in dry THF. Indeed, in presence of Pd/C, ammonium formate can actually decompose to give H_2, CO_2 and ammonia[86]. However, this reaction gave a messy and incomplete reaction. This could be explained by a leak in the set-up, allowing the formed hydrogen to leave the reaction flask since the argon balloon was found deflated after the night. Moreover, NH_4COOH was dissolved in water and added by fractions in the reaction mixture but, as the reaction was not complete due to the hydrogen leak, more ammonium formate and water were added which made the product precipitate since it is not soluble in water.

Therefore, as this reaction demonstrated too many problems, the last attempt of reduction was realized by simply using H_2 and Pd/C but with distilled THF. In this way, the reagent was perfectly soluble in the solvent and the reaction worked perfectly to give quantitative yields and a pure product. The formation of the product was confirmed by comparing the ^1H NMR spectra of the product **2.4** and the nitro dimer reagent **2.3**. Indeed, a shielding of the aromatic protons was observed as well as a substantial deshielding of the amide proton. Moreover, a new broad signal integrating for two protons appeared at 6,72 ppm which corresponds to the two protons of the newly formed amine.

II. Activation of the monomer

The next step in the synthesis of the trimer consisted in the activation of the *methyl quinoline monomer **1.8*** into the *corresponding acid chloride **2.5*** (scheme 28).

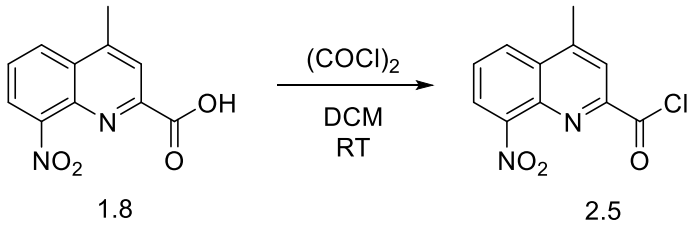

Scheme 28. Activation of the methyl quinoline monomer into an acid chloride.

Whereas thionyl chloride $SOCl_2$ was used in dimer synthesis, oxalyl chloride $(COCl)_2$ was used in trimer synthesis. Indeed, the reaction was first realized with thionyl chloride but the signal corresponding to the methyl group disappeared on the NMR spectrum (figure 38).

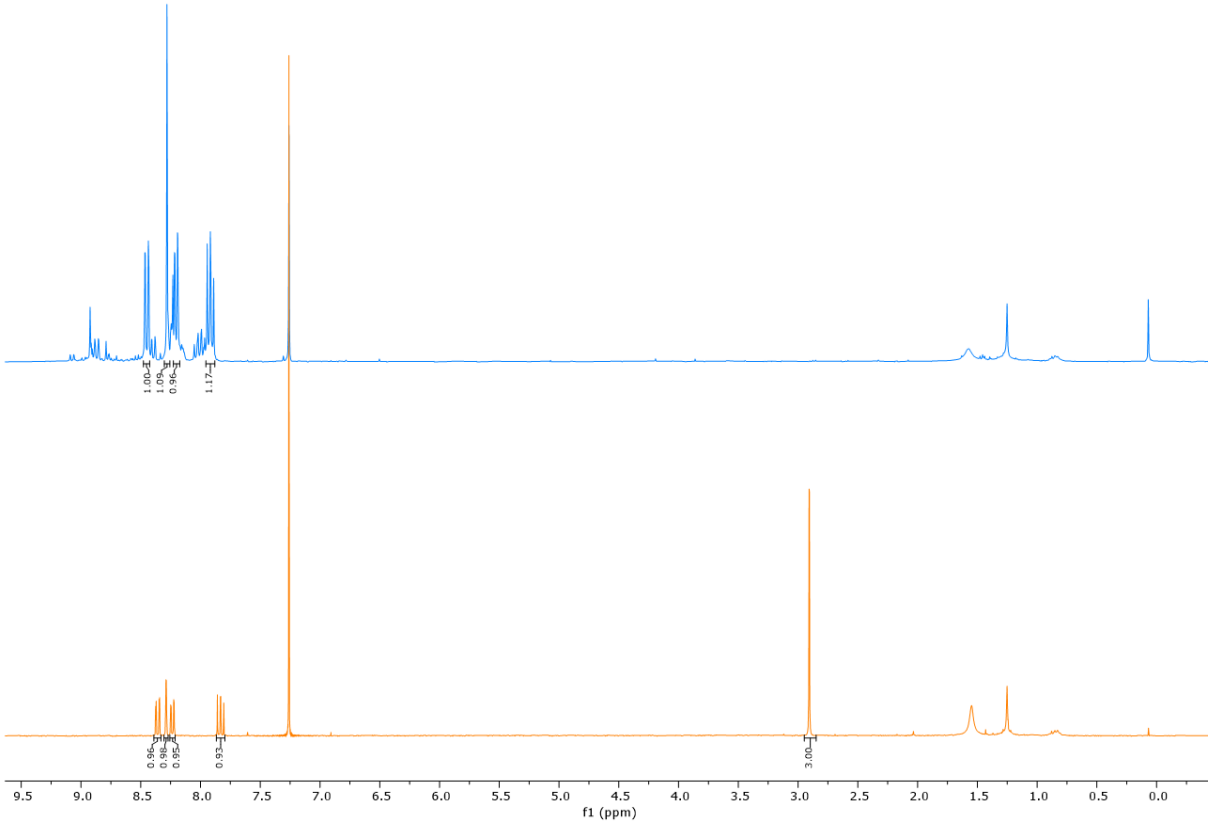

Figure 38. Comparison of the ^1H NMR spectra before (orange) and after (blue) activation of the monomer. The blue spectrum displays no peak for the methyl group due to the hypothesized formation of a trichloromethyl group.

What we propose is that the acid chloride was not formed and the methyl group was rather transformed into a trichloromethyl group when using $SOCl_2$ (scheme 29).

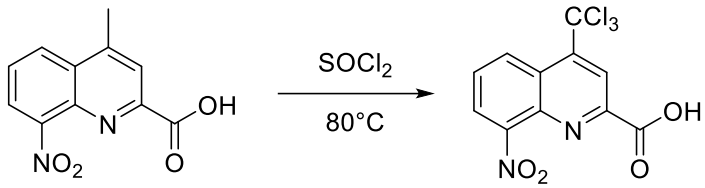

Scheme 29. Formation of a trichloromethyl group.

Such anomaly has actually already been reported several times and thus, some studies were led on this subject. It appeared that bicyclic compounds bearing a nitrogen in para or ortho position of the methyl group undergo this reaction rapidly. Several hypotheses were suggested but the most plausible one is that $SOCl_2$ decomposes into SO and Cl_2 when heated.

Since these compounds are strongly pi-deficient, the methyl group could easily be attacked by Cl_2 to give this trichloromethyl group[87].

Therefore, the reaction was realized with $(COCl)_2$, without heating, and with a drop of DMF as catalyst. Indeed, DMF is able to form a Vilsmeier reagent with oxalyl chloride which is a highly electrophilic species that can then be easily attacked by the oxygen of the carboxylic acid. For the same reasons than with $SOCl_2$ (acid chloride is really reactive and has to be maintained under vacuum), this reaction was never analyzed by ^1H NMR spectroscopy and was always considered to give quantitative yields.

III. Amide coupling

Finally, two trimers were synthesized by an amide coupling as described in the dimer synthesis; one bearing the methyl quinoline monomer and that will finally be oxidized into a PLP-mimic and one with no PLP-mimic for further synthesis of hexamers (scheme 30).

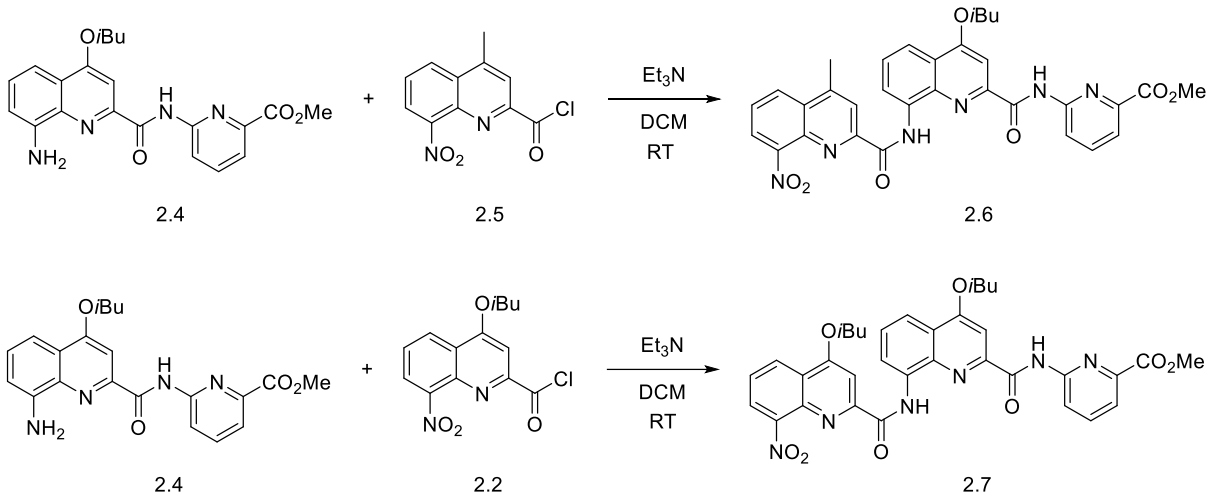

Scheme 30. Synthesis of two trimers 2.7 and 2.8 by amide coupling between the dimer and, respectively, the methyl quinoline monomer 2.6 and the isobutoxy quinoline monomer 1.5.

Surprisingly, the synthesis of the *trimer **2.6*** gave yields ranging between 40 and 50% while the synthesis of the *trimer **2.7*** gave better yields up to 91%. One of the major differences between these two reactions lies in the type of chlorinating agent that was used to form the acid chloride; $(COCl)_2$ for trimer **2.6** and $SOCl_2$ for trimer **2.7**. This difference could explain the difference of yields. Indeed, the purity of the product **2.5** was never validated by NMR spectroscopy, contrary to the product **2.2** and thus, nothing ensures that the product was quantitatively formed. For example, the synthesis of the product **2.5** was assisted by a drop of

DMF as catalyst to form a Vilsmeier reagent but if some of this intermediate is still present in the medium when the dimer **2.4** is added, it can also react with it, reducing the yield. Therefore, in the future of this project, this step should be optimized to ensure the purity of the acid chloride obtained before any further reaction.

The formation of the two trimers **2.6** and **2.7** was, once again, confirmed by ^{1}H NMR spectroscopy thanks to the appearance of a second peak in the amide region, corresponding to the second amide bond forming in this reaction.

3.3.3 Trimer oxidation

The last step in the synthesis of the *PLP-mimic trimer **2.8*** consisted in the oxidation of the methyl group into the aldehyde group. This oxidation was first tried the same way it was previously tried for the monomer; thanks to a Riley oxidation using five equivalents of selenium dioxide SeO_2 (scheme 31). Even though this reaction worked and allowed quite good yields (around 60%) for the oxidation of the monomer, it did not work as well for the oxidation of the trimer.

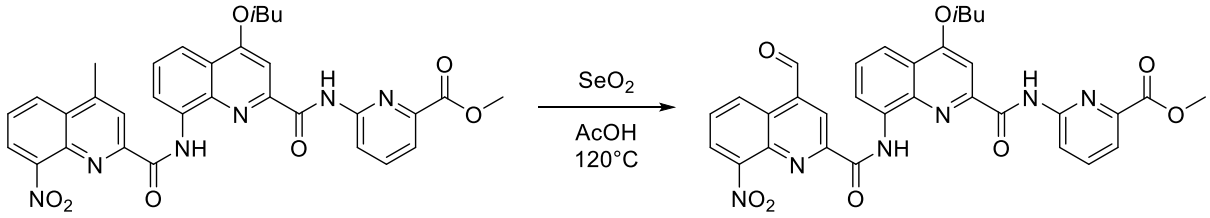

Scheme 31. Riley oxydation of the trimer.

Indeed, this reaction allowed the formation of the aldehyde group, as could be seen on the ^{1}H NMR spectrum that displayed a new peak at 10,6 ppm corresponding to the proton of the aldehyde group, but the product was not pure at all and could not be purified, neither by recrystallisation, nor column. The hypothesis on this bad purity could be that the oxidation was pushed up to the formation of an unknown impurity and that these two species were too similar to be separated by column or recrystallisation. Therefore, to try to avoid the over-oxidation, the exact same reaction was tested without heating, at room temperature, but even after two days of reaction, no change was observed on the NMR spectrum and the *methyl trimer **2.6*** was simply recovered.

Therefore, another reaction was tried; a Vismara oxidation thanks to a procedure reported in the literature[88] (scheme 32).

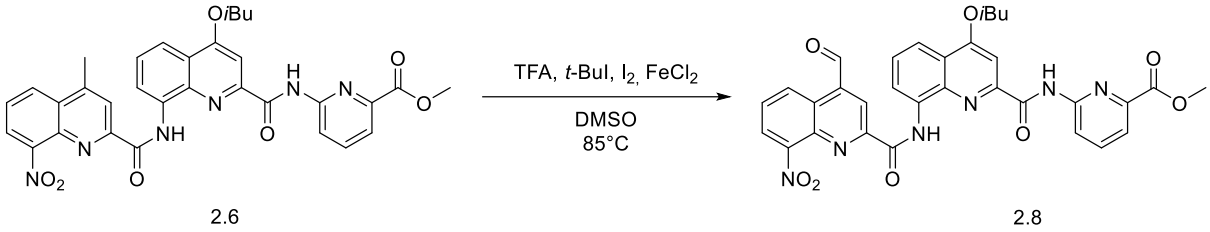

Scheme 32. Vismara oxidation of the trimer.

These conditions were developed by Vismara and Minisci but their article is inaccessible. Even though this reaction has already been used by several groups, it has not been widely investigated and its mechanism is still roughly debated.

The hypothesis on the mechanism of a Vismara oxidation is that it would seem to involve a Kornblum-like oxidation. The first step would consist in the formation of a C-I bond on the benzylic position thanks to t-BuI (radical initiatior) giving an iodine radical by action with I_2, and thanks to $FeCl_2$ which serves as an initiator for this first step. The second step would consist in the Kornblum-like oxidation of the benzylic position into an aldehyde thanks to DMSO[89] (scheme 33).

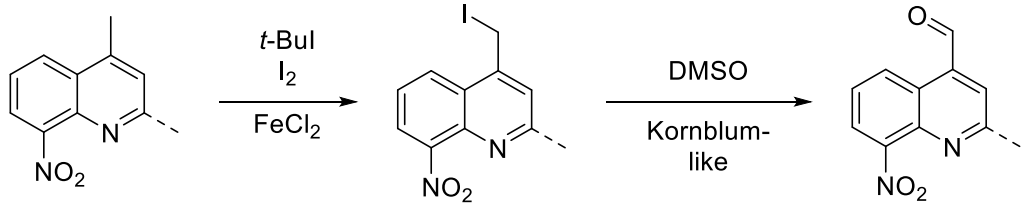

Scheme 33. Hypothesized mechanism for the Vismara oxidation, involving a Kornblum-like oxidation.

Even though the mechanism behind this oxidation is still highly unclear, the reaction worked really well to afford our *PLP-mimic trimer **2.8*** with a moderate yield of 53% as shown by the appearance of a new signal around 10,75 ppm on the ^{1}H NMR spectrum corresponding to the aldehyde (figure 39). This reaction took 5 to 6 days to reach completion but it afforded a pure product with almost no need of purification, except a simple extraction with saturated $Na_2S_2O_3$ and Na_2CO_3 (10%) and a quick silica pad to get rid of two small aliphatic signals. Importantly, being able to perform this reaction on the oligomer, helps to avoid additional protection deprotection steps during the synthesis and further represents a rare example of post-synthetic modification of aromatic oligoamide foldamers.

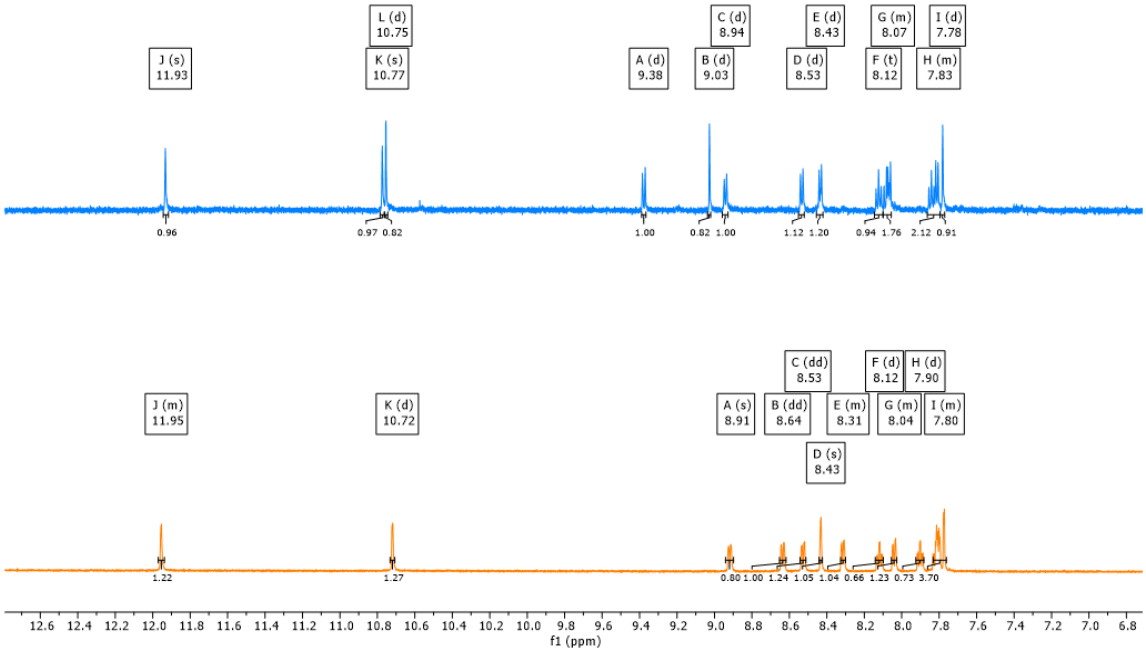

Figure 39. Comparison of the ^{1}H NMR spectra before (orange) and after (blue) Vismara oxidation of the trimer. The top spectrum displays a new peak at 10,75 ppm corresponding to the aldehyde proton.

3.4 Reactivity assays

Whereas the reactivity of the PLP-mimic as a monomer was investigated last year to determine if its reactivity was similar to the one of the PLP, the next crucial part of this project is to study the reactivity of the *PLP-mimic trimer **2.8*** to determine how the introduction of the PLP-mimic into a foldamer influences the reactivity. Indeed, as the environment around the PLP-mimic is modified by the foldamer, some effects could be seen on the reactivity, either negative or positive effects.

Two types of reactions have been conducted on the monomer last year: transamination and decarboxylation. As the transamination gave better results, it is this one that we wanted to further investigate with the trimer. However, last year, only the catalytic loading of the monomer was screened but no other conditions were. Therefore, before entering in the trimer reactivity assays, we wanted to see if any better conditions could be found for the monomer.

3.4.1 Conditions of the transamination reaction

Last year, after making sure that the monomer was able to form the important catalytic imine species with the amine substrate, the transamination was investigated by adding one equivalent of NaOH to a solution of one equivalent of benzylamine and 10 mol% of the monomer in ethanol. Moreover, one equivalent of a sacrificial ketone (2-oxobutanoic acid) was added in the solution in order to regenerate the catalyst (scheme 34).

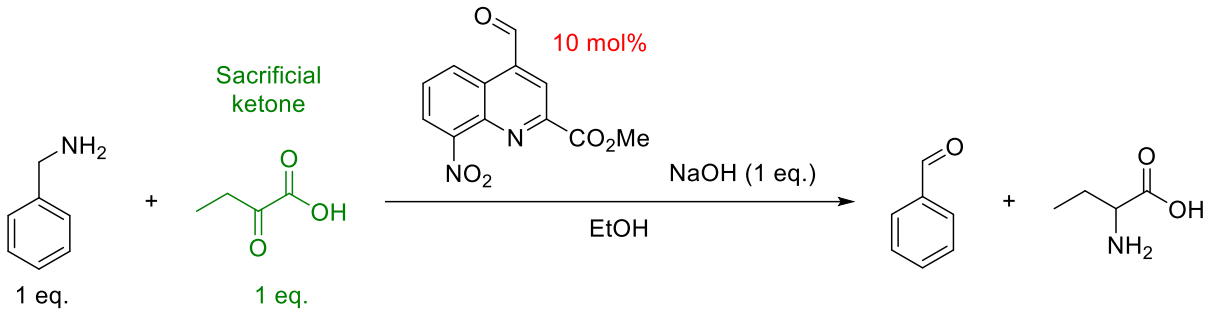

Scheme 34. Transamination reaction investigated last year.

Indeed, during a transamination reaction, benzylamine is transformed into benzaldehyde but, in the same way, the catalyst is transformed into its amine counterpart and must be converted back into its aldehyde form thanks to a sacrificial ketone for which the only purpose is to regenerate the catalyst (scheme 35).

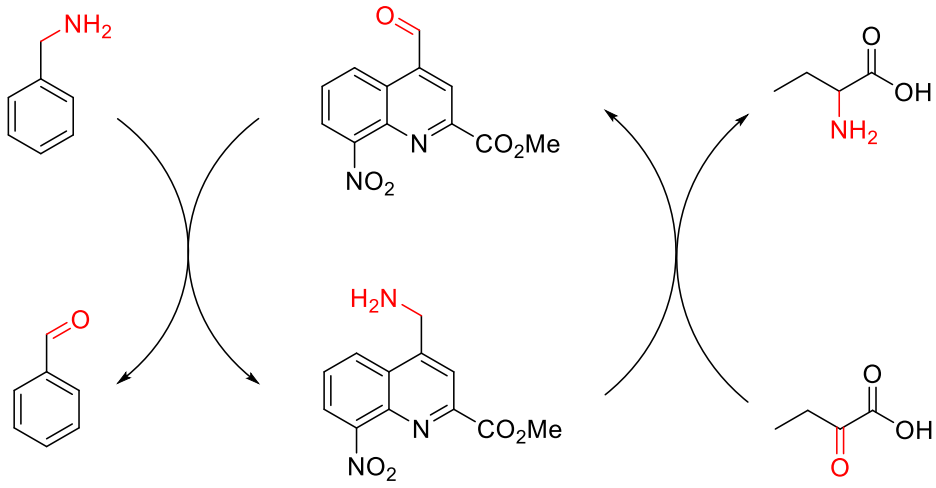

Scheme 35. Catalytic cycle of the transamination reaction, requiring a sacrificial ketone.

This reaction was determined to work in a catalytic way since a yield of 28% was obtained with 10 mol% catalytic loading. However, to determine if there were any better conditions for the transamination reaction than these ones, it was decided to change different parameters such as the type of sacrificial ketone or the solvent and study the influence on the transamination reaction.

I. Different sacrificial ketones

The first sacrificial ketone to be tested was pyruvic acid which is quite similar to 2-oxobutanoic acid but with one less carbon. In the exact same way than last year, one equivalent of benzylamine, one equivalent of pyruvic acid and 10 mol% of catalyst were put in presence of one equivalent of NaOH in ethanol (scheme 36). One can note that these conditions will be the ones used for every reactivity assays.

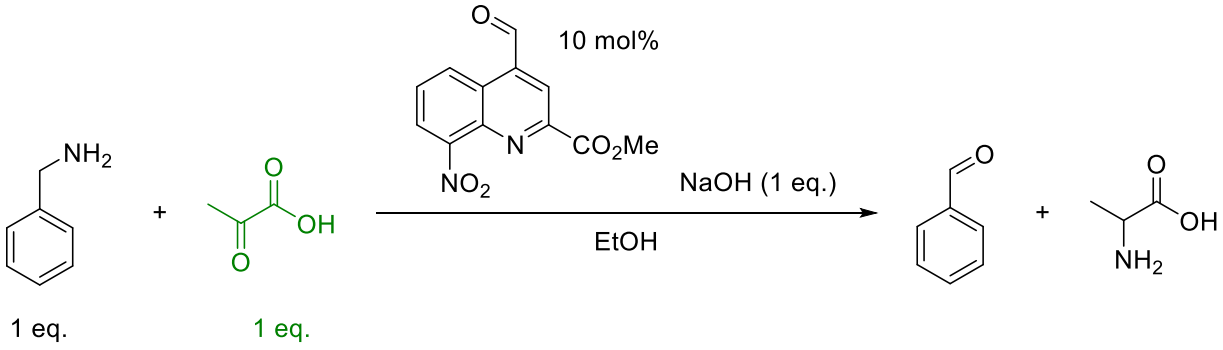

Scheme 36. Transamination reaction with pyruvic acid as the sacrificial ketone.

This reaction was followed by ^{1}H NMR spectroscopy in which the yield of the reaction was estimated with an internal standard (figure 40). Indeed, trimethoxybenzene (TMB) was added

to the reaction mixture as an internal standard since this compound does not react with any other species in presence. By integrating its peak (around 6 ppm) at the same value on every spectrum, the evolution of the different species in the mixture can be followed.

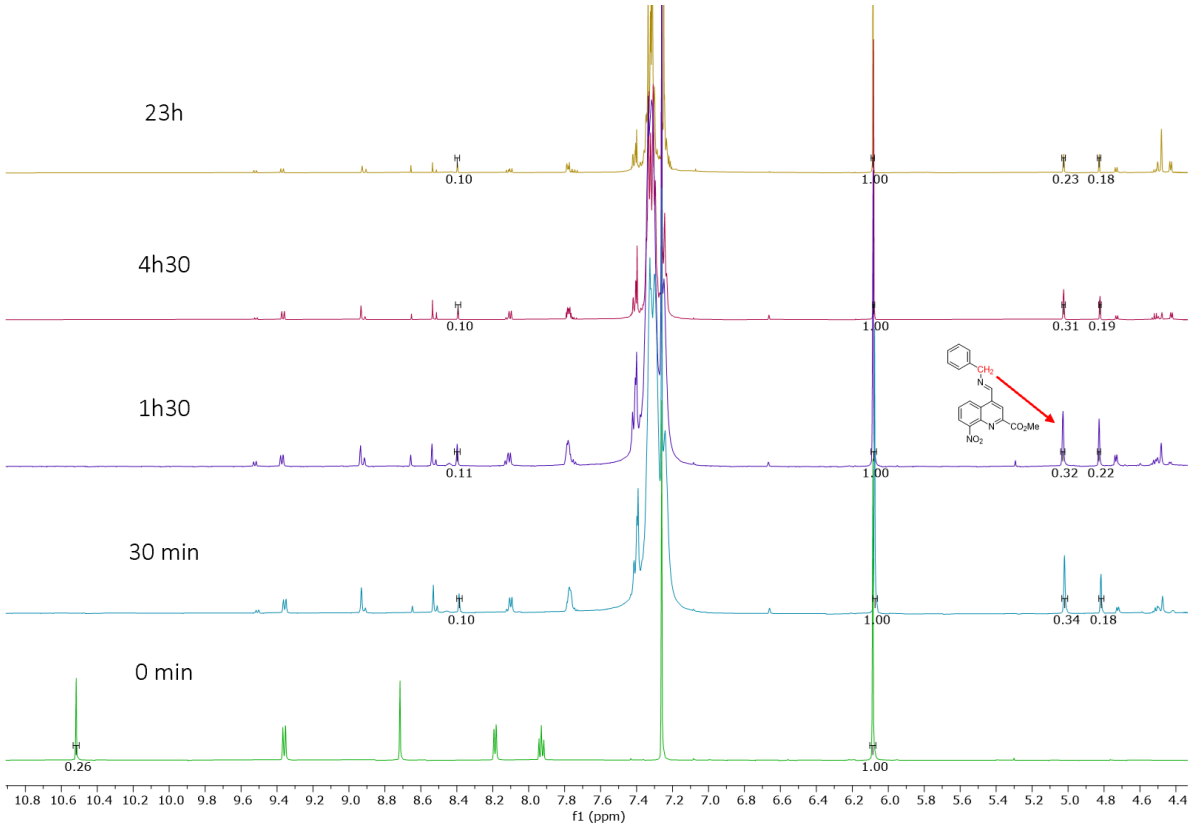

Figure 40. Evolution of the ^{1}H NMR spectra during the transamination reaction using pyruvic acid as the sacrificial ketone.

Therefore, no benzaldehyde seems to form since the characteristic peak of the benzaldehyde, at 10 ppm, is not visible. However, three interesting peaks are appearing at 4,8 ppm, 5 ppm and 8,4 ppm. The peak around 5 ppm has previously been determined to be the imine species forming between the catalyst and benzylamine. The other two peaks, at 4,8 ppm and 8,4 ppm are actually related to the benzaldehyde product. Indeed, benzaldehyde is formed but it quickly reacts with benzylamine to give a benzaldehyde-benzylamine imine (scheme 37).

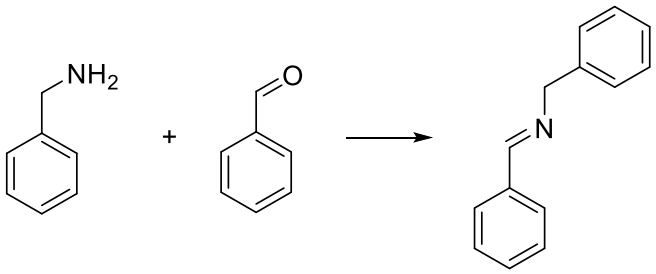

Scheme 37. Condensation between benzylamine and formed benzaldehyde to yield the corresponding imine.

This hypothesis was further validated by mixing benzylamine and benzaldehyde together and analysing the mixture by ^{1}H NMR spectroscopy (figure 41). This NMR spectrum highlights two things: first, it is normal not to observe the benzaldehyde peak on the reactivity assays since benzaldehyde condenses quickly with benzylamine to give a benzaldehyde-benzylamine imine (BBI). Secondly, the two peaks corresponding to this BBI are, indeed, observed at 4,8 ppm and 8,4 ppm.

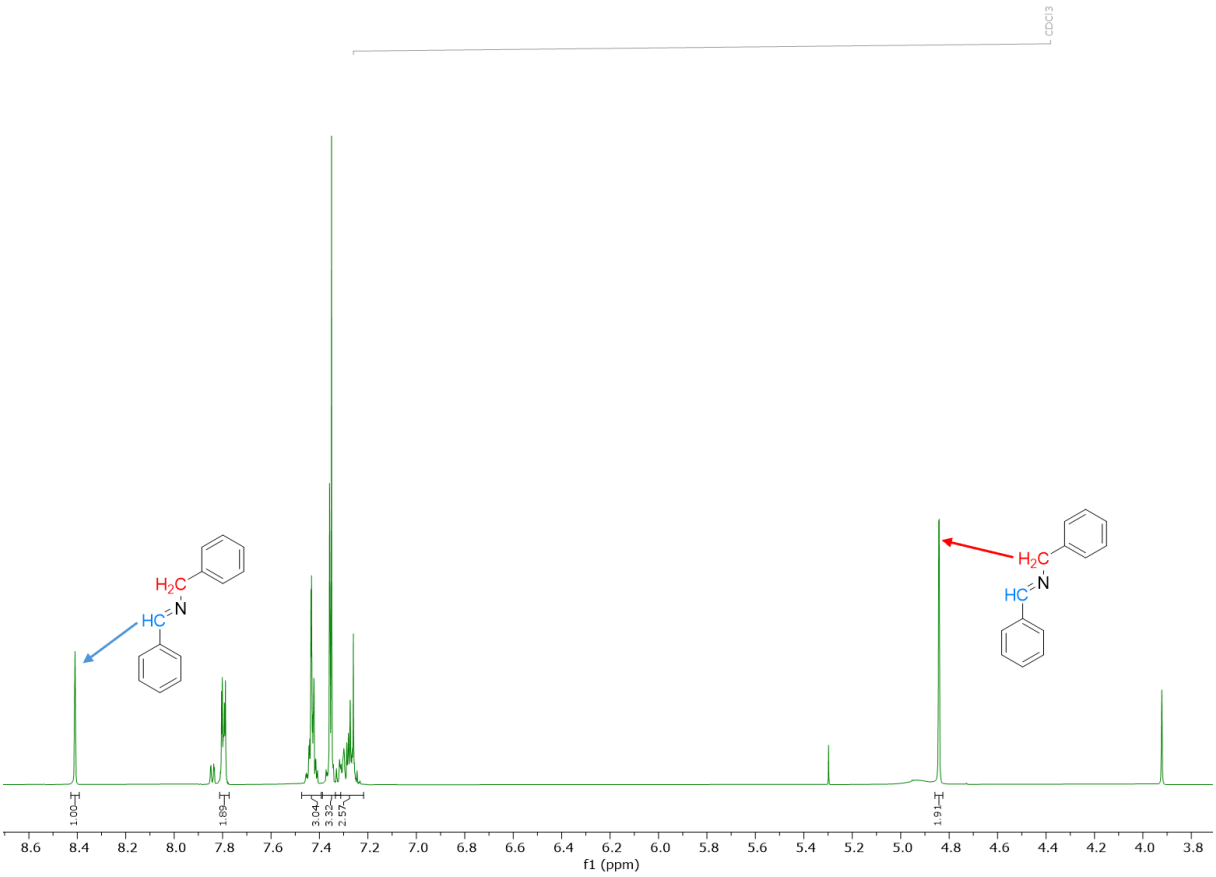

Figure 41. ^{1}H NMR spectrum of the condensation reaction between benzaldehyde and benzylamine. This spectrum displays the two characteristic peaks of the imine formed at 4,8 and 8,4 ppm.

Once the interesting peaks were attributed, we were able to estimate the yield of the reaction and determine if, first, it is working in a catalytic way and secondly, if these conditions afford a better reaction than with the conditions used previously. To estimate this yield, we simply needed to compare the integration value of the peaks before and after the reaction. Since the product (benzaldehyde) quickly reacts to give the BBI, we needed to compare the signals of this BBI (4,8 ppm or 8,4 ppm) with the signal of the aldehyde proton of the catalyst (10,5 ppm).

Therefore, the yield can be calculated with the following formula:

$$Yield\ (\%) = \frac{n_{products}}{n_{reagents}}.100 = \frac{n_{BBimine}}{n_{catalyst}}.100 = \frac{0{,}5.Int_{4{,}8\ ppm}}{Int_{10{,}5\ ppm}}.100$$

It is important to note that this yield is calculated considering that the catalyst is the limiting reagent and thus, a yield over 100% would indicate that the reaction works in a catalytic way. Therefore, by using this equation, we can see that, even after 23 hours, the reaction is still not working in a catalytic way since the yield is $\frac{0{,}5.0{,}18}{0{,}26}$ = 31%. Moreover, the yield is already 31% after only 30 minutes and does not increase anymore during the whole reaction.

As the 2-oxobutanoic acid allowed a catalytic reaction with a yield of 283% (last year conditions and result), these new conditions are not improving the transamination reaction and were thus not further investigated.

The second sacrificial ketone to be tested was methyl pyruvate which is the ester counterpart of the pyruvic acid. Indeed, as the mixture was not well soluble when using pyruvic acid, we tried to use its ester counterpart hoping it would allow a better solubility. The same conditions than for pyruvic acid were used but with one equivalent of methyl pyruvate instead of pyruvic acid (scheme 38).

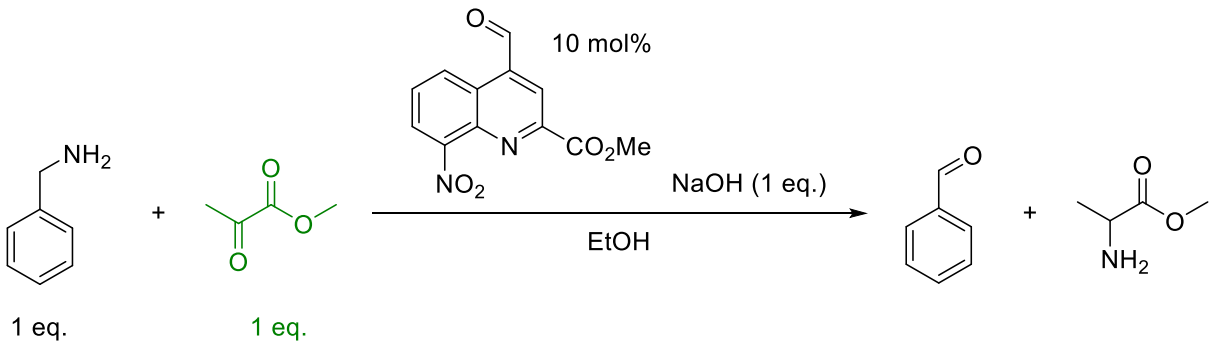

Scheme 38. Transamination reaction with methyl pyruvate as the sacrificial ketone.

The reaction was, once again followed by ^{1}H NMR spectroscopy with TMB as the internal standard (figure 42).

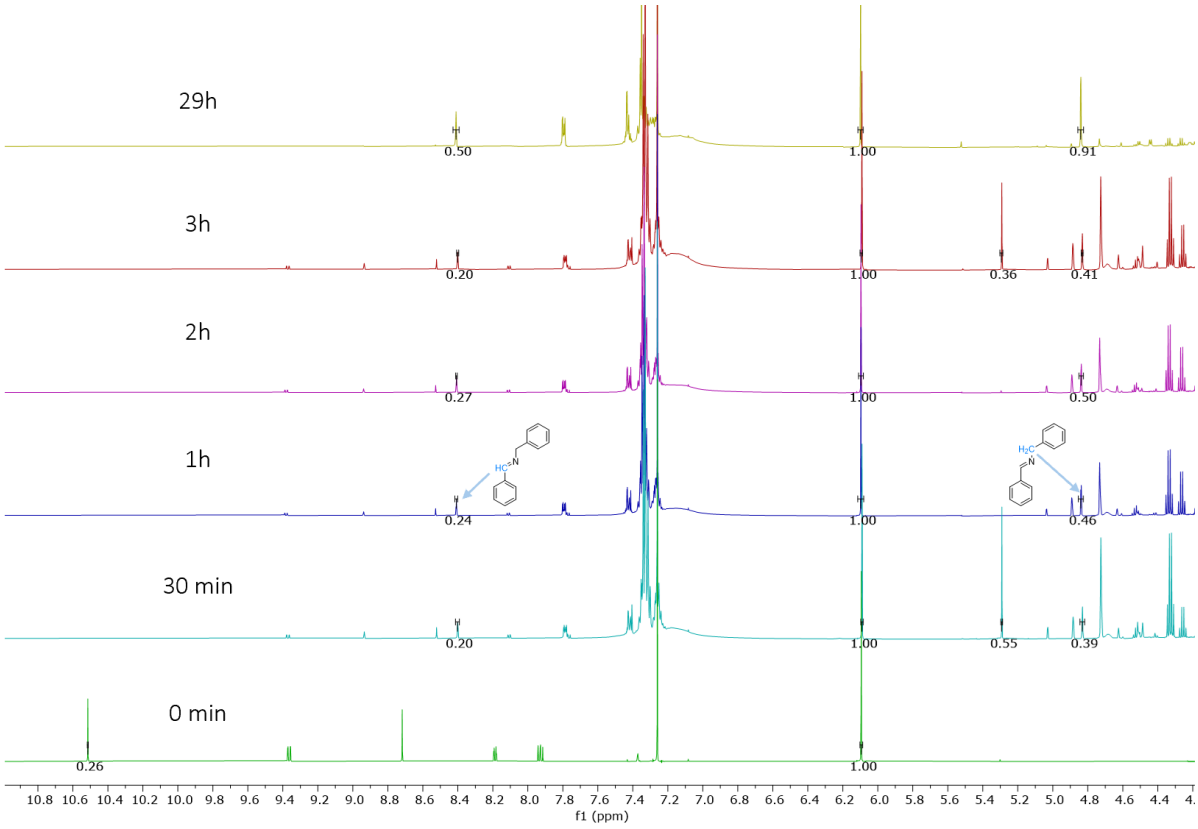

Figure 42. Evolution of the ^{1}H NMR spectra during the transamination reaction using methyl pyruvate as the sacrificial ketone.

First, in these spectra, we sometimes observe a peak at 5,3 ppm which has been attributed to a contamination with DCM during the work-up. Secondly, here too, the transamination reaction is happening since the two characteristic peaks of the BBI (4,8 and 8,4 ppm) are visible and therefore, the yield of this reaction can be estimated:

$$Yield\ (\%) = \frac{0{,}5.\,Int_{4{,}8\ ppm}}{Int_{10{,}5\ ppm}}.100 = \frac{0{,}5.\,0{,}91}{0{,}26} = 175\%$$

This reaction is showing a yield of 175% (based on the catalyst as the limiting reagent) after 29 hours and the catalyst is therefore reacting in a catalytic way towards the transamination reaction. These conditions, using methyl pyruvate as the sacrificial ketone, seemed thus promising for the transamination reaction but, after a few tests with it, we noticed that all the obtained ^{1}H NMR spectra displayed numerous signals in the aliphatic region compared to those obtained with pyruvic acid. Therefore, we decided to do a control reaction by mixing methyl pyruvate and benzylamine together which gave a rapid and strongly exothermic reaction (scheme 39).

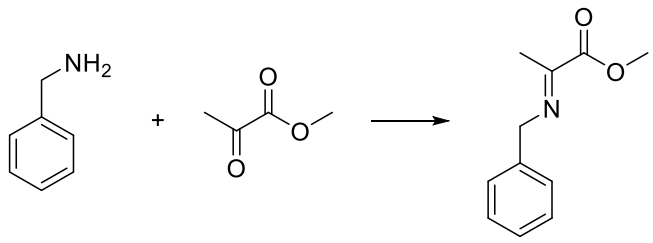

Scheme 39. Condensation between methyl pyruvate and benzylamine.

Indeed, the NMR spectrum revealed that, whereas 2-oxobutanoic acid and pyruvic acid first undergo an acid-base reaction with benzylamine due to their carboxylic acid group, methyl pyruvate rather undergo a condensation to give a mixture of different products, probably including the corresponding imine.

Therefore, we concluded that methyl pyruvate was not a so promising sacrificial ketone as it can react with benzylamine and thus, make a part of it unavailable for the transamination reaction. However, as this was discovered later in the experiments, the following solvent screening was performed using methyl pyruvate.

II. Different solvents

The influence of the solvents on this transamination reaction was also tested with two solvents; $CHCl_3$ and DCM since both of them allow the complete solubilization of the mixture. Therefore, we were also looking at the influence of the solubility on the transamination reaction.

The first solvent to be tested was $CHCl_3$. The same conditions than above were used except that the reaction was let to run in $CHCl_3$ instead of ethanol and that DBU was used instead of NaOH since NaOH is not soluble in $CHCl_3$ (scheme 40).

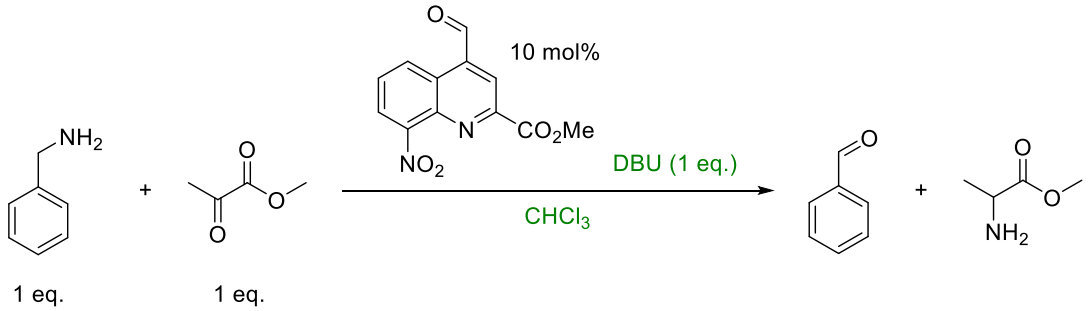

Scheme 40. Transamination reaction with chloroform as the solvent and DBU as the base.

Once again, the reaction was followed by ^1H NMR spectroscopy with TMB as the internal standard (figure 43).

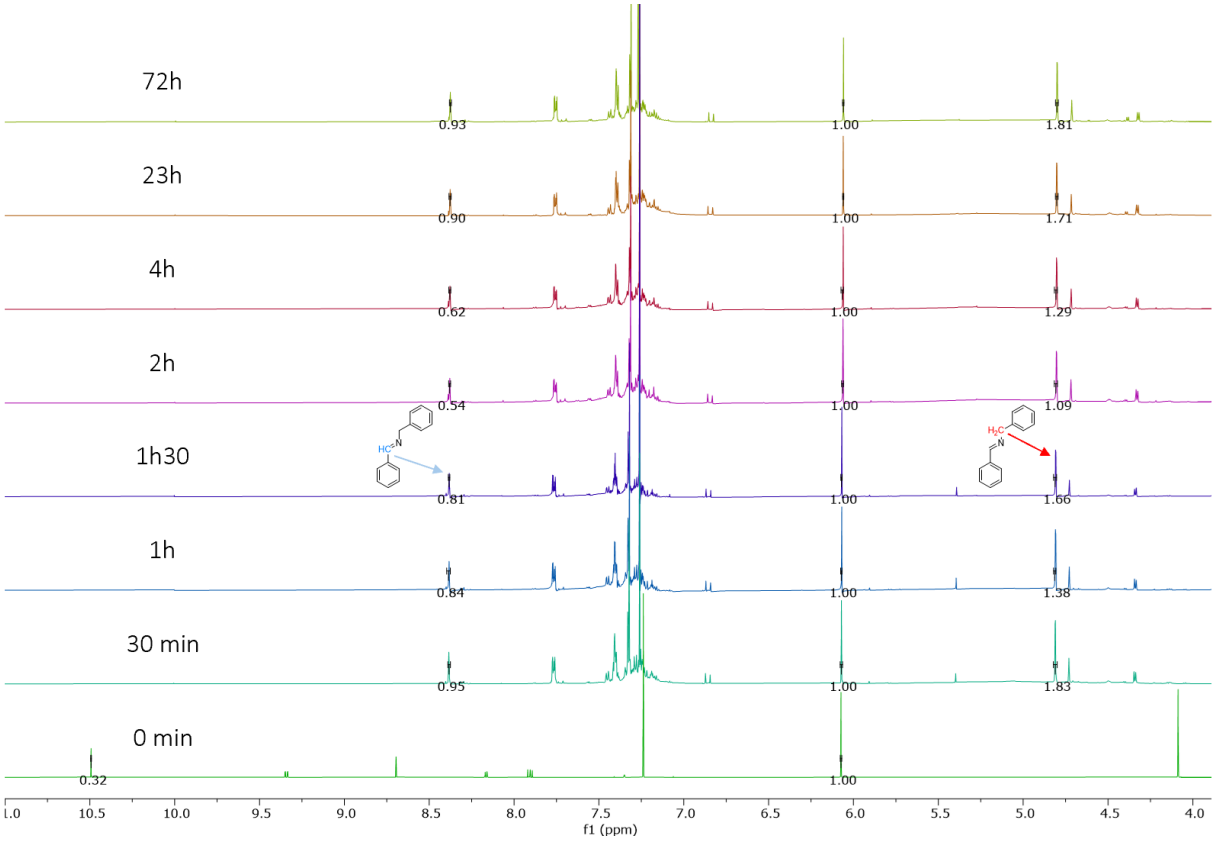

Figure 43. Evolution of the ^{1}H NMR spectra during the transamination reaction using chloroform as the solvent.

The transamination reaction is happening as showed by the two characteristic peaks of the BBI and what is really interesting here is that we can notice that the reaction is working in a catalytic way after only 30 minutes (yield of 286% based on the catalyst). However, some strange behaviour can also be highlighted since the integration values of the BBI peaks are randomly increasing and decreasing throughout the reaction, but this could be due to the broadening of a signal from 4,5 ppm to 5,5 ppm. Indeed, as the BBI peak is included in this broad signal, the integration values are not trustworthy. Another strange behaviour happening is that the maximal integration value for the BBI peaks is obtained after 30 minutes but no evolution is noticed during the next 3 days. The hypothesis on this would be that the catalyst gives a really fast reaction but that it is also deactivated in only 30 minutes since no more peak of the catalyst is observed in the aromatic region.

Therefore, these conditions seem quite interesting but they need to be studied with great caution due to the fast deactivation of the catalyst and the fluctuation in the integration values.

The second solvent to be tested was DCM by using the same conditions than above but in DCM instead of $CHCl_3$. Once again, DBU was used instead of NaOH (scheme 41).

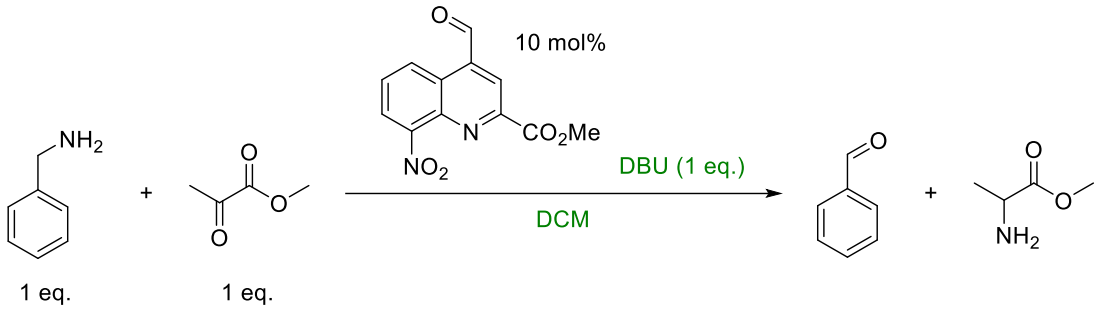

Scheme 41. Transamination reaction with DCM as the solvent and DBU as the base.

The transamination reaction was followed by ^1H NMR spectroscopy using TMB as an internal standard (figure 44).

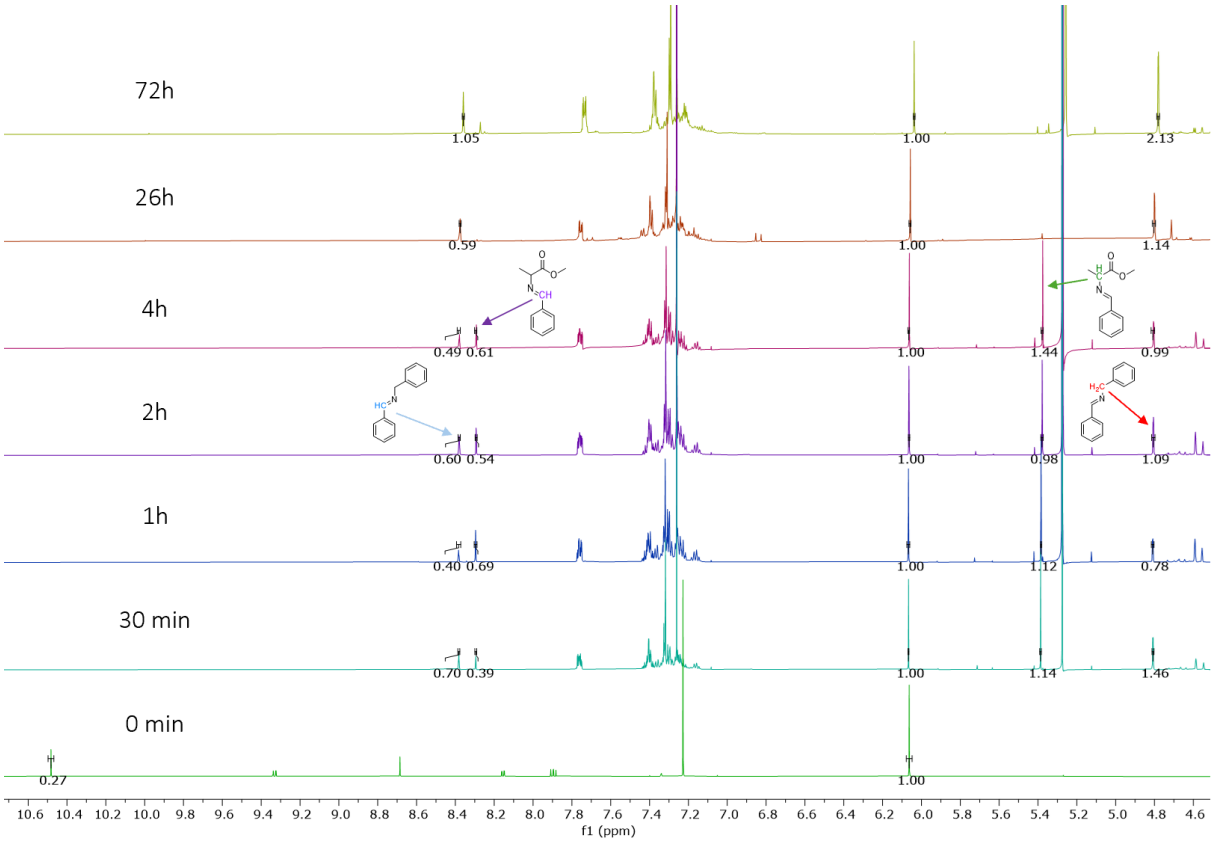

Figure 44. Evolution of the ^1H NMR spectra during the transamination reaction using DCM as the solvent.

Globally, the same observations can be made for DCM than for $CHCl_3$. Indeed, here too the reaction is working in a catalytic way in only 30 minutes (yield of 211% based on the catalyst) but some fluctuations in the integration values of the BBI peaks are observed and the catalyst again seems deactivated in 30 minutes.

But, if the catalyst indeed seems deactivated after only 30 minutes of reaction, then, how to explain the great increase in the integration value of the BBI peaks between 26 hours and 72 hours (from 1,14 to 2,13 for the peak at 4,8ppm)? The hypothesis was that the reaction was happening even without the assistance of the catalyst. This hypothesis was validated by realizing the exact same reaction without adding the catalyst in the mixture and the two characteristic peaks of the BBI were observed. Therefore, the reaction is happening without the presence of the catalyst and this can explain why more product is forming even once the catalyst is deactivated.

Therefore, these conditions for the transamination reaction were not selected for reactivity assays with the trimer since the reaction does not require the assistance of a catalyst.

Finally, as no real better condition was found for this transamination reaction, we decided to get back to the conditions used last year (ethanol as the solvent and 2-oxobutanoic acid as the sacrificial ketone) for the reactivity assays with the trimer.

3.4.2 Reactivity assays with the trimer

I. Imine condensation

The very first step that must be verified is the condensation of the trimer with benzylamine in order to form the reactive imine species. Indeed, if the imine species is not forming, no subsequent reaction is possible. Therefore, the ability of the trimer to form an imine has been investigated by adding one equivalent of benzylamine to a solution of the trimer **2.8** in $CDCl_3$ (scheme 42) and the reaction was followed by ^1H NMR spectroscopy (figure 45).

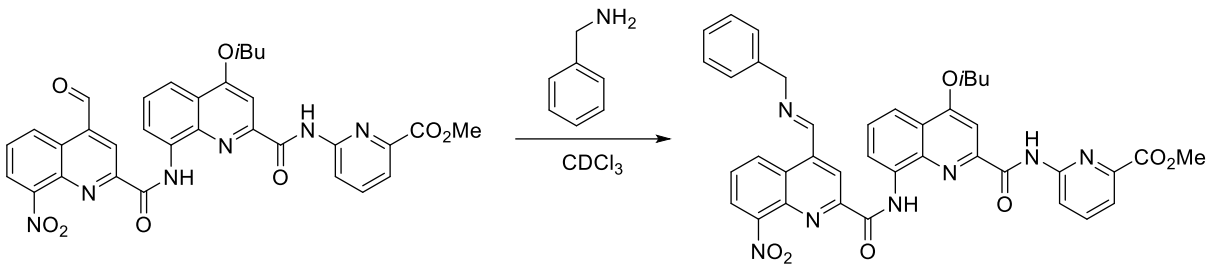

Scheme 42. Imine condensation of the trimeric catalyst with benzylamine to form the corresponding imine.

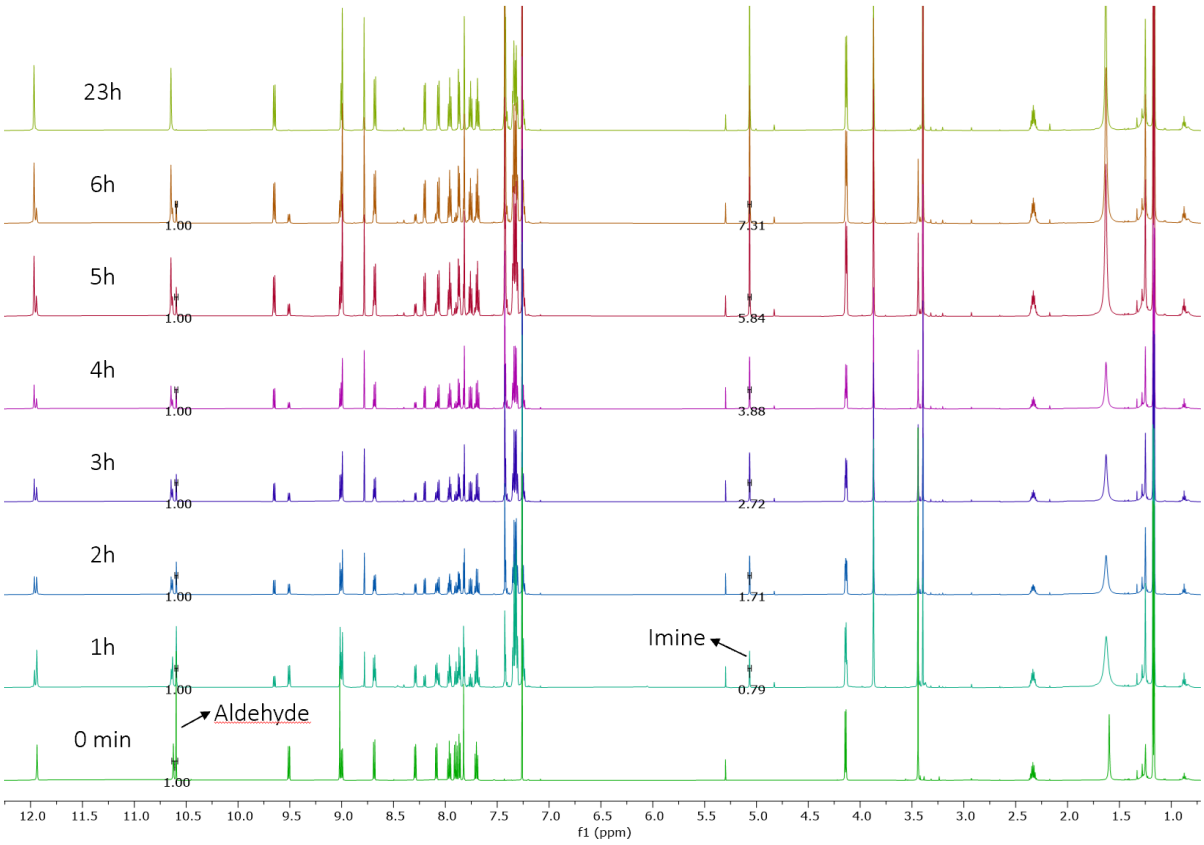

Figure 45. Evolution of the ^1H NMR spectra of the imine formation over time.

During this reaction, we observed the disappearance of the aldehyde peak throughout time and the appearance of a new signal around 5 ppm corresponding to the imine in formation.

Moreover, we clearly saw the appearance of two set of signals when both species were present in the mixture. The disappearance of the aldehyde species (and thus, the appearance of the imine species) was plotted over time to see that the reaction took more than 6 hours to reach equilibrium (figure 46).

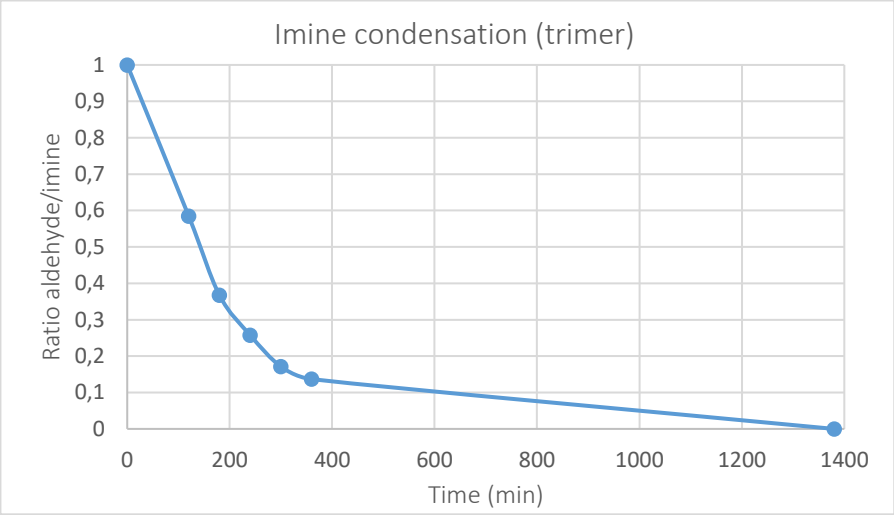

Figure 46. Plot of the disappearance of the aldehyde species over time.

This same experiment was realized last year for the monomer for which a complete reaction was observed after 4 hours only. Therefore, the imine formation takes longer for the trimer but this can be explained by two hypothesis. First, the trimer being bulkier and larger than the monomer, it could take longer for the imine to form. Secondly, this reaction was directly realized in a NMR tube with no stirring whereas the same experiment for the monomer was realized in a flask with stirring which could have made the reaction faster.

II. Transamination

Once we knew for sure that the trimer was also able to form the imine species, we could start the reactivity assays on it. The whole purpose of these reactivity assays is to determine if the trimeric catalyst demonstrates a different reactivity than the monomeric catalyst. Therefore, in order to compare the reactivity of these two species, the reactivity assays must be realized with the same concentration of trimer than monomer. Two transamination reactions were tested with the trimer; one in ethanol and one in chloroform.

For both experiments, the same conditions than above were used but with 10 mol% of the trimer (with a concentration of 0,016 M) in ethanol or $CDCl_3$ (scheme 43).

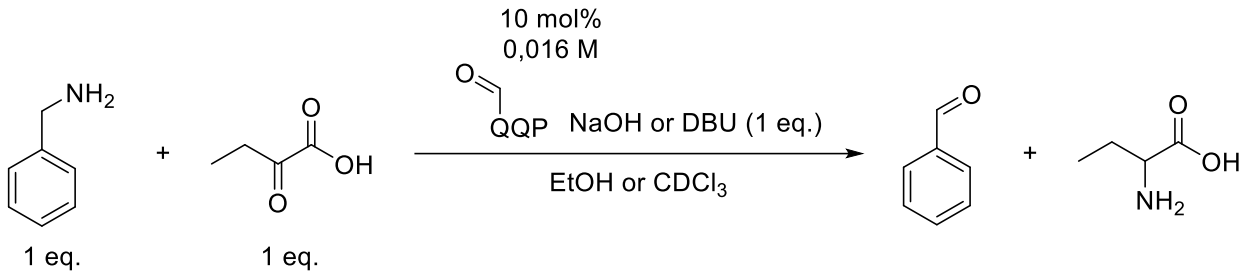

Scheme 43. Transamination reaction in ethanol with the trimer as the catalyst.

As for the experiments with the monomer, these two reactions were followed by ^1H NMR spectroscopy using TMB as the internal standard (figures 47 and 48).

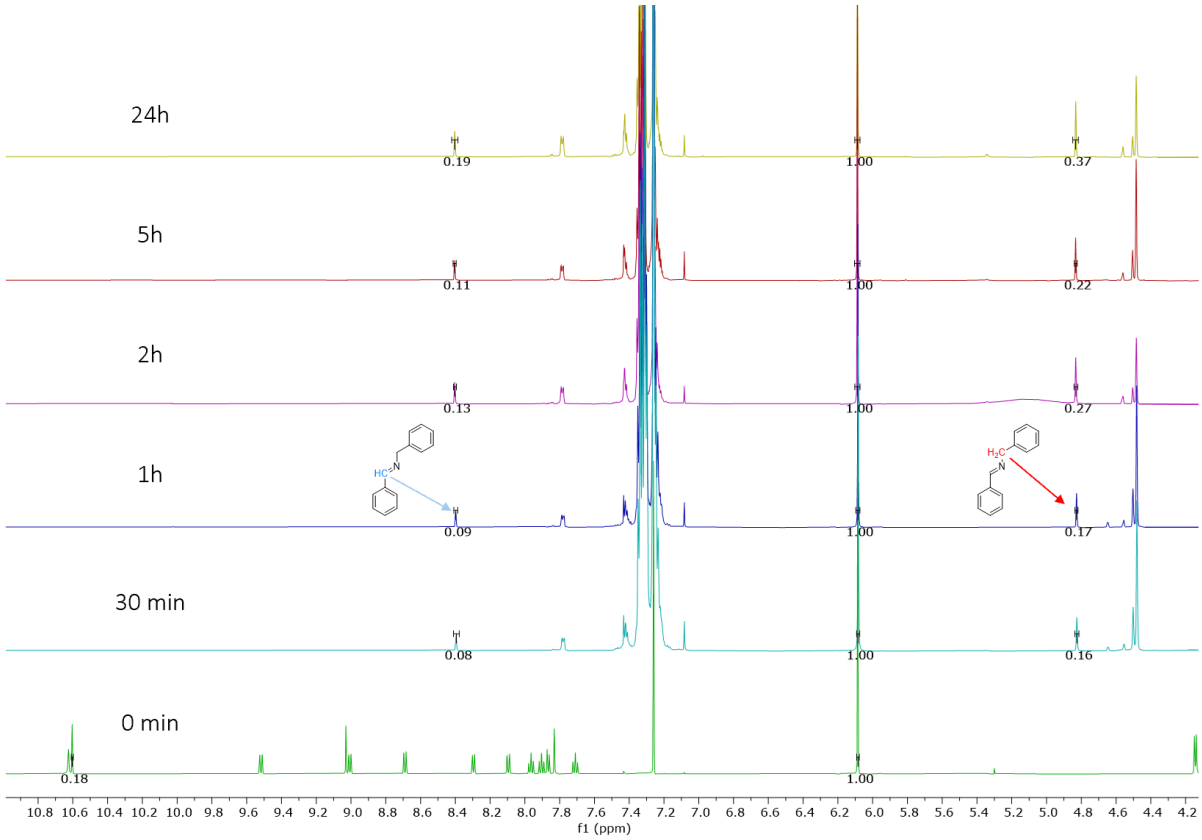

Figure 47. Evolution of the ^1H NMR spectra during the transamination reaction in ethanol using the trimer as the catalyst.

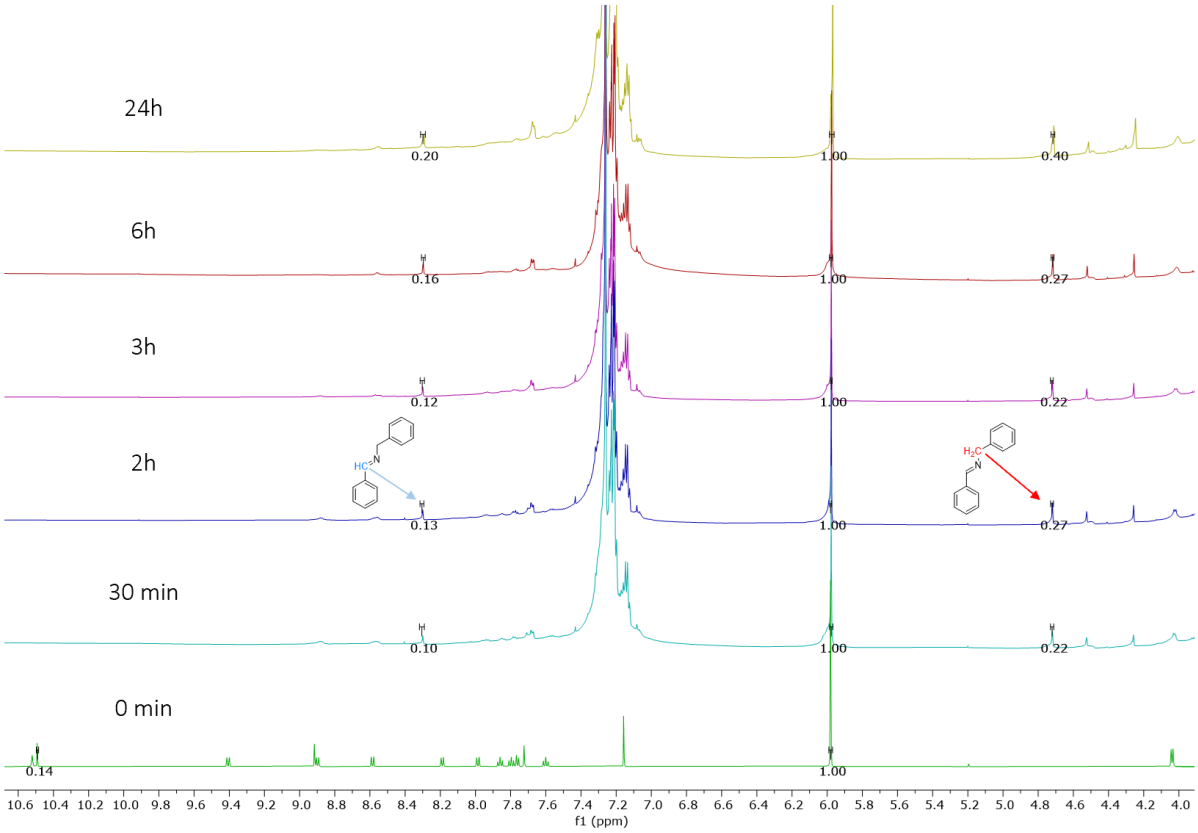

Figure 48. Evolution of the ^{1}H NMR spectra during the transamination reaction in chloroform using the trimer as the catalyst.

For both experiments, the transamination reaction is happening with the trimeric catalyst since the two characteristic peaks of the BBI are visible. However, what interests us here is to compare the reactivity obtained for the trimer with the one obtained for the monomer in the exact same conditions. Therefore, these reactions were also realized with the monomer catalyst (with a concentration of 0,016 M as well) and the yields obtained for these four reactions were plotted over time (figure 49). It is important to note that every time an integration value included part of a broad peak leading to some variation in the values (as for the trimer in ethanol after 2 hours), these points were not used when plotting the graphs.

The trimer and the monomer behave really similarly in ethanol whereas they follow a completely different trend in chloroform. Indeed, in chloroform, the trimer allows a faster reaction and, above all, only the trimer allows a catalytic reaction in 24 hours whereas the yield obtained with the monomer never surpasses 60% in 24 hours.

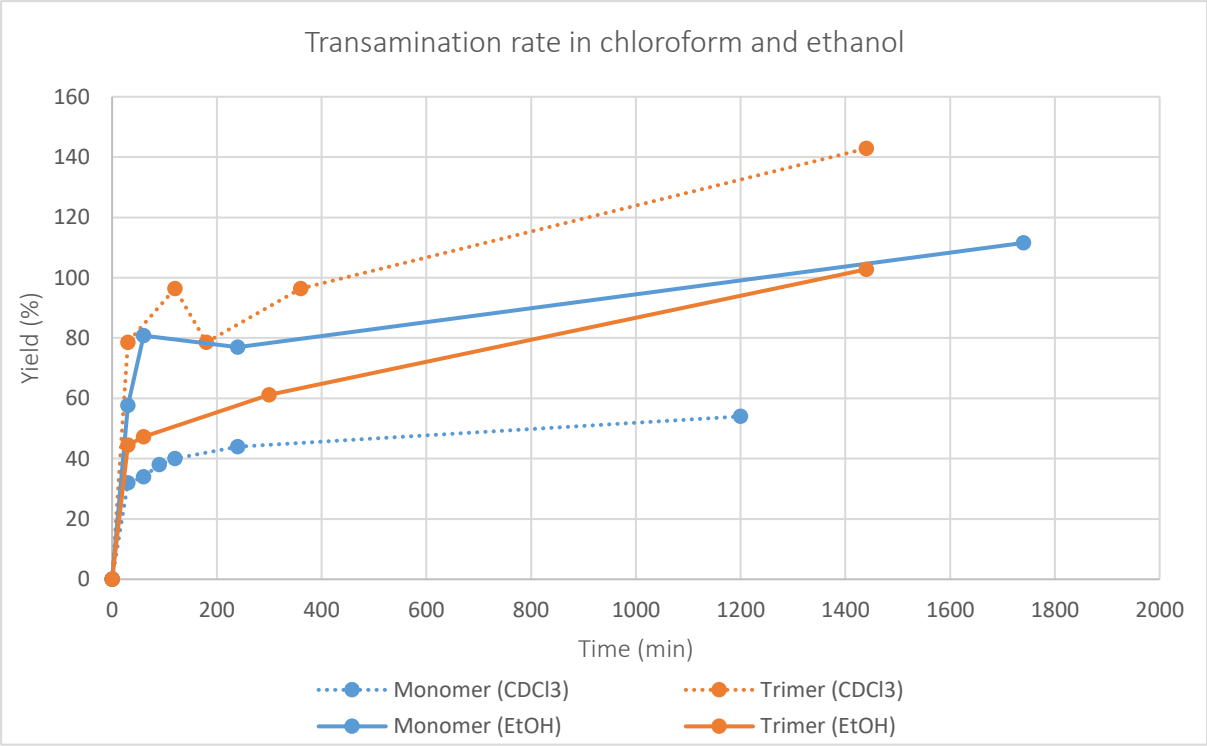

Figure 49. Comparison of the yields obtained for the transamination reaction in ethanol (solid lines) or chloroform (dotted lines) with the trimer (orange) or the monomer (blue) over time.

This difference between the two solvents could be explained in two ways; the ability of the solvent to stabilize the negative charge formed during the transamination reaction or the ability of the solvent to form hydrogen bonds with the quinoline nitrogen.

Indeed, for the first hypothesis, it was suggested previously that the monomer was able to react with itself and thus, self-deactivate. Therefore, during the transamination reaction, trimer and monomer in ethanol showed the same behaviour since both of them could see their negative charge rapidly reprotonated, avoiding the self-deactivation. On the contrary, as chloroform is not able to provide this stabilization, it could explain the difference of reactivity. It is proposed that, in chloroform, the monomer would not be rapidly reprotonated and could easily react with itself and self-deactivate, causing a drop in the yield of the reaction. On the opposite, the trimer, even though its negative charge would also not be rapidly reprotonated, is bulkier and larger which could make it more difficult to react with itself. The trimer would then show less self-deactivation and could more easily react in a transamination reaction, increasing the yield of the reaction.

For the second hypothesis, it could be possible that, in ethanol, both the monomer and the trimer have hydrogen bonding with the quinoline nitrogen thanks to the solvent. This could

make them as electron-withdrawing as each other and thus, lead to the same reactivity. On the opposite, in chloroform, the monomer would lack hydrogen bonding but not the trimer thanks to intramolecular hydrogen bonding. Only the electron-withdrawing effect of the trimer would be enhanced and the trimer would demonstrate a better reactivity than the monomer. Such a hypothesis would be potential evidence that the foldamer scaffold provides non-covalent interactions that enhance reactivity.

For ease, the conditions used and the results obtained for all reactivity assays are summarized in table 1.

	Catalyst	Sacrificial ketone	Solvent	[M]	Yield and results after 24 hours
1	Monomer	Pyruvic acid	EtOH	0,02	Not catalytic (31%)
2	Monomer	Methyl pyruvate	EtOH	0,02	Catalytic (175%) but unwanted side reactions
3	Monomer	Methyl pyruvate	$CHCl_3$	0,02	Catalytic (286%) but fast deactivation of the catalyst
4	Monomer	Methyl pyruvate	DCM	0,02	No need for a catalyst
5	Monomer	2-oxobutanoic acid	EtOH	0,016	Catalytic (111%)
6	Trimer	2-oxobutanoic acid	EtOH	0,016	Catalytic (103%)
7	Monomer	2-oxobutanoic acid	$CHCl_3$	0,016	Not catalytic (54%)
8	Trimer	2-oxobutanoic acid	$CHCl_3$	0,016	Catalytic (143%)

Table 1. Conditions and results for all reactivity assays. For all these tests, the substrate is benzylamine and the catalytic loading is 10 mol%. The yields are calculated based on the catalyst as the limiting reagent. NaOH is used as the base in EtOH and DBU is used in $CHCl_3$ and DCM. The concentration values correspond to the catalyst concentration.

4 Conclusion and outlooks

4.1 Conclusion

This work described the successful synthesis of a trimeric PLP-mimic based aromatic oligoamide foldamer. In the first place, the three monomers of the trimeric sequence were synthesized and later assembled in dimeric and trimeric sequences, as shown on scheme 44.

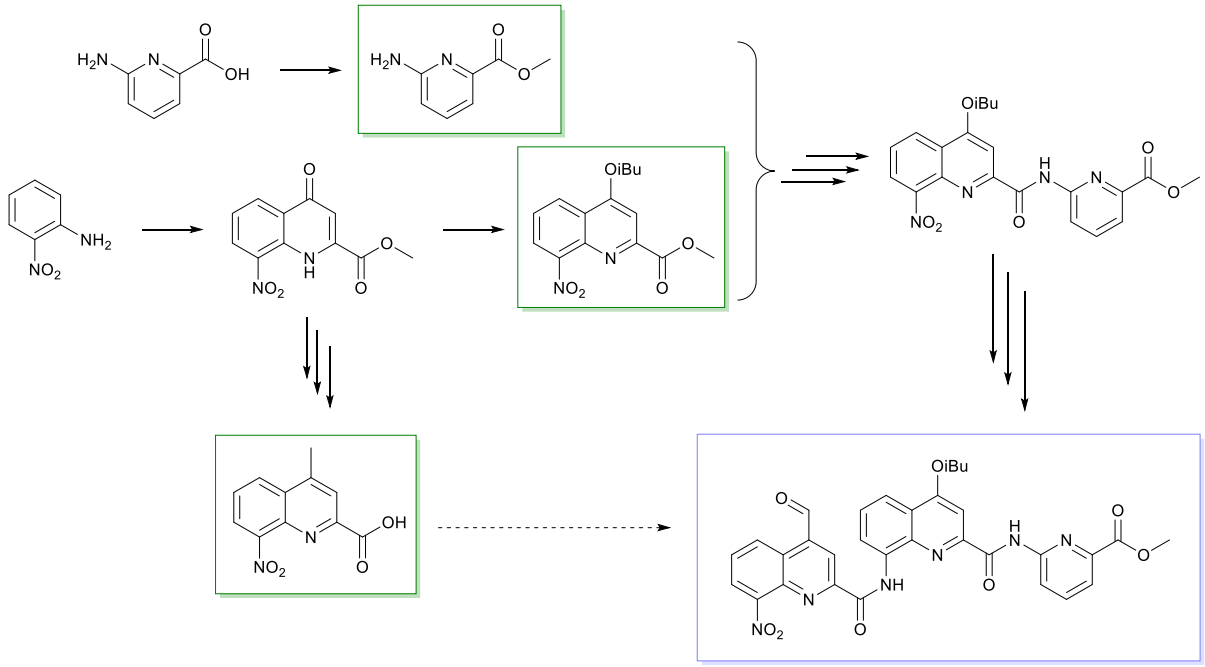

Scheme 44. Synthetic representation of the synthesis of the trimeric PLP-mimic catalyst (framed in purple) by assembling the monomeric units (framed in green).

The aldehyde group of the trimer was obtained by direct functionalization of the trimer by a Vismara oxidation of the methyl group. This allowed to avoid additional protecting and deprotecting steps of the aldehyde group but moreover, it provided a new example of direct functionalization of AOF.

The reactivity of this new species towards a transamination reaction was then tested and demonstrated some encouraging results. Indeed, the trimeric species showed a faster rate of reaction than the monomeric species when the transamination reaction was investigated by adding one equivalent of benzylamine, one equivalent of 2-oxobutanoic acid (sacrificial ketone) and one equivalent of DBU to 10 mol% of the trimeric catalyst in chloroform (scheme 45). In these conditions, the rate of reaction was more than 2 times faster with the trimer than the monomer.

The same experiment was investigated in ethanol but the trend was almost identical between monomer and trimer and it was thus hypothesized that the protic nature of the solvent plays an important role in this catalyzed transamination reaction.

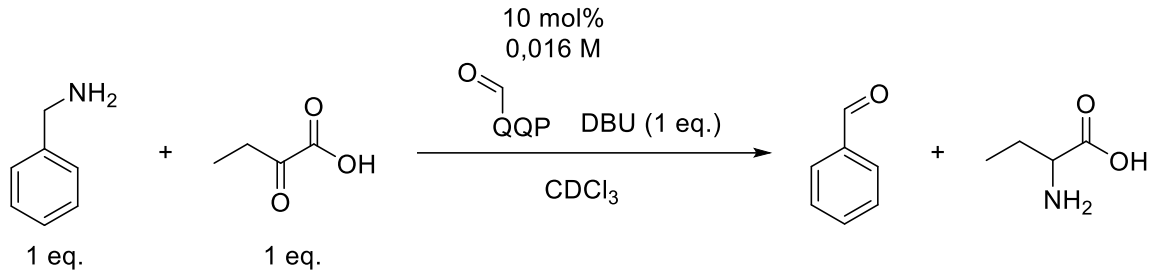

Scheme 45. Conditions of the catalyzed transamination reaction investigated with the trimeric species.

Therefore, such results provide some encouraging insights on the development of a novel type of organocatalyst showing a new type of reactivity not previously reported.

4.2 Outlooks

Concerning the future of this project, in the first place, it could be interesting to investigate other types of reaction with this trimer, such as α-replacement or decarboxylation.

It could also be interesting to synthesize a similar trimer bearing the PLP-mimic unit in position 2 to study the influence of the position of the PLP-mimic on the reactivity (figure 50). Indeed, by modifying its position, we also modify the bulkiness around the PLP-mimic, as well as the nitro group. Changing this strongly electron-withdrawing group by a weaker one could decrease the H-bond donor ability of the opposite hydrogen and therefore make the H-bond with the aldehyde less strong. By doing so, the rotation of the aldehyde will not be as slow as with the nitro group and this could have an influence on the reactivity.

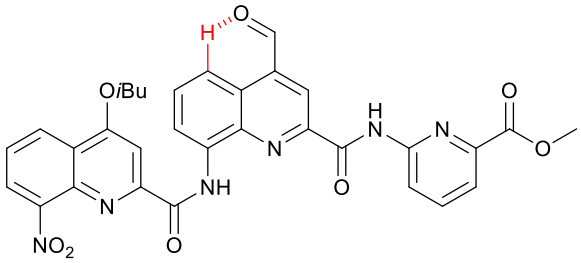

Figure 50. Trimer bearing the PLP-mimic in position 2.

However, the main objective of this project lies in the synthesis of hexamers bearing the PLP-mimic unit. This should be achieved quickly thanks to the combinatorial approach used in this project and thus, by coupling the two trimers synthesized in this work. Hexamers are the

main objective of this project because longer oligomers will allow the folding into a helix presenting more than one turn. For example, hexamers, with their 6 monomers, will allow the folding into a helix presenting 2 turns. In this way, we will be able to functionalize the aromatic unit above the aldehyde group to influence the reactivity of the PLP-mimic (figure 51).

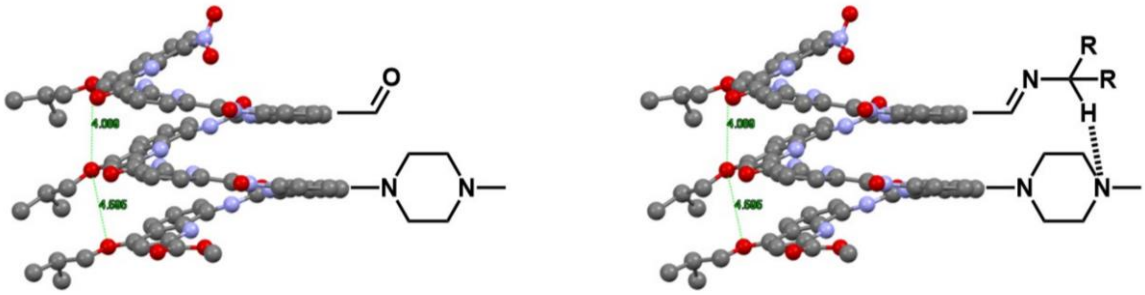

Figure 51. Schematic representation of the functionalization of a residue in close proximity with the PLP-mimic.

For example, we could include a basic group on this residue, that will act as a H-bond acceptor group, in order to form a H-bond with the hydrogen on the C_α of the imine species. By doing so, we could avoid the addition of an exogenous base in the solution for deprotonation, and this would thus give multiple reactivity roles to the foldamer, similarly to what occurs in the PLP-dependent enzymes. This could maybe also provide a method to have selectivity over the type of reaction performed (example: deprotonation versus decarboxylation) by controlling the orientation of the substituents, as suggested by the Dunathan stereoelectronic hypothesis.

5 Experimental section

5.1 Synthesis

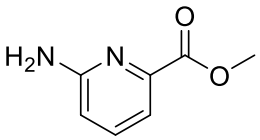

Methyl 6-aminopicolinate (1.2) : *6-amino-picolinic acid* (1.1; 1 eq, 141 mmol, 20 g) is dissolved in 280 mL of methanol and cooled down to 0°C. *Thionyl chloride* (5 eq, 733 mmol, 52 mL) is added and the mixture is stirred at 0°C for 30 minutes and then heated up to 70°C. After 72 hours, the mixture is concentrated by rotary evaporator. The obtained solid is redissolved in DCM and $NaHCO_3$ is added. The aqueous phase is extracted twice and the combined organic layers are then dried over Na_2SO_4 and concentrated by rotary evaporator to yield the pure product 1.2 as a white solid (19.96 g, 82%). **^{1}H NMR (300 MHz, DMSO)** δ 7.51 (dd, *J* = 8.3, 7.3 Hz, 1H), 7.18 (dd, *J* = 7.3, 0.9 Hz, 1H), 6.64 (dd, *J* = 8.3, 0.9 Hz, 1H), 3.79 (s, 3H).

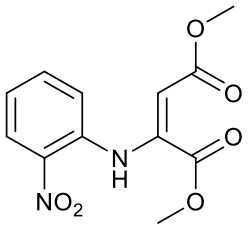

Dimethyl 2-((2-nitrophenyl)amino)maleate : *2-nitroaniline* (1.3, 1 eq, 362 mmol, 50 g) is dissolved in 500 mL of methanol and *dimethyl acetylene dicarboxylate DMAD* (1 eq, 362 mmol, 51.44 g) is added. The mixture is stirred at reflux for 72 hours. The solution is cooled down to room temperature and is evaporated up to ca. 70 mL. The flask is placed at -18°C and let to crystallize for 4 hours. The mixture is filtered and washed with cold methanol to afford the pure product as a yellow solid (43.24 g, 43%). **^{1}H NMR (300 MHz, $CDCl_3$)** δ 11.12 (br s, 1H), 8.14 (dd, *J* = 8.4, 1.6 Hz, 1H), 7.46 (ddd, *J* = 8.6, 7.2, 1.6 Hz, 1H), 7.08 (ddd, *J* = 8.5, 7.3, 1.2 Hz, 1H), 6.76 (dd, *J* = 8.3, 1.2 Hz, 1H), 5.84 (s, 1H), 3.81 (s, 3H), 3.75 (s, 3H).

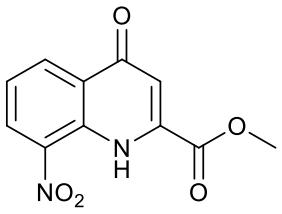

Methyl 8-nitro-4-oxo-1,4-dihydroquinoline-2-carboxylate (1.4; according to a previously reported procedure): A mixture of *2-(2-nitrophenylamino)fumerate* and *polyphosphoric acid PPA* is placed in a round-bottomed flask equipped with a rotor and a mechanical stirrer. Reaction mixture is stirred at 130°C for 3 hours. The solution is cooled to 50°C and poured slowly into a bucket containing saturated $NaHCO_3$ at 0°C for neutralisation. The resulting slurry is filtered with a fine sintered glass funnel and washed several times with distilled water. The brown solid is triturated in methanol and stirred for one hour at room temperature. The flask is subsequently placed at -20°C for 2h for precipitation. The precipitate is filtered, washed with cold methanol and dried under reduced pressure to yield the pure product.

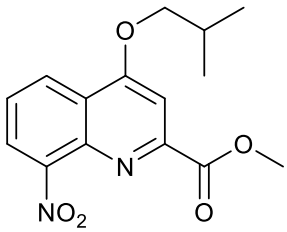

Methyl 4-isobutoxy-8-nitroquinoline-2-carboxylate (1.5): In a flame dried flask under argon atmosphere, *methyl 8-nitro-4-oxo-1,4-dihydroquinoline-2-carboxylate* (1.4, 1 eq, 60.4 mmol, 15 g), *triphenylphosphine* PPh_3 (1.05 eq, 63.5 mmol, 16.64 g) and *isobutanol* (1.1 eq, 66.5 mmol, 6.14 mL) are dissolved in 100 mL of distilled THF. The mixture is cooled down to 0°C and *diisopropyl azodicarboxylate DIAD* (1.05 eq, 63.5 mmol, 12.46 mL) is added dropwise. The mixture is stirred at 0°C for 1 hour and at room temperature for 23 hours. The solvent is evaporated by rotary evaporator and the obtained solid is recrystallized in MeOH/$CHCl_3$ (3:1). The mixture is filtered and the solid is washed with cold methanol to yield the pure product 1.5 (16.31 g, 87%). **^{1}H NMR (600 MHz, $CDCl_3$)** δ 8.48 (ddd, *J* = 8.4, 1.4, 0.5 Hz, 1H), 8.11 (ddd, *J* = 7.5, 1.4, 0.5 Hz, 1H), 7.67 – 7.63 (m, 2H), 4.09 (d, *J* = 6.2 Hz, 2H), 4.06 – 4.02 (m, 3H), 2.31 (hept, *J* = 6.7 Hz, 1H), 1.15 (dd, *J* = 6.8, 0.5 Hz, 6H).

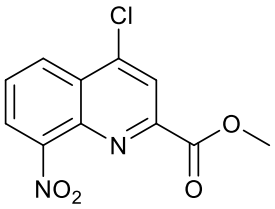

Methyl 4-chloro-8-nitroquinoline-2-carboxylate (1.6): In a flame dried flask under argon atmosphere equipped with a condenser, *methyl 8-nitro-4-oxo-1,4-dihydroquinoline-2-carboxylate* (1.4, 1 eq, 40 mmol, 10 g) is dissolved in $OPCl_3$ (6 eq, 25 mmol, 22.53 mL) and the solution is stirred at reflux for 4 hours. The mixture is poured into 600 mL of icy water and stirred for 30 minutes. The mixture is then filtered and washed with water. The obtained solid is dissolved in DCM and filtrated on silica pad. The filtrate is concentrated by rotary evaporator to yield the pure product 1.6 (10.149 g, 95%). **^{1}H NMR (300 MHz, $CDCl_3$)** δ 8.52 (dd, *J* = 8.6, 1.3 Hz, 1H), 8.40 (s, 1H), 8.16 (dd, *J* = 7.5, 1.4 Hz, 1H), 7.88 – 7.80 (m, 1H), 4.06 (d, *J* = 0.5 Hz, 3H).

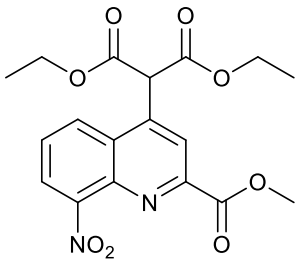

Diethyl 2-(2-(methoxycarbonyl)-8-nitroquinolin-4-yl)malonate (1.7): In a flame dried flask under inert atmosphere, *methyl 4-chloro-8-nitroquinoline-2-carboxylate* (1.6, 1 eq, 7.5 mmol, 2g), K_2CO_3 (3 eq, 22.5 mmol, 3.1 g) and *diethylmalonate* (3 eq, 22.5 mmol, 3.43 mL) are dissolved in 40 mL of anhydrous THF and the mixture is heated up to 75°C. After 48 hours, the solvent is evaporated by rotary evaporator and the obtained solid is dissolved in DCM and washed twice with HCl 0,5 M until the end of the gaseous emission. The combined organic layers are dried over Na_2SO_4 and concentrated by rotary evaporator. The obtained oil is recrystallised in methanol. The precipitate is filtered and washed with cold methanol to yield the pure product 1.7 (2.17 g, 74%). **^{1}H NMR (300 MHz, $CDCl_3$)** δ 8.37 (s, 1H), 8.25 (dd, *J* = 8.7, 1.3 Hz, 1H), 8.08 (dd, *J* = 7.5, 1.3 Hz, 1H), 7.76 (dd, *J* = 8.7, 7.5 Hz, 1H), 5.35 (s, 1H), 4.27 (qd, *J* = 7.1, 1.6 Hz, 4H), 4.04 (s, 3H), 1.25 (t, *J* = 7.1 Hz, 6H).

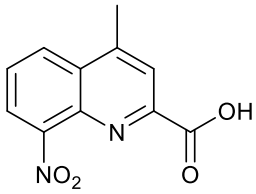

4-methyl-8-nitroquinoline-2-carboxylic acid (1.8): *Diethyl 2-(2-(methoxycarbonyl)-8-nitroquinolin-4-yl)malonate* (1.7,1 eq, 3.7 mmol, 1.45 g) is dissolved in a mixture of 1,4-dioxane/HCl 2M (10:1) and heated up to 110°C for 18 hours. The mixture is concentrated by rotary evaporator and the obtained solid is dissolved in DCM and washed with water. The combined organic layers are dried over Na_2SO_4 and concentrated by rotary evaporator. The obtained solid is recrystalized in $CHCl_3$ to yield the pure product 1.8 (0.2 g, 23%). **^{1}H NMR (300 MHz, DMSO)** δ 8.45 (dd, *J* = 8.5, 1.3 Hz, 1H), 8.33 (dd, *J* = 7.5, 1.3 Hz, 1H), 8.13 (d, *J* = 1.1 Hz, 1H), 7.89 (dd, *J* = 8.5, 7.5 Hz, 1H), 2.83 (d, *J* = 0.9 Hz, 3H).

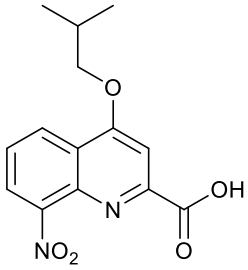

4-isobutoxy-8-nitroquinoline-2-carboxylic acid (2.1): *Methyl 4-isobutoxy-8-nitroquinoline-2-carboxylate* (1.5, 1 eq, 32.7 mmol, 10 g) is dissolved in 440 mL of a mixture THF/water (2:1) and *sodium hydroxide* (2.5 eq, 82.2 mmol, 3.29 g) is added. The mixture is stirred at room temperature for 5 hours and solvents are then evaporated by rotary evaporator. The obtained solid is redissolved in DCM and extracted with citric acid (the aqueous phase must be acidic) and then $NaHCO_3$. The combined organic layers are dried over Na_2SO_4 and concentrated by rotary evaporator to yield the pure product 2.1 (9.44 g, Quant.). **^{1}H NMR (600 MHz, $CDCl_3$)** δ 8.55 (dd, *J* = 8.4, 1.4 Hz, 1H), 8.23 (dd, *J* = 7.5, 1.4 Hz, 1H), 7.76 – 7.71 (m, 2H), 4.14 (d, *J* = 6.4 Hz, 2H), 2.33 (dp, *J* = 13.4, 6.7 Hz, 1H), 1.16 (d, *J* = 6.6 Hz, 6H).

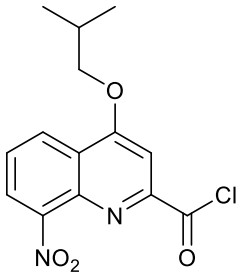

4-isobutoxy-8-nitroquinoline-2-carbonyl chloride (2.2): In a flame dried flask under inert atmosphere, *4-isobutoxy-8-nitroquinoline-2-carboxylic acid* (2.1, 1 eq, 13.2 mmol, 3.82 g) is dissolved in 70 mL of $SOCl_2$ and stirred at 80°C for 3 hours. $SOCl_2$ is then evaporated twice with dry toluene (azeotrope) and dried on the vacuum line to yield the product 2.2 (Quant). **^{1}H NMR (300 MHz, $CDCl_3$)** δ 8.49 (dd, *J* = 8.5, 1.4 Hz, 1H), 8.13 (dd, *J* = 7.5, 1.4 Hz, 1H), 7.73 (dd, *J* = 8.5, 7.5 Hz, 1H), 7.52 (s, 1H), 4.09 (d, *J* = 6.5 Hz, 2H), 2.35 – 2.25 (m, 1H), 1.16 (d, *J* = 6.7 Hz, 6H).

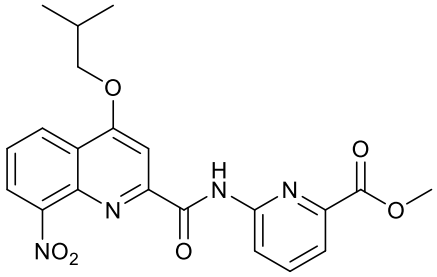

Methyl 3-(4-isobutoxy-8-nitroquinoline-2-carboxamido)picolinate (2.3): In a flame dried flask under inert atmosphere, *methyl 6-aminopicolinate* (1.2, 1 eq, 30.9 mmol, 4.71 g) is dissolved in 100 mL of dry DCM and *triethylamine* Et_3N (5.5 eq, 170.1 mmol, 23.71 mL) is added. The mixture is cooled down to 0°C and a solution of *4-isobutoxy-8-nitroquinoline-2-carbonyl chloride* (2.2, 1 eq, 30.9 mmol, 9.55 g) in 130 mL of dry DCM is added dropwise. The mixture is stirred at room temperature for 18 hours and is then extracted with water (2 times) and $NaHCO_3$ (6 times). The combined organic layers are dried overs Na_2SO_4 and concentrated by rotary evaporator. The obtained solid is recrystalized slowly in MeOH/DCM to yield the pure product 2.3 (6.67 g, 51%). **^{1}H NMR (600 MHz, $CDCl_3$)** δ 10.53 (s, 1H), 8.63 – 8.59 (m, 1H), 8.53 (ddd, *J* = 8.4, 1.4, 0.6 Hz, 1H), 8.18 (ddd, *J* = 7.5, 1.4, 0.6 Hz, 1H), 7.97 – 7.92 (m, 2H), 7.87 – 7.84 (m, 1H), 7.68 (ddd, *J* = 8.2, 7.5, 0.6 Hz, 1H), 4.15 (d, *J* = 6.5 Hz, 2H), 4.04 (d, *J* = 0.7 Hz, 3H), 2.33 (dp, *J* = 13.4, 6.7 Hz, 1H), 1.16 (dd, *J* = 6.8, 0.6 Hz, 6H).

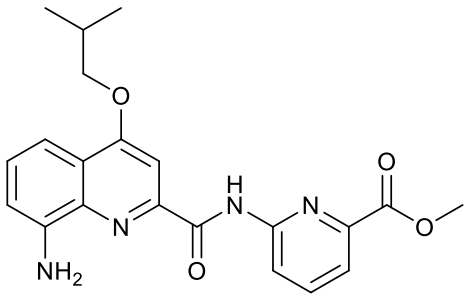

Methyl 6-(8-amino-4-isobutoxyquinoline-2-carboxamido)picolinate (2.4): *Methyl 3-(4-isobutoxy-8-nitroquinoline-2-carboxamido)picolinate* (2.3, 1 eq, 7.1 mmol, 3 g) is dissolved in 300 mL of dry THF and. The mixture is placed under inert atmosphere and *Pd/C 10%* and *ammonium metavanadate* (spatula tip) are added. The flask is placed under hydrogen atmosphere and stirred at room temperature for 18 hours. The mixture is filtered on celite, washed with dry THF and concentrated by rotary evaporator to yield the pure product 2.4 (2.65 g, Quant). **^{1}H NMR (600 MHz, DMSO)** δ 11.49 (s, 1H), 8.39 (dt, *J* = 8.3, 0.9 Hz, 1H), 8.12 – 8.08 (m, 1H), 7.88 (dt, *J* = 7.5, 0.9 Hz, 1H), 7.61 (d, *J* = 0.9 Hz, 1H), 7.36 (ddd, *J* = 8.3, 7.6, 0.9 Hz, 1H), 7.25 (dt, *J* = 8.2, 1.1 Hz, 1H), 6.88 (dt, *J* = 7.7, 1.1 Hz, 1H), 6.72 (br s, 2H), 4.10 (d, *J* = 6.4 Hz, 2H), 3.91 (d, *J* = 0.9 Hz, 3H), 2.20 (dt, *J* = 13.3, 6.7 Hz, 1H), 1.09 (dd, *J* = 6.7, 0.9 Hz, 6H).

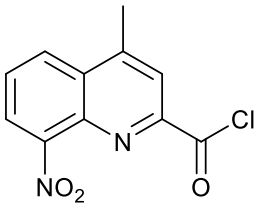

4-methyl-8-nitroquinoline-2-carbonyl chloride (2.5): In a flame dried flask under inert atmosphere, *4-methyl-8-nitroquinoline-2-carboxylic acid* (1.8, 1 eq, 1.1 mmol, 0.25 g) is dissolved in 8 mL of dry DCM. *Oxalyl chloride* (10 eq, 10.8 mmol, 1 mL) and a drop of DMF are then added and the mixture is stirred at room temperature for 4 hours. The solvent is evaporated by rotary evaporator and dried on the vacuum line to yield the product 2.5 and is directly used in the next step.

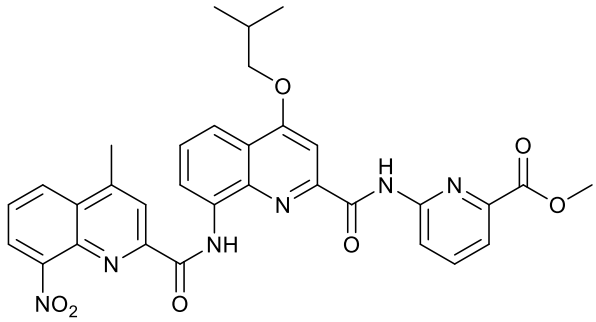

Methyl 6-(4-isobutoxy-8-(4-methyl-8-nitroquinoline-2-carboxamido)quinoline-2-carboxamido) picolinate (2.6): In a flame dried flask under inert atmosphere, *methyl 6-(8-amino-4-isobutoxyquinoline-2-carboxamido)picolinate* (2.4, 1 eq, 1.8 mmol, 708 mg) is dissolved in 25 mL of dry DCM and *triethylamine* Et_3N (5.5 eq, 9.9 mmol, 1.38 mL) is added. The mixture is cooled down to 0°C and a solution of *4-methyl-8-nitroquinoline-2-carbonyl chloride* (2.5, 1 eq, 1.8 mmol, 450 mg) in 20 mL of dry DCM is added dropwise. The mixture is stirred at room temperature for 18 hours and is then extracted with water (1 time), $NaHCO_3$ (3 times) and citric acid (1 time). The combined organic layers are dried overs Na_2SO_4 and concentrated by rotary evaporator. The obtained solid is purified by column chromatography using DCM/AcOEt (from 94/6 to 85/15) to yield the pure product 2.6 (0.485 g, 46%). **^{1}H NMR (300 MHz, DMSO)** δ 11.94 (s, 1H), 10.71 (s, 1H), 8.91 (d, *J* = 7.8 Hz, 1H), 8.62 (d, *J* = 8.1 Hz, 1H), 8.51 (d, *J* = 8.3 Hz, 1H), 8.42 (s, 1H), 8.30 (d, *J* = 6.9 Hz, 1H), 8.14 – 8.07 (m, 1H), 8.03 (d, *J* = 7.4 Hz, 1H), 7.92 – 7.86 (m, 1H), 7.84 – 7.75 (m, 3H), 4.24 (d, *J* = 6.4 Hz, 2H), 3.30 (s, 3H), 2.98 – 2.93 (m, 3H), 1.12 (d, *J* = 6.8 Hz, 6H). The signal for one proton is hidden behind solvents signals.

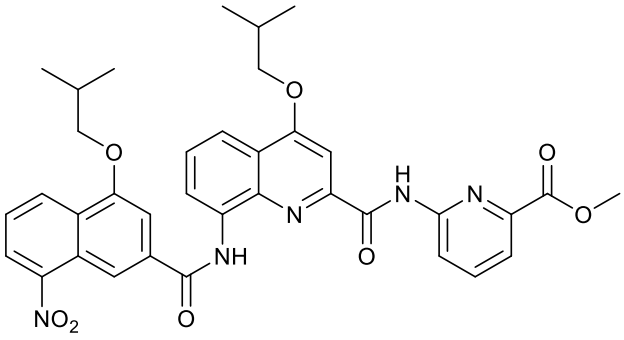

Methyl 6-(4-isobutoxy-8-(4-isobutoxy-8-nitro-2-naphthamido)quinoline-2-carboxamido)picolinate (2.7): In a flame dried flask under inert atmosphere, *methyl 6-(8-amino-4-isobutoxyquinoline-2-carboxamido)picolinate* (2.4, 1 eq, 2.3 mmol, 894 mg) is dissolved in 30 mL of dry DCM and *triethylamine* Et_3N (5.5 eq, 12.5 mmol, 1.74 mL) is added. The mixture is

cooled down to 0°C and a solution of *4-isobutoxy-8-nitroquinoline-2-carbonyl chloride* (2.2, 1 eq, 2.3 mmol, 700 mg) in 20 mL of dry DCM is added dropwise. The mixture is stirred at room temperature for 18 hours and is then extracted with water (3 times), $NaHCO_3$ (3 times) and citric acid (1 time). The combined organic layers are dried overs Na_2SO_4 and concentrated by rotary evaporator to yield the pure product 2.6 (1.38 g, 91%). **^{1}H NMR (600 MHz, $CDCl_3$)** δ 12.10 (d, *J* = 4.5 Hz, 1H), 10.68 (d, *J* = 4.4 Hz, 1H), 9.02 – 8.95 (m, 1H), 8.65 (ddd, *J* = 41.7, 8.4, 4.4 Hz, 2H), 8.25 – 8.18 (m, 1H), 8.06 (dd, *J* = 8.5, 4.5 Hz, 1H), 7.96 (dd, *J* = 10.8, 5.5 Hz, 2H), 7.88 (dd, *J* = 7.8, 4.4 Hz, 1H), 7.82 (d, *J* = 4.5 Hz, 1H), 7.67 (dq, *J* = 31.8, 5.8, 3.6 Hz, 2H), 4.17 (dt, *J* = 36.5, 5.6 Hz, 4H), 3.43 – 3.37 (m, 3H), 2.35 (tq, *J* = 14.1, 7.6, 7.1 Hz, 2H), 1.18 (dt, *J* = 7.1, 5.0 Hz, 12H).

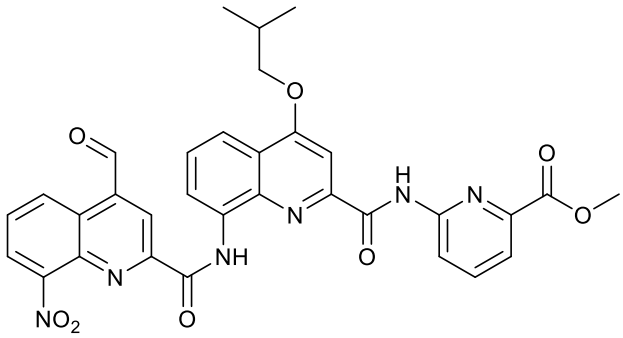

Methyl 6-(8-(4-formyl-8-nitroquinoline-2-carboxamido)-4-isobutoxyquinoline-2-carboxamido) picolinate (2.8): *Methyl 6-(4-isobutoxy-8-(4-methyl-8-nitroquinoline-2-carboxamido)quinoline-2-carboxamido)picolinate* (2.6, 1 eq, 164 µmol, 100 mg) is dissolved in 0,72 mL of DMSO and *trifluoroacetic acid* (1.25 eq, 205 µmol, 0.015 mL), *tert-butyl iodide* (0.22 eq, 36 µmol, 0.004 mL), *diiodine* (1 eq, 164 µmol, 41.7 mg) and *iron(II) chloride* (spatula tip) are added. The mixture is let to run for 72 hours at 80°C and then, for 18 hours at 120°C. DCM is added and the organic phase is extracted with large quantities (compared to DMSO) of saturated $Na_2S_2O_3$ (3 times) and then, with Na_2CO_3 10% (3 times). The combined organic layers are dried over Na_2SO_4 and concentrated by rotary evaporator. The obtained product is filtered on a silica pad (DCM/AcOEt 90/10) to afford the pure product 2.8 (54 mg, 53%). **^{1}H NMR (600 MHz, DMSO)** δ 11.93 (s, 1H), 10.77 (s, 1H), 10.75 (d, *J* = 1.1 Hz, 1H), 9.38 (d, *J* = 8.5 Hz, 1H), 9.03 (d, *J* = 1.1 Hz, 1H), 8.94 (d, *J* = 7.6 Hz, 1H), 8.53 (d, *J* = 8.2 Hz, 1H), 8.43 (d, *J* = 7.4 Hz, 1H), 8.12 (t, *J* = 7.9 Hz, 1H), 8.10 – 8.06 (m, 2H), 7.86 – 7.80 (m, 2H), 7.78 (d, *J* = 0.9 Hz, 1H), 4.26 (d, *J* = 6.5 Hz, 2H), 2.27 (dt, *J* = 13.4, 6.7 Hz, 1H), 1.13 (dd, *J* = 6.7, 1.1 Hz, 6H). The signal for three protons of a methyl group is hidden behind solvent signals.

5.2 Catalytic assays

For all trimeric catalytic assays carried out in this master's thesis, the protocol is the following:

In a flask, vial or NMR tube, the *trimeric PLP-mimic* (10 mol%) and *trimethoxybenzene* (0.1 eq.) are dissolved in the chosen solvent (0,016 M). A first ^{1}H NMR spectrum is realized. *Benzylamine* (1 eq.) and *sacrificial oxygen donor* (1 eq.) are added to the mixture, followed by *the base* (1 eq.). The reaction is let to run for several days and ^{1}H NMR spectra are realized after 30 minutes, 60 minutes, 90 minutes, 2 hours, 5 hours, 24 hours and 72 hours.

5.3 ^{1}H NMR spectra

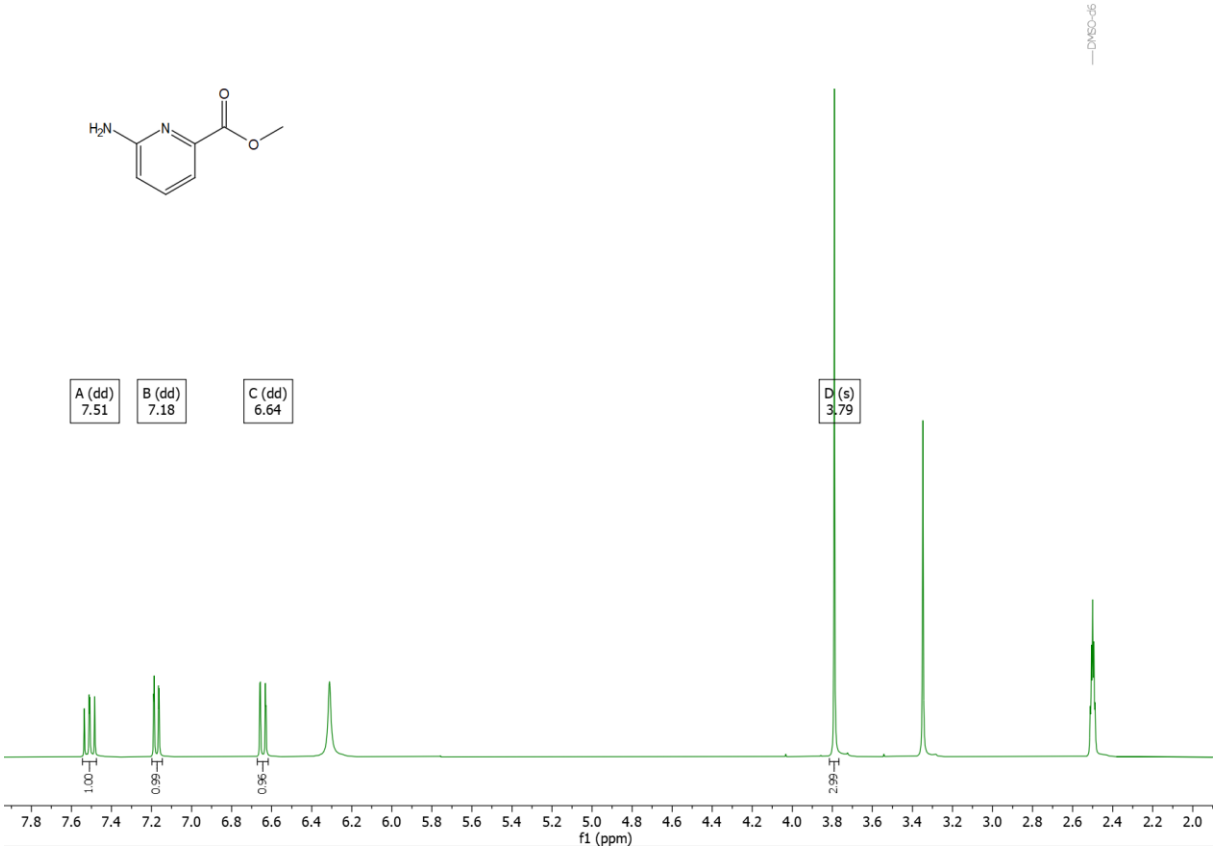

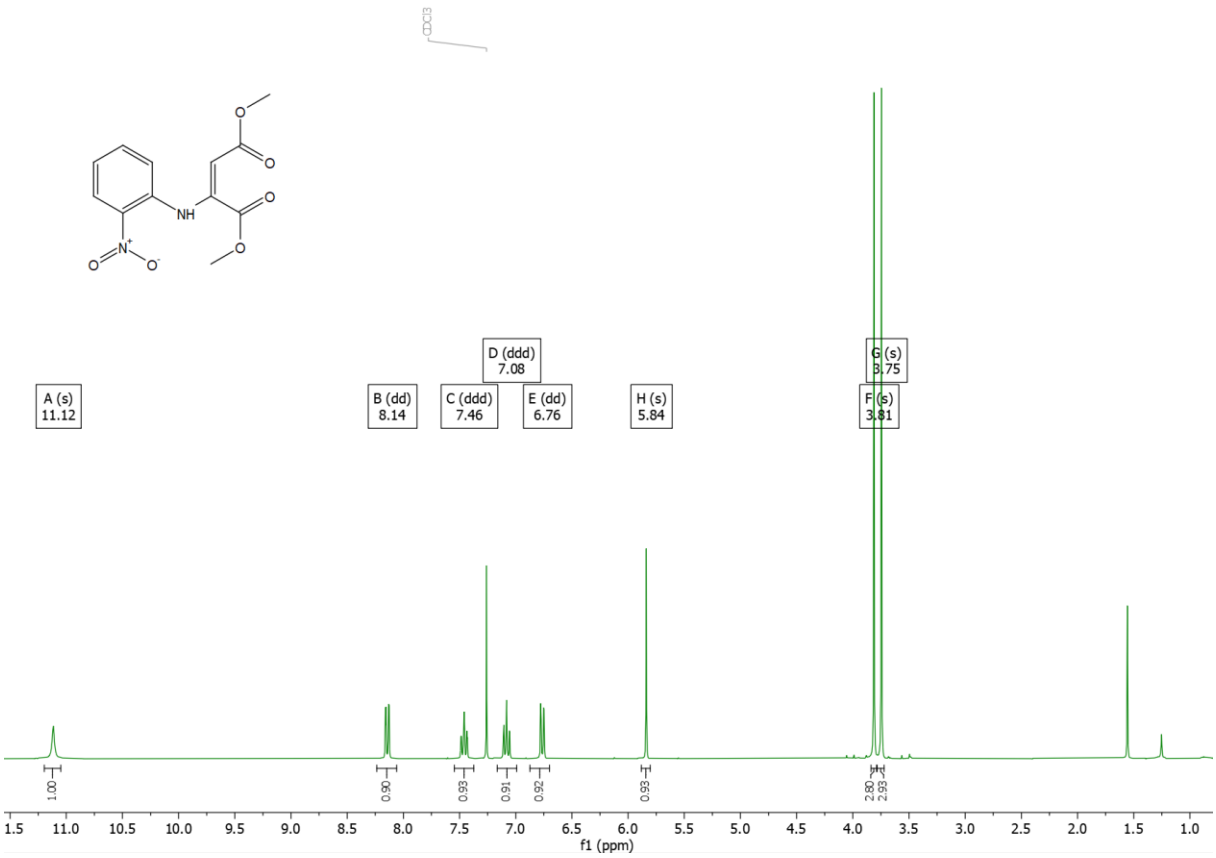
CDCl3
NH
A (s)
11.12
B (dd)
8.14
C (ddd)
7.46
D (ddd)
7.08
E (dd)
6.76
H (s)
5.84
F (s)
3.81
G (s)
3.75
1.00
0.90
0.93
0.91
0.92
0.93
2.80
2.93
f1 (ppm)

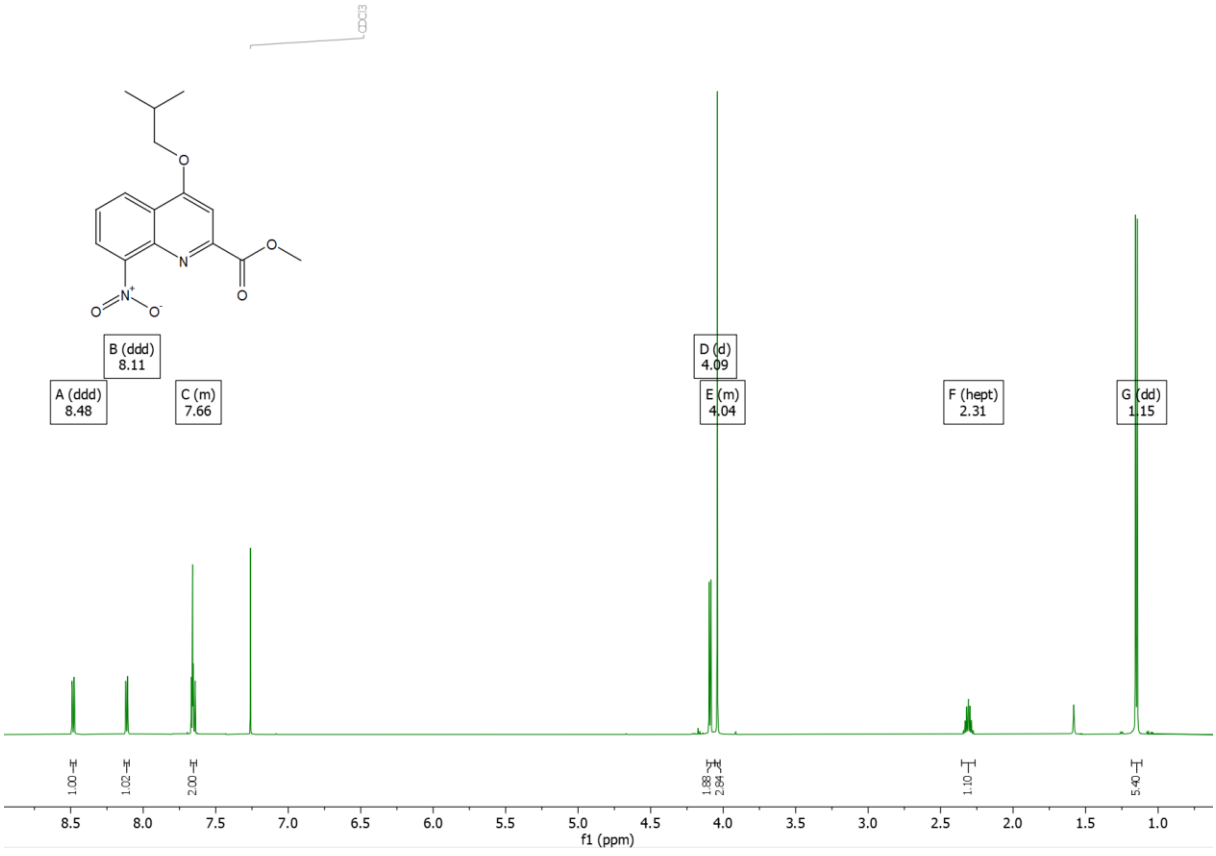
CDCl3
A (ddd)
8.48
B (ddd)
8.11
C (m)
7.66
D (d)
4.09
E (m)
4.04
F (hept)
2.31
G (dd)
1.15
1.00
1.02
2.00
1.88
2.84
1.10
5.40
f1 (ppm)

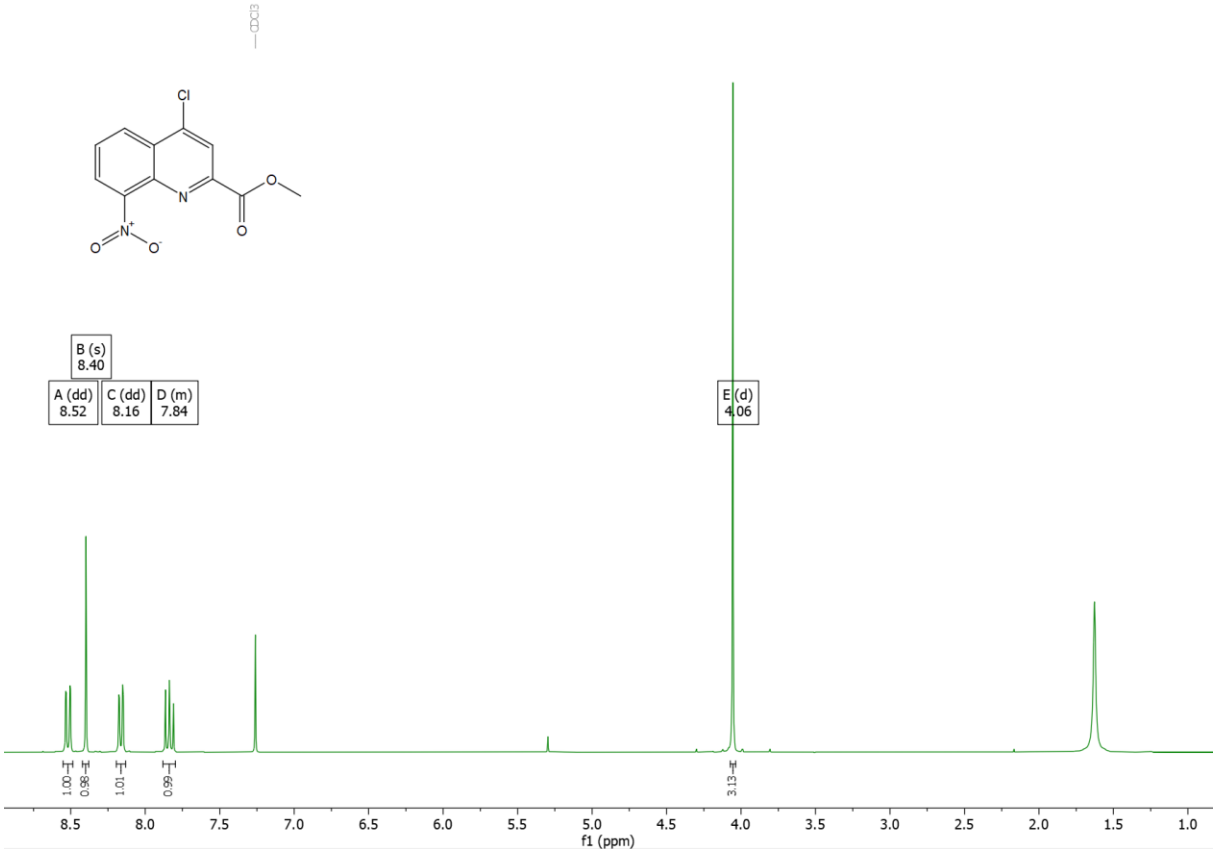
Cl
N
O
O
O
N+
O-
B (s)
8.40
A (dd)
8.52
C (dd)
8.16
D (m)
7.84
E (d)
4.06
1.00
0.98
1.01
0.99
3.13
8.5
8.0
7.5
7.0
6.5
6.0
5.5
5.0
4.5
4.0
3.5
3.0
2.5
2.0
1.5
1.0
f1 (ppm)

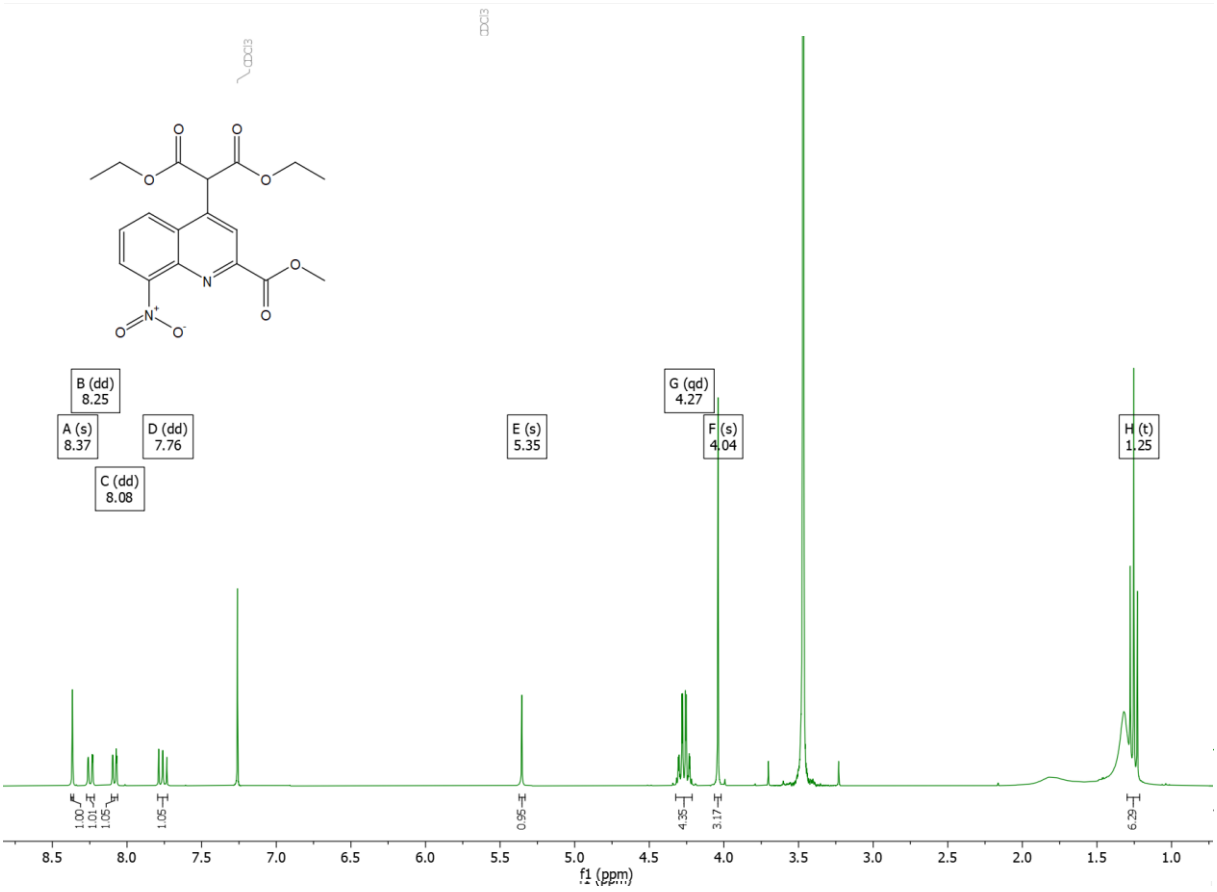
O
O
O
O
N
O
O
N+
O-
B (dd)
8.25
A (s)
8.37
D (dd)
7.76
C (dd)
8.08
E (s)
5.35
G (qd)
4.27
F (s)
4.04
H (t)
1.25
1.00
1.01
1.05
1.05
0.95
4.35
3.17
6.29
8.5
8.0
7.5
7.0
6.5
6.0
5.5
5.0
4.5
4.0
3.5
3.0
2.5
2.0
1.5
1.0
f1 (ppm)

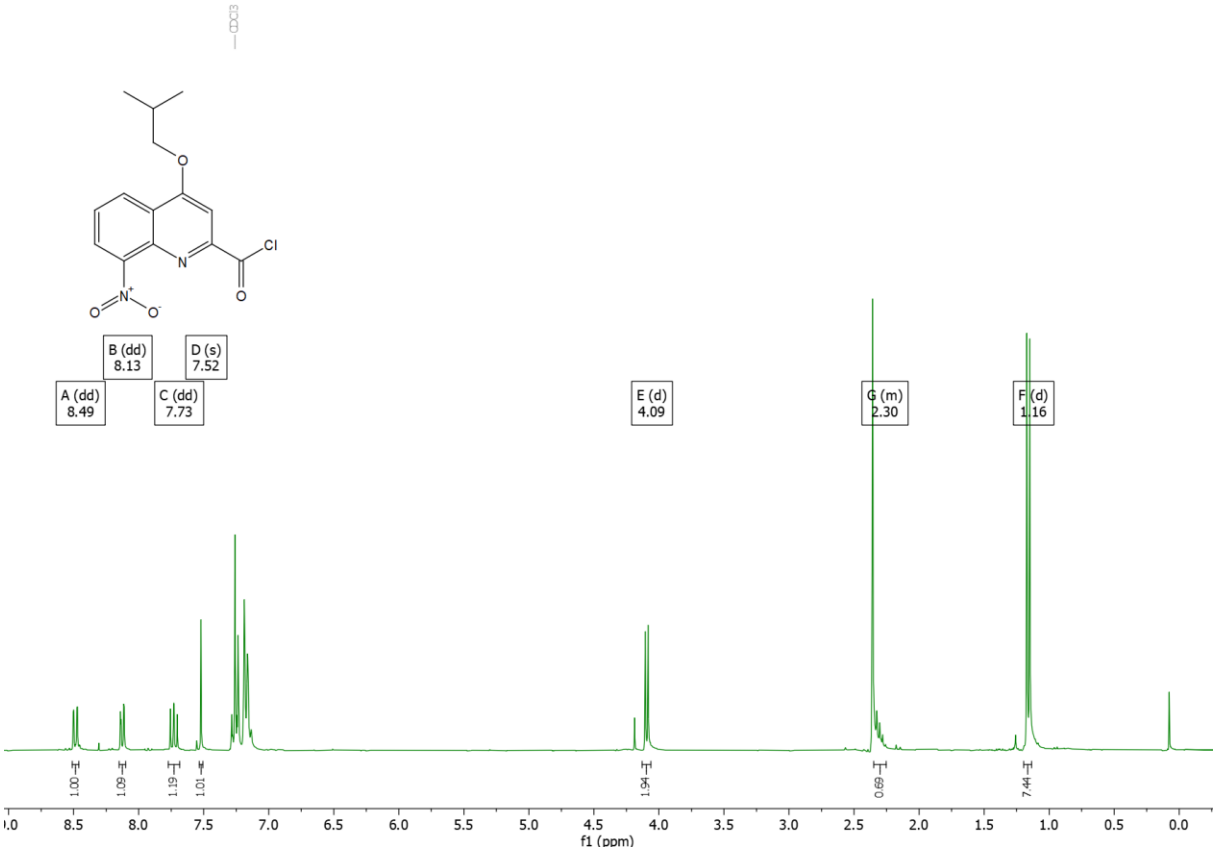
B (dd)
8.13
D (s)
7.52
A (dd)
8.49
C (dd)
7.73
E (d)
4.09
G (m)
2.30
F (d)
1.16
1.00
1.09
1.19
1.01
1.94
0.69
7.44
f1 (ppm)

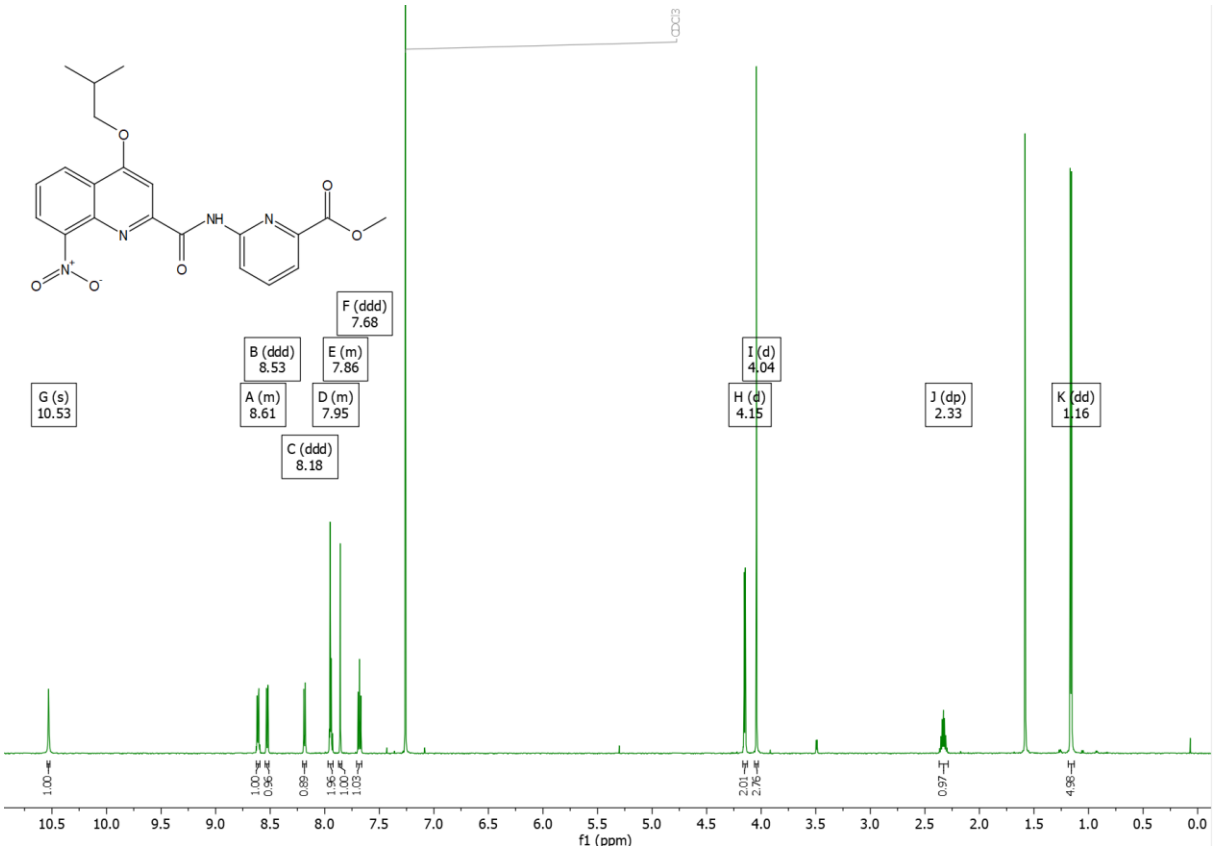
F (ddd)
7.68
B (ddd)
8.53
E (m)
7.86
I (d)
4.04
G (s)
10.53
A (m)
8.61
D (m)
7.95
H (d)
4.15
J (dp)
2.33
K (dd)
1.16
C (ddd)
8.18
1.00
1.00
0.96
0.89
1.96
1.00
1.03
2.01
2.76
0.97
4.98
f1 (ppm)

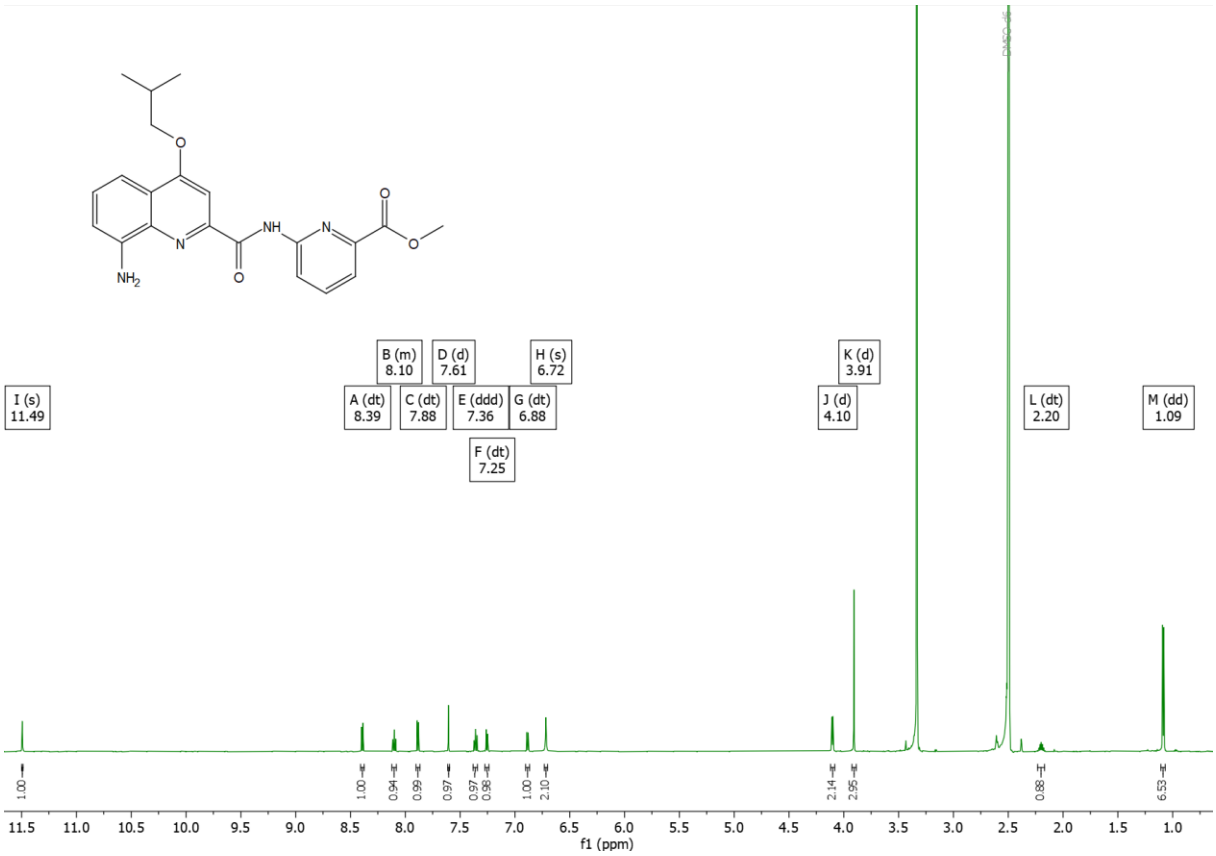
I (s) 11.49
A (dt) 8.39
B (m) 8.10
C (dt) 7.88
D (d) 7.61
E (ddd) 7.36
F (dt) 7.25
G (dt) 6.88
H (s) 6.72
J (d) 4.10
K (d) 3.91
L (dt) 2.20
M (dd) 1.09
f1 (ppm)

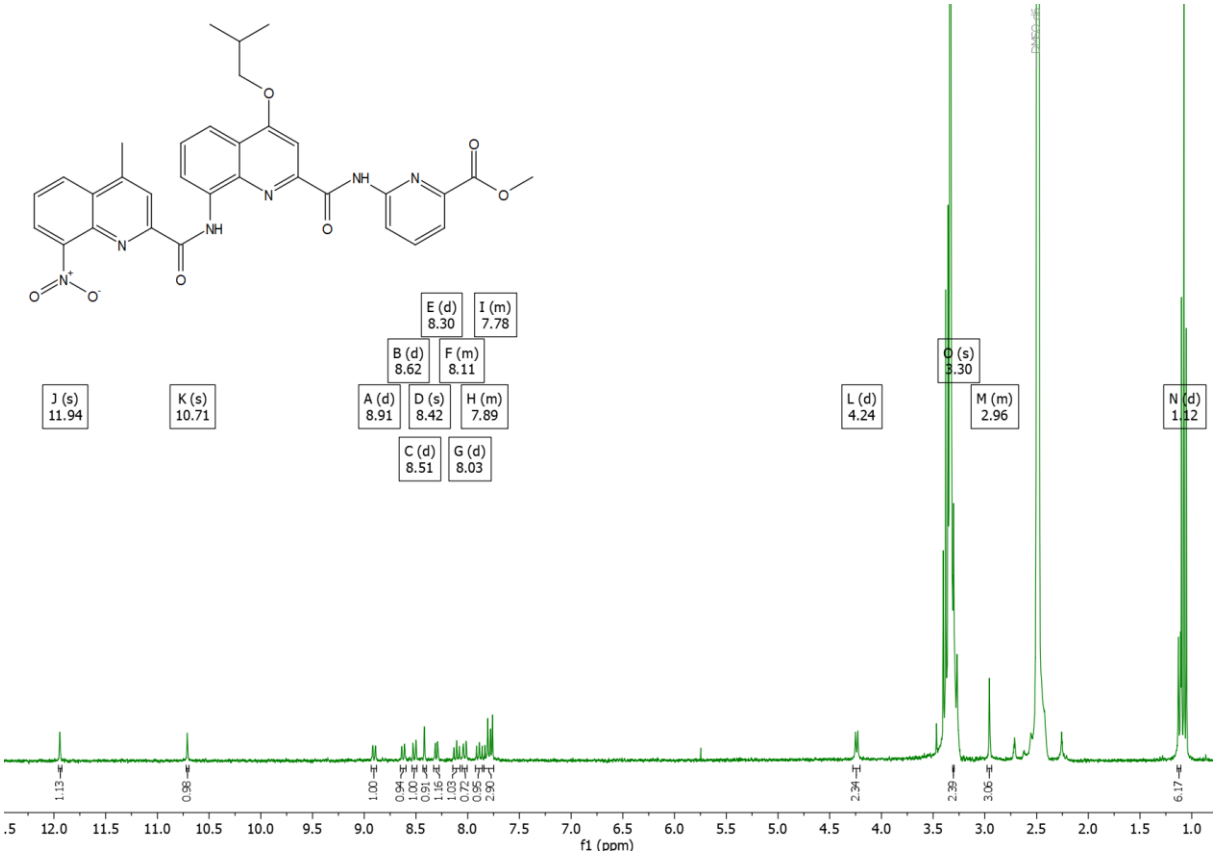
J (s) 11.94
K (s) 10.71
A (d) 8.91
B (d) 8.62
C (d) 8.51
D (s) 8.42
E (d) 8.30
F (m) 8.11
G (d) 8.03
H (m) 7.89
I (m) 7.78
L (d) 4.24
M (m) 2.96
N (d) 1.12
O (s) 8.30
f1 (ppm)

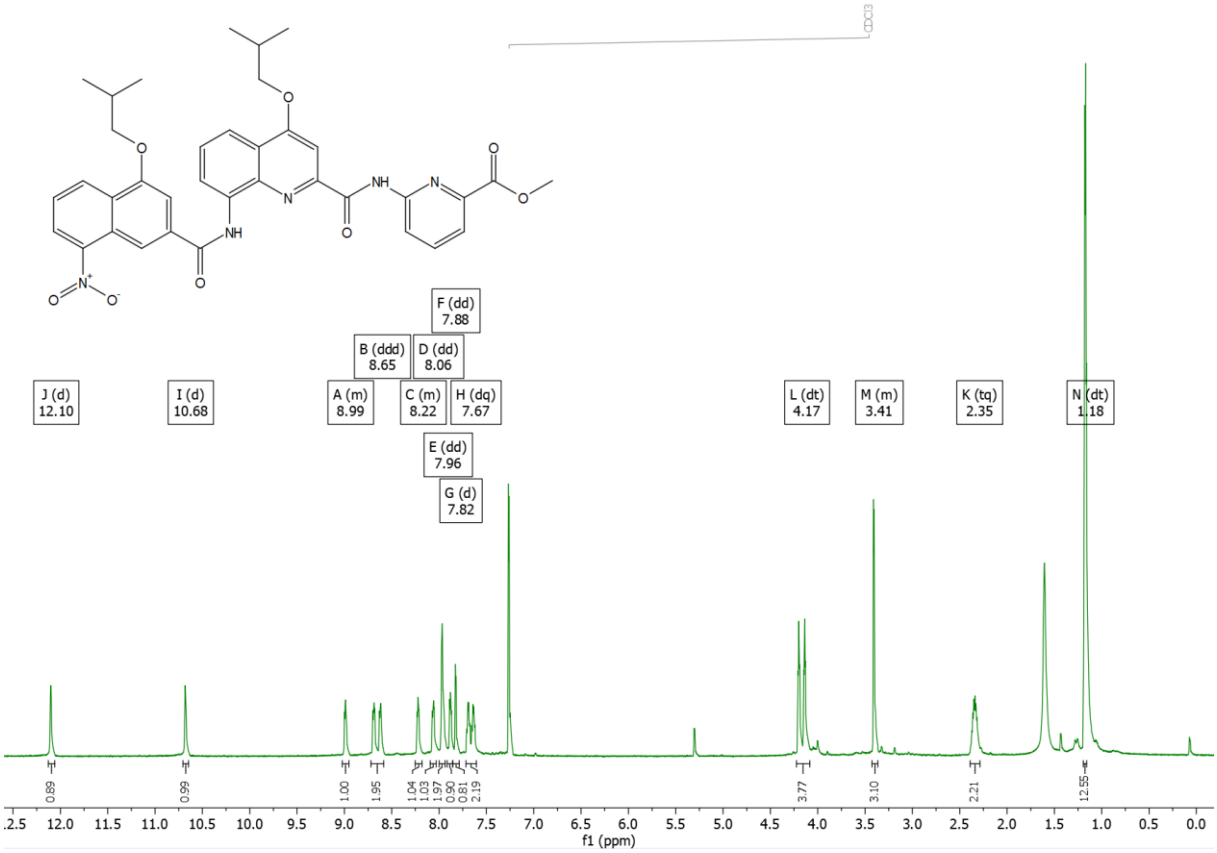
F (dd) 7.88
B (ddd) 8.65
D (dd) 8.06
J (d) 12.10
I (d) 10.68
A (m) 8.99
C (m) 8.22
H (dq) 7.67
L (dt) 4.17
M (m) 3.41
K (tq) 2.35
N (dt) 1.18
E (dd) 7.96
G (d) 7.82
f1 (ppm)

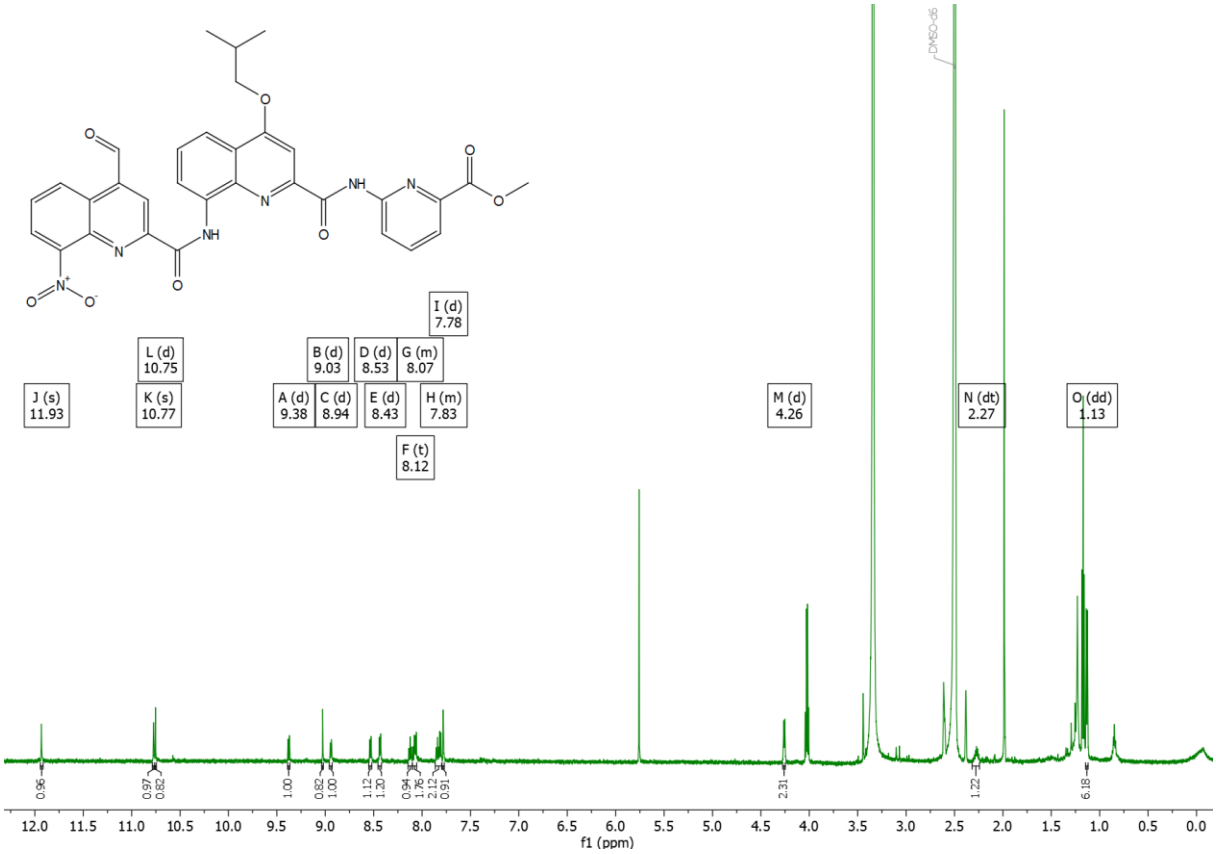
I (d) 7.78
L (d) 10.75
B (d) 9.03
D (d) 8.53
G (m) 8.07
J (s) 11.93
K (s) 10.77
A (d) 9.38
C (d) 8.94
E (d) 8.43
H (m) 7.83
F (t) 8.12
M (d) 4.26
N (dt) 2.27
O (dd) 1.13
f1 (ppm)

[1] Breslow, R. (2009). Biomimetic Chemistry : Biology as an inspiration. *Journal of Biological Chemistry*, *284*(3), 1337-1342. https://doi.org/10.1074/jbc.x800011200

[2] Breslow, R. (1995). Biomimetic Chemistry and Artificial Enzymes : Catalysis by design. *Accounts of Chemical Research*, *28*(3), 146-153. https://doi.org/10.1021/ar00051a008

[3] Piumetti, M., & Illanes, A. (2022). Enzymes and Their Function. Dans *Springer eBooks* (p. 23-53). https://doi.org/10.1007/978-3-030-88500-7_2

[4] Robinson, P. (2015). Enzymes : principles and biotechnological applications. *Essays In Biochemistry*, *59*, 1-41. https://doi.org/10.1042/bse0590001

[5] Blanco, A., & Blanco, G. (2022). Enzymes. Dans *Elsevier eBooks* (p. 165-190). https://doi.org/10.1016/b978-0-323-91599-1.00029-8

[6] Jennings, I. (1970). Enzymes. Dans *Elsevier eBooks* (p. 11-24). https://doi.org/10.1016/b978-0-433-17320-5.50006-5

[7] Kirschning, A. (2020). Coenzymes and Their Role in the Evolution of Life. *Angewandte Chemie*, *60*(12), 6242-6269. https://doi.org/10.1002/anie.201914786

[8] Stach, K., Stach, W., & Augoff, K. (2021). Vitamin B6 in Health and Disease. *Nutrients*, *13*(9), 3229. https://doi.org/10.3390/nu13093229

[9] Parra, M., Stahl, S., & Hellmann, H. (2018). Vitamin B6 and Its Role in Cell Metabolism and Physiology. *Cells*, *7*(7), 84. https://doi.org/10.3390/cells7070084

[10] Harris, E. D. (2013). Cofactors : organic. Dans *Elsevier eBooks* (p. 366-377). https://doi.org/10.1016/b978-0-12-375083-9.00058-1

[11] Mooney, S., Leuendorf, J., Hendrickson, C. L., & Hellmann, H. (2009). Vitamin B6 : A Long Known Compound of Surprising Complexity. *Molecules*, *14*(1), 329-351. https://doi.org/10.3390/molecules14010329

[12] John, R. A. (1995). Pyridoxal phosphate-dependent enzymes. *Biochimica et Biophysica Acta (BBA) - Proteins And Proteomics*, *1248*(2), 81-96. https://doi.org/10.1016/0167-4838(95)00025-p

[13] Rocha, J. F., Pina, A. F., Sousa, S. F., & Cerqueira, N. M. F. S. A. (2019). PLP-dependent enzymes as important biocatalysts for the pharmaceutical, chemical and food industries : a structural and mechanistic perspective. *Catalysis Science & Technology*, *9*(18), 4864-4876. https://doi.org/10.1039/c9cy01210a

[14] Sagong, H., & Kim, K. (2017). Lysine Decarboxylase with an Enhanced Affinity for Pyridoxal 5-Phosphate by Disulfide Bond-Mediated Spatial Reconstitution. *PLOS ONE*, *12*(1), e0170163. https://doi.org/10.1371/journal.pone.0170163

[15] Rui, J., You, S., Zheng, Y., Wang, C., Gao, Y., Zhang, W., Qi, W., Su, R., & He, Z. (2020). High-efficiency and low-cost production of cadaverine from a permeabilized-cell bioconversion by a Lysine-induced engineered Escherichia coli. *Bioresource Technology*, *302*, 122844. https://doi.org/10.1016/j.biortech.2020.122844

[16] Ma, W., Cao, W., Zhang, B., Chen, K., Liu, Q., Li, Y., & Ouyang, P. (2015). Engineering a pyridoxal 5'-phosphate supply for cadaverine production by using Escherichia coli whole-cell biocatalysis. *Scientific Reports*, *5*(1). https://doi.org/10.1038/srep15630

[17] Kino, K., Nakajima, Y., Yanagawa, H., Gawasawa, R., & Hirasawa, I. (2021). Enzymatic Synthesis of l - threo -β-Hydroxy-α-Amino Acids via Asymmetric Hydroxylation Using 2-Oxoglutarate-Dependent Hydroxylase from Sulfobacillus thermotolerans Strain Y0017. *Applied And Environmental Microbiology*, *87*(20). https://doi.org/10.1128/aem.01335-21

[18] Xi, Z., Li, L., Zhang, X., Jiang, Z., Zhang, R., Xu, Y., & Zhang, W. (2023). Expanding the L-threonine transaldolase toolbox for the diastereomeric synthesis of β-hydroxy-α-amino acids. *Molecular Catalysis*, *543*, 113139. https://doi.org/10.1016/j.mcat.2023.113139

[19] Martino, L., Budiša, N., & Contestabile, R. (2013). PLP-dependent Enzymes : a Powerful Tool for Metabolic Synthesis of Non-canonical Amino Acids 1. *Beilstein Institut*. https://www.beilstein-institut.de/download/65/plp-dependent_enzymes_a_powerful_tool_for_metabolic_synthesis_of_non-canonical_amino_acids_.pdf

[20] Du, Y., & Ryan, K. S. (2019). Pyridoxal phosphate-dependent reactions in the biosynthesis of natural products. *Natural Product Reports*, *36*(3), 430-457. https://doi.org/10.1039/c8np00049b

[21] Alexander, F. W., Sandmeier, E., Mehta, P. K., & Christen, P. (1994). Evolutionary relationships among pyridoxal-5′-phosphate-dependent enzymes. *European Journal Of Biochemistry*, *219*(3), 953-960. https://doi.org/10.1111/j.1432-1033.1994.tb18577.x

[22] Schneider, G., Käck, H., & Lindqvist, Y. (2000). The manifold of vitamin B6 dependent enzymes. *Structure*, *8*(1), R1-R6. https://doi.org/10.1016/s0969-2126(00)00085-x

[23] Jansonius, J. N. (1998). Structure, evolution and action of vitamin B6-dependent enzymes. *Current Opinion In Structural Biology*, *8*(6), 759-769. https://doi.org/10.1016/s0959-440x(98)80096-1

[24] Dunathan, H. C. (1966). Conformation and reaction specificity in pyridoxal phosphate enzymes. *Proceedings Of The National Academy Of Sciences Of The United States Of America*, *55*(4), 712-716. https://doi.org/10.1073/pnas.55.4.712

[25] Eliot, A. C., & Kirsch, J. F. (2004). Pyridoxal Phosphate Enzymes : Mechanistic, Structural, and Evolutionary Considerations. *Annual Review Of Biochemistry*, *73*(1), 383-415. https://doi.org/10.1146/annurev.biochem.73.011303.074021

[26] Toney, M. D. (2005). Reaction specificity in pyridoxal phosphate enzymes. *Archives Of Biochemistry And Biophysics*, *433*(1), 279-287. https://doi.org/10.1016/j.abb.2004.09.037

[27] Metzler, D. E., & Snell, E. E. (1952). DEAMINATION OF SERINE. *Journal Of Biological Chemistry*, *198*(1), 353-361. https://doi.org/10.1016/s0021-9258(18)55589-7

[28] Kuzuhara, H., Komatsu, T., & Emoto, S. (1978). Synthesis of a chiral pyridoxamine analog and nonenzymatic stereoselective transamination. *Tetrahedron Letters*, *19*(38), 3563-3566. https://doi.org/10.1016/s0040-4039(01)94995-0

[29] Tachibana, Y., Ando, M., & Kuzuhara, H. (1982). ASYMMETRIC SYNTHESIS OF A-AMINO ACIDS BY NONENZYMATIC TRANSAMINATION. VERSATILITY OF THE REACTION AND ENANTIOMERIC EXCESSES OF THE PRODUCTS. *Chemistry Letters*, *11*(11), 1765-1768. https://doi.org/10.1246/cl.1982.1765

[30] Zhou, W., Yerkes, N., Chruma, J. J., Liu, L., & Breslow, R. (2005). Chiral polyamines from reduction of polypeptides : asymmetric pyridoxamine-mediated transaminations. *Bioorganic & Medicinal Chemistry Letters*, *15*(5), 1351-1355. https://doi.org/10.1016/j.bmcl.2005.01.021

[31] Zimmerman, S. C., Czarnik, A. W., & Breslow, R. (1983). Intramolecular general base-acid catalysis in transaminations catalyzed by pyridoxamine enzyme analogs. *Journal Of The American Chemical Society*, *105*(6), 1694-1695. https://doi.org/10.1021/ja00344a069

[32] Breslow, R. (1986). Biomimetic Control of Chemical Selectivity. Dans *Springer eBooks* (p. 185-197). https://doi.org/10.1007/978-3-642-70926-5_15

[33] Breslow, R., Czarnik, A. W., Lauer, M., Leppkes, R., Winkler, J. D., & Zimmerman, S. C. (1986). Mimics of transaminase enzymes. *Journal Of The American Chemical Society*, *108*(8), 1969-1979. https://doi.org/10.1021/ja00268a040

[34] Breslow, R., Chmielewski, J., Foley, D., Johnson, B. D., Kumabe, N., Varney, M. D., & Mehra, R. (1988). Optically Active Amino Acid Synthesis by Artificial Transaminase Enzymes. *Tetrahedron*, *44*(17), 5515-5524. https://doi.org/10.1016/s0040-4020(01)86057-9

[35] Chen, J., Gong, X., Li, J., Li, Y., Ma, J., Hou, C., Zhao, G., Yuan, W., & Zhao, B. (2018). Carbonyl catalysis enables a biomimetic asymmetric Mannich reaction. *Science*, *360*(6396), 1438-1442. https://doi.org/10.1126/science.aat4210

[36] Gellman, S. H. (1998). Foldamers : A manifesto. *Accounts Of Chemical Research*, *31*(4), 173-180. https://doi.org/10.1021/ar960298r

[37] Huc, I., Kwon, S., & Lee, H. (2021). Synthetic Foldamers : Rational Design of Advanced Structures with Diverse Applications. *ChemPlusChem*, *86*(8), 1042-1043. https://doi.org/10.1002/cplu.202100288

[38] Hill, D. J. T., Mio, M. J., Prince, R. B., Hughes, T. S., & Moore, J. S. (2001). A Field Guide to Foldamers. *Chemical Reviews*, *101*(12), 3893-4012. https://doi.org/10.1021/cr990120t

[39] Goodman, C., Choi, S., Shandler, S. J., & DeGrado, W. F. (2007). Foldamers as versatile frameworks for the design and evolution of function. *Nature Chemical Biology*, *3*(5), 252-262. https://doi.org/10.1038/nchembio876

[40] Pasco, M., Dolain, C., & Guichard, G. (2017). Foldamers in Medicinal Chemistry. Dans *Elsevier eBooks* (p. 89-125). https://doi.org/10.1016/b978-0-12-409547-2.12565-x

[41] Seebàch, D., Overhand, M., Kühnle, F. N. M., Martinoni, B., Oberer, L., Hommel, U., & Widmer, H. (1996). β-Peptides : Synthesis by Arndt-Eistert homologation with concomitant peptide coupling. Structure determination by NMR and CD spectroscopy and by X-ray crystallography. Helical secondary structure of a β-hexapeptide in solution and its stability towards pepsin. *Helvetica Chimica Acta*, *79*(4), 913-941. https://doi.org/10.1002/hlca.19960790402

[42] Appella, D. H., Christianson, L. A., Karle, I. L., Powell, A. D. R., & Gellman, S. H. (1996). β-Peptide Foldamers : Robust Helix Formation in a New Family of β-Amino Acid Oligomers. *Journal Of The American Chemical Society*, *118*(51), 13071-13072. https://doi.org/10.1021/ja963290l

[43] Seebàch, D., & Matthews, J. L. (1997). β-Peptides : a surprise at every turn. *Chemical Communications*, *21*, 2015-2022. https://doi.org/10.1039/a704933a

[44] Raguse, T. L., Lai, J. R., LePlae, P. R., & Gellman, S. H. (2001). Toward β-Peptide Tertiary Structure : Self-Association of an Amphiphilic 14-Helix in Aqueous Solution. *Organic Letters*, *3*(24), 3963-3966. https://doi.org/10.1021/ol016868r

[45] Horne, W. S., & Gellman, S. H. (2008). Foldamers with Heterogeneous Backbones. *Accounts Of Chemical Research*, *41*(10), 1399-1408. https://doi.org/10.1021/ar800009n

[46] Girvin, Z. C., & Gellman, S. H. (2020). Foldamer catalysis. *Journal Of The American Chemical Society*, *142*(41), 17211-17223. https://doi.org/10.1021/jacs.0c07347

[47] Müller, M. A., Windsor, M. A., Pomerantz, W. C., Gellman, S. H., & Hilvert, D. (2009). A rationally designed Aldolase foldamer. *Angewandte Chemie*, *121*(5), 940-943. https://doi.org/10.1002/ange.200804996

[48] Semetey, V., Rognan, D., Hemmerlin, C., Graff, R., Briand, J., Marraud, M., & Guichard, G. (2002b). Stable Helical Secondary Structure in Short-Chain N,N′-Linked Oligoureas Bearing

Proteinogenic Side Chains. *Angewandte Chemie*, *114*(11), 1973. https://doi.org/10.1002/1521-3757(20020603)114:11

[49] Bécart, D., Diemer, V., Salaün, A., Oiarbide, M., Nelli, Y. R., Kauffmann, B., Fischer, L., Palomo, C., & Guichard, G. (2017). Helical Oligourea Foldamers as Powerful Hydrogen Bonding Catalysts for Enantioselective C–C Bond-Forming Reactions. *Journal Of The American Chemical Society*, *139*(36), 12524-12532. https://doi.org/10.1021/jacs.7b05802

[50] Tsutsumi, H., Hamasaki, K., Mihara, H., & Ueno, A. (2000). Rate enhancement and enantioselectivity in ester hydrolysis catalysed by cyclodextrin–peptide hybrids. *Perkin 2*, *9*, 1813-1818. https://doi.org/10.1039/b004031m

[51] Chou, P. Y., & Fasman, G. D. (1979). Prediction of the Secondary Structure of Proteins from their Amino Acid Sequence. *Advances In Enzymology And Related Areas Of Molecular Biology*, 45-148. https://doi.org/10.1002/9780470122921.ch2

[52] Serrano, L., Horovitz, A., Avron, B., Bycroft, M., & Fersht, A. R. (1990). Estimating the contribution of engineered surface electrostatic interactions to protein stability by using double-mutant cycles. *Biochemistry*, *29*(40), 9343-9352. https://doi.org/10.1021/bi00492a006

[53] Baltzer, L., Broo, K., Nilsson, H., & Nilsson, J. (1999). Designed four-helix bundle catalysts—the engineering of reactive sites for hydrolysis and transesterification reactions of p-nitrophenyl esters. *Bioorganic & Medicinal Chemistry*, *7*(1), 83-91. https://doi.org/10.1016/s0968-0896(98)00218-1

[54] Choudhuri, S. (2014). Additional bioinformatic analyses involving protein sequences. Dans *Elsevier eBooks* (p. 183-207). https://doi.org/10.1016/b978-0-12-410471-6.00008-6

[55] Hamuro, Y., Geib, S. J., & Hamilton, A. D. (1997). Novel Folding Patterns in a Family of Oligoanthranilamides : Non-Peptide Oligomers That Form Extended Helical Secondary Structures. *Journal Of The American Chemical Society*, *119*(44), 10587-10593. https://doi.org/10.1021/ja963449u

[56] Saraogi, I., & Hamilton, A. D. (2009). Recent advances in the development of aryl-based foldamers. *Chemical Society Reviews*, *38*(6), 1726. https://doi.org/10.1039/b819597h

[57] Malone, J. F., Murray, C. M., Dolan, G. M., Docherty, R., & Lavery, A. J. (1997). Intermolecular Interactions in the Crystal Chemistry of N,N′-Diphenylisophthalamide, Pyridine-2,6-dicarboxylic Acid Bisphenylamide, and Related Compounds. *Chemistry Of Materials*, *9*(12), 2983-2989. https://doi.org/10.1021/cm970350t

[58] Huc, I. (2003). Aromatic oligoamide foldamers. *European Journal Of Organic Chemistry*, *2004*(1), 17-29. https://doi.org/10.1002/ejoc.200300495

[59] Hamuro, Y., Geib, S. J., & Hamilton, A. D. (1996). Oligoanthranilamides. Non-Peptide Subunits That Show Formation of Specific Secondary Structure. *Journal Of The American Chemical Society*, *118*(32), 7529-7541. https://doi.org/10.1021/ja9539857

[60] Delnoye, D., Sijbesma, R. P., Vekemans, J. A. J. M., & Meijer, E. W. (1996). π-Conjugated Oligomers and Polymers with a Self-Assembled Ladder-like Structure. *Journal Of The American Chemical Society*, *118*(36), 8717-8718. https://doi.org/10.1021/ja9614171

[61] Ernst, J. T., Becerril, J., Park, H. S., Yin, H., & Hamilton, A. D. (2003). Design and Application of an α-Helix-Mimetic Scaffold Based on an Oligoamide-Foldamer Strategy : Antagonism of the Bak BH3/Bcl-xL Complex. *Angewandte Chemie International Edition*, *42*(5), 535-539. https://doi.org/10.1002/anie.200390154

[62] Zhu, J., Parra, R. D., Zeng, H., Skrzypczak-Jankun, E., Zeng, X. C., & Gong, B. (2000). A New Class of Folding Oligomers : Crescent Oligoamides. *Journal Of The American Chemical Society*, *122*(17), 4219-4220. https://doi.org/10.1021/ja994433h

[63] Jiang, H., Léger, J., Dolain, C., Guionneau, P., & Huc, I. (2003). Aromatic δ-peptides : design, synthesis and structural studies of helical, quinoline-derived oligoamide foldamers. *Tetrahedron*, *59*(42), 8365-8374. https://doi.org/10.1016/j.tet.2003.08.058

[64] Gong, B. (2001). Crescent Oligoamides : From Acyclic "Macrocycles" to Folding Nanotubes. *Chemistry - A European Journal*, *7*(20), 4336-4342. https://doi.org/10.1002/1521-3765(20011015)7:20

[65] Berl, V., Huc, I., Khoury, R. G., Krische, M. J., & Lehn, J. M. (2000). Interconversion of single and double helices formed from synthetic molecular strands. *Nature*, *407*(6805), 720-723. https://doi.org/10.1038/35037545

[66] Berl, V., Huc, I., Khoury, R. G., & Lehn, J. (2001). Helical Molecular Programming : Supramolecular Double Helices by Dimerization of Helical Oligopyridine-dicarboxamide Strands. *Chemistry - A European Journal*, *7*(13), 2810-2820. https://doi.org/10.1002/1521-3765(20010702)7:13

[67] Huc, I., Maurizot, V., Gornitzka, H., & Léger, J. (2002). Hydroxy-substituted oligopyridine dicarboxamide helical foldamers. *Chemical Communications*, *6*, 578-579. https://doi.org/10.1039/b111612f

[68] Zheng, L., Zheng, D., Wang, Y., Yu, C., Zhang, K., & Jiang, H. (2019). Chiral bisphosphine ligands based on quinoline oligoamide foldamers : application in asymmetric hydrogenation. *Organic And Biomolecular Chemistry*, *17*(44), 9573-9577. https://doi.org/10.1039/c9ob01649j

[69] Zhao, H., Shen, J., Ren, C., Zeng, W., & Zeng, H. (2017). A Foldamer-Based Organocatalyst for Direct Arylations of Unactivated Arenes. *Organic Letters*, *19*(8), 2190-2193. https://doi.org/10.1021/acs.orglett.7b00921

[70] Dumont de Chassart, C.; Singleton, M. L. Aromatic Oligoamide Foldamer as a modular scaffold for the control of the reactivity of a PLP-mimic, Master thesis, Université Catholique de Louvain, 2023

[71] Velaerts, M.; Singleton, M. L. Synthesis and Design of Foldamers for Organocatalysis, Master thesis, Université catholique de Louvain, 2022.

[72] Liu, R., Li, X., & Lam, K. S. (2017). Combinatorial chemistry in drug discovery. *Current Opinion In Chemical Biology*, *38*, 117-126. https://doi.org/10.1016/j.cbpa.2017.03.017

[73] Zhang, R., Mahjour, B., Outlaw, A., McGrath, A., Hopper, T., Kelley, B., Walters, W. P., & Cernak, T. (2024). Exploring the combinatorial explosion of amine–acid reaction space via graph editing. *Communications Chemistry*, *7*(1). https://doi.org/10.1038/s42004-024-01101-w

[74] Massolo, E., Pirola, M., & Benaglia, M. (2020). Amide Bond Formation Strategies : Latest Advances on a Dateless Transformation. *European Journal Of Organic Chemistry*, *2020*(30), 4641-4651. https://doi.org/10.1002/ejoc.202000080

[75] Hosangadi, B. D., & Dave, R. H. (1996). An efficient general method for esterification of aromatic carboxylic acids. *Tetrahedron Letters*, *37*(35), 6375-6378. https://doi.org/10.1016/0040-4039(96)01351-2

[76] But, T. Y. S., & Toy, P. H. (2007). The Mitsunobu Reaction : Origin, Mechanism, Improvements, and Applications. *Chemistry - An Asian Journal*, *2*(11), 1340-1355. https://doi.org/10.1002/asia.200700182

[77] Wang, H., Wen, K., Wang, L., Ye, X., Xu, X., Shen, Y., & Sun, Z. (2012). Large-Scale Solvent-Free Chlorination of Hydroxy-Pyrimidines, -Pyridines, -Pyrazines and -Amides Using Equimolar POCl3. *Molecules/Molecules Online/Molecules Annual*, *17*(4), 4533-4544. https://doi.org/10.3390/molecules17044533

[78] Kwan, E. E., Zeng, Y., Besser, H. A., & Jacobsen, E. N. (2018). Concerted nucleophilic aromatic substitutions. *Nature Chemistry*, *10*(9), 917-923. https://doi.org/10.1038/s41557-018-0079-7

[79] Bunnett, J. F., & Zahler, R. E. (1951). Aromatic nucleophilic substitution reactions. *Chemical Reviews*, *49*(2), 273-412. https://doi.org/10.1021/cr60153a002

[80] Terrier, F. (2013). *Modern nucleophilic aromatic substitution*. https://doi.org/10.1002/9783527656141

[81] Logue, M. W., Pollack, R. M., & Vitullo, V. P. (1975b). Nature of the transition state for the decarboxylation of .beta.-keto acids. *Journal Of The American Chemical Society*, *97*(23), 6868-6869. https://doi.org/10.1021/ja00856a047

[82] Bases. (s. d.). https://reagents.acsgcipr.org/reagent-guides/ester-deprotection/list-of-reagents/bases

[83] Montalbetti, C., & Falque, V. M. (2005). Amide bond formation and peptide coupling. *Tetrahedron*, *61*(46), 10827-10852. https://doi.org/10.1016/j.tet.2005.08.031

[84] Li, X., Takale, B. S., Gallou, F., & Lipshutz, B. H. (2021). High Turnover Pd/C Catalyst for Nitro Group Reductions in Water. One-Pot Sequences and Syntheses of Pharmaceutical Intermediates. Organic Letters, 23(20), 8114-8118. https://doi.org/10.1021/acs.orglett.1c03258

[85] Catalytic Hydrogenation : Catalytic Reduction of Pd/C, Deprotection and Lindlar Catalyst. (s. d.). Hatsudy. https://hatsudy.com/pd.html

[86] De Miranda, A. S., De Souza, R. O. M. A., & Miranda, L. S. M. (2014). Ammonium formate as a green hydrogen source for clean semi-continuous enzymatic dynamic kinetic resolution of (+/−)-α-methylbenzylamine. *RSC Advances*, *4*(26), 13620-13625. https://doi.org/10.1039/c4ra00462k

[87] Davis, M. M., & Scanlon, D. B. (1977). The reaction of thionyl chloride with methyl-substituted heteroaromatic compounds. *Australian Journal Of Chemistry*, *30*(2), 433. https://doi.org/10.1071/ch9770433

[88] Roberts, D., Joule, J. A., Bros, M. A., & Alvarez, M. (1997). Synthesis of Pyrrolo[4,3,2-de]quinolines from 6,7-Dimethoxy-4-methylquinoline. Formal Total Syntheses of Damirones A and B, Batzelline C, Isobatzelline C, Discorhabdin C, and Makaluvamines A−D. *Journal Of Organic Chemistry*, *62*(3), 568-577. https://doi.org/10.1021/jo961743z

[89] Jayram, J., Xulu, B. A., & Jeena, V. (2019). Iodine/DMSO promoted oxidation of benzylic Csp3–H bonds to diketones – A mechanistic investigation. *Tetrahedron*, *75*(43), 130617. https://doi.org/10.1016/j.tet.2019.130617

UNIVERSITÉ CATHOLIQUE DE LOUVAIN
Faculté des sciences
Place des sciences, 2 bte L6.06.01, 1348 Louvain-la-Neuve, Belgique | **www.uclouvain.be/sc**